FEDERAL UNIVERSITY OF SÃO CARLOS
EXACT SCIENCES AND TECHNOLOGY CENTER
GRADUATE PROGRAM IN CHEMICAL ENGINERRING

SYNTHESIS OF ISOAMYL ESTERS FROM SOYBEAN OIL DEODORIZER DISTILLATE BY ENZYMATIC CATALYSIS FOR BIOLUBRICANT APPLICATIONS

RAFAEL DE ARAUJO SILVA

São Carlos
2022

UNIVERSIDADE FEDERAL DE SÃO CARLOS
CENTRO DE CIÊNCIAS EXATAS E DE TECNOLOGIA
PROGRAMA DE PÓS-GRADUAÇÃO EM ENGENHARIA QUÍMICA

SÍNTESE DE ÉSTERES ISOAMÍLICOS A PARTIR DO DESTILADO DA DESODORIZAÇÃO DO ÓLEO DE SOJA POR CATÁLISE ENZIMÁTICA PARA APLICAÇÕES COMO BIOLUBRIFICANTE

RAFAEL DE ARAUJO SILVA

São Carlos
2022

FEDERAL UNIVERSITY OF SÃO CARLOS
EXACT SCIENCES AND TECHNOLOGY CENTER
GRADUATE PROGRAM OF CHEMICAL ENGINEERING

SYNTHESIS OF ISOAMYL ESTERS FROM SOYBEAN OIL DEODORIZER DISTILLATE BY ENZYMATIC CATALYSIS FOR BIOLUBRICANT APPLICATIONS

RAFAEL DE ARAUJO SILVA

Doctoral thesis presented to the Graduate Program in Chemical Engineering of the Federal University of São Carlos to obtain the title of Doctor in Chemical Engineering.

Advisor: Prof. Dr. Paulo W. Tardioli

São Carlos
2022

Rafael de Araujo, Silva

Synthesis of isoamyl esters from soybean oil deodorizer distillate by enzymatic catalysis for biolubricant applications / Silva Rafael de Araujo -- 2022.
143f.

Tese de Doutorado - Universidade Federal de São Carlos, campus São Carlos, São Carlos
Orientador (a): Paulo Waldir Tardioli
Banca Examinadora: Paulo Waldir Tardioli, Felipe Fernando Furlan, Caterina Gruenwaldt Cunha Marques Netto, Adriano Aguiar Mendes, Débora de Oliveira
Bibliografia

1. Engenharia Química. 2. Desenvolvimento de Processos Químicos. 3. Ésteres Biolubrificantes. I. Rafael de Araujo, Silva. II. Título.

Ficha catalográfica desenvolvida pela Secretaria Geral de Informática (SIn)

DADOS FORNECIDOS PELO AUTOR

Bibliotecário responsável: Ronildo Santos Prado - CRB/8 7325

UNIVERSIDADE FEDERAL DE SÃO CARLOS

Centro de Ciências Exatas e de Tecnologia
Programa de Pós-Graduação em Engenharia Química

Folha de Aprovação

Defesa de Tese de Doutorado do candidato Rafael de Araujo Silva, realizada em 26/07/2022.

Comissão Julgadora:

Prof. Dr. Paulo Waldir Tardioli (UFSCar)

Prof. Dr. Felipe Fernando Furlan (UFSCar)

Profa. Dra. Caterina Gruenwaldt Cunha Marques Netto (UFSCar)

Prof. Dr. Adriano Aguiar Mendes (UNIFAL - MG)

Profa. Dra. Débora de Oliveira (UFSC)

O Relatório de Defesa assinado pelos membros da Comissão Julgadora encontra-se arquivado junto ao Programa de Pós-Graduação em Engenharia Química.

AGRADECIMENTOS

Gostaria de agradecer a todos e todas que de forma direta ou indireta contribuíram, em qualquer grau, para a realização deste trabalho. Foi uma jornada longa, repleta de desafios e sacrifícios, que agora chegou a seu fim. Toda ajuda e incentivo fizeram a diferença.

Agradeço ao meu orientador, o Prof. Dr. Paulo Waldir Tardioli, pela orientação, suporte, zelo, paciência e amizade ao longo destes anos.

Aos membros das bancas de acompanhamento, qualificação e defesa de tese, o Prof. Dr. Adriano Aguiar Mendes (acompanhamento, qualificação e defesa de tese), a Dra. Simone de Carvalho Miyoshi (acompanhamento), o Prof. Dr. André Bernardo (qualificação), a Profa. Dra. Débora de Oliveira (defesa de tese), a Profa. Dra. Caterina Gruenwaldt Cunha Marques Netto (defesa de tese) e o Prof. Dr. Felipe Fernando Furlan (defesa de tese), por aceitarem compor as bancas e pelas sugestões nestas mesmas oportunidades.

Aos professores Dra. Fernanda Perpétua Casciatori e Dr. Adilson José da Silva, pela oportunidade de estágio de livre docência.

Aos colegas de laboratório e de pós-graduação pela amizade, ajuda e suporte ao longo dos anos.

Aos demais professores do departamento de engenharia química da UFSCar dos quais fui aluno ou tive algum tipo de contato ao longo destes anos.

Ao corpo técnico-administrativo do departamento de engenharia química da UFSCar, em especial as técnicas Alyne Bernardes Veroli, Natália Gonçalves dos Santos e Thais Correa Castral Paranhos, assim como aos prestadores de serviço e fornecedores de suprimentos.

Às empresas Cocamar (Maringá, PR, Brasil), Novozymes Latin America (Araucária, PR, Brasil) e São Martinho (Pradópolis, SP, Brasil) por cederem amostras para este projeto.

Aos meus familiares, amigos e amigas de longa data, que me apoiaram, ajudaram e/ou incentivaram a seguir em frente, me lembrando ou fazendo me lembrar porque escolhi o caminho que segui.

Ao meu irmão e aos meus pais, em especial minha mãe, que me ajudou financeiramente ao longo dos anos para que pudesse me manter no programa de pós-graduação e concluir este doutorado.

A todos vocês, meu profundo e sincero agradecimento. Muito obrigado!

ACKNOWLEDGEMENTS

I would like to thank to all the people which contributed direct or indirect, in any degree, for the accomplishment of this work. It was a long journey, full of challenges and sacrifices, that now becomes to its ending. Every help and encouragement did the difference.

I thank my adviser, Prof. Dr. Paulo Waldir Tardioli, for the advising, support, care, patience and friendship for all those years.

To the members of the examination boards of thesis preliminary examination, qualifying examination and/or thesis defense, Prof. Dr. Adriano Aguiar Mendes (thesis preliminary examination, qualifying examination and thesis defense), Dr. Simone de Carvalho Miyoshi (thesis preliminary examination), Prof. Dr. André Bernardo (qualifying examination), Prof. Dr. Débora de Oliveira (thesis defense), Prof. Dr. Caterina Gruenwaldt Cunha Marques Netto (thesis defense) and Prof. Dr. Felipe Fernando Furlan (thesis defense), to accepted to participate as examination board members of this doctorate and for the comments and suggestions to improve the quality of the thesis text.

To the professors Dr. Fernanda Perpétua Casciatori and Dr. Adilson José da Silva, for the teaching training opportunities.

To the laboratory and graduate program fellows for the friendship, help and support in all those years.

To other professors of UFSCar chemical engineering department which I was student or had any kind of proximity in all those years.

To the technic-administrative body of UFSCar chemical engineering department, in special the technicians Alyne Bernardes Veroli, Natália Gonçalves dos Santos and Thais Correa Castral Paranhos, likewise to the service providers and suppliers.

To the companies Cocamar (Maringá, PR, Brasil), Novozymes Latin America (Araucária, PR, Brasil) and São Martinho (Pradópolis, SP, Brasil), for the donated samples to this project.

To my relatives and long-term friends, that supported, helped, and/or encouraged me to move on, reminding me or making me remember why I choused the way I am following.

To my brother and my parents, in special my mother, which financially aid me in all those years to maintaining me in the graduate program a finish this doctorate.

To all of you, my deep and sincere thanks. Thank you very much!

FINANCIAMENTO

O presente trabalho foi realizado com apoio da Fundação de Amparo à Pesquisa do Estado de São Paulo (FAPESP, Processo 2016/10636-8), Conselho Nacional de Desenvolvimento Científico e Tecnológico (CNPq, Processo 308212/2017-7) e Coordenação de Aperfeiçoamento de Pessoal de Nível Superior – Brasil (CAPES) – Código de Financiamento 001 e Processo 8887.335022/2019-00 (Bolsa de Doutorado, de 01/03/2019 a 30/06/2022).

FUNDING

This work was funded by São Paulo Research Foundation (FAPESP, grant #2016/10636-8), Conselho Nacional de Desenvolvimento Científico e Tecnológico (CNPq, grant #308212/2017-7), and in part by the Coordenação de Aperfeiçoamento de Pessoal de Nível Superior – Brasil (CAPES) – Finance Code 001 and grant #8887.335022/2019-00 (Doctoral Fellowship, from 01/03/2019 to 30/06/2022).

O Brasil é uma potência agrícola porque é uma potência hídrica, e só é uma potência hídrica porque é uma potência florestal. Sem a floresta vamos entrar num processo dramático, não só em relação à agricultura, mas da própria indústria, são regiões absolutamente densas sofrendo problemas de abastecimento da água. Meio ambiente e economia podem andar juntos e eu nem digo que é uma questão de compatibilizar, é integrar. O mundo está caminhando nessa direção.

Marina Silva

Brazil is Only an agricultural power because it is a hydric power, and it is only a hydric power because it is a forestal power. Without the forest we will going to enter in a dramatic process, not only regarding the agriculture, but for the industry as well, absolutely dense regions suffering from water supply problems. Environment and economy can walk side by side, and I am not saying that this is a compatibilization issue, it is an integration one. The world is walking in this direction.

Marina Silva

Falar de clima é falar de meio ambiente, assim como falar de justiça climática é falar de pessoas, falar de uma pauta antirracista, anticapitalista, por igualdade de gênero, contra as desigualdades sociais. São coisas que a gente pode abordar separadamente, mas elas nunca se separam.
Txai Suruí

Talking about clime is talking about environment, as talking about clime justice is talking about people, talking about an agenda of antiracism, anticapitalism, by gender equality, against social inequality. They are subjects that we can approach separately, but they never separated.
Txai Suruí

RESUMO

Os lubrificantes são produtos cuja fabricação atualmente é muito dependente de recursos fósseis não renováveis, possuem mercado e produção expressivos e se encontram na mira de várias leis ambientais em todo o planeta. Atualmente já existem alguns produtos de base biológicas inseridos neste mercado, denominados de biolubrificantes, porém compõem uma fração muito pequena deste segmento e possuem limitações. Estudos que envolvam o desenvolvimento de novos produtos, insumos e processos são essenciais para o sucesso e a ampliação dos biolubrificantes neste mercado. Assim, esta tese de doutorado teve como objetivo: avaliar a produção de bases biolubrificantes na forma de ésteres isoamílicos de ácidos graxos ("fatty acid isoamyl ester" – FAIE), a partir do destilado da desodorização do óleo de soja (DDOS – como fonte de ácidos graxos) com álcool isoamílico (coproduto gerado na fermentação de bioetanol e o principal constituinte do óleo fúsel) catalisada por lipase comercial Eversa Transform 2.0 (ETL 2.0) na sua forma livre, e por lipase de *Pseudomonas fluorescens* (PFL) imobilizada pelo método "hybrid nanoflower" (hNF). Planejamento experimental e metodologia de superfície de resposta foram utilizadas para definir parâmetros tanto para a imobilização da PFL por hNF (hNF-PFL), sendo estes parâmetros: a concentração de proteína, a concentração de metal e o pH de imobilização; quanto para a produção dos FAIEs, sendo estes parâmetros: a relação molar DDOS/álcool isoamílico, a temperatura de reação, a quantidade de enzima (para as reações com ETL 2.0) e a massa de material secante (para as reações com hNF-PFL). Estudos voltados para a etapa de incubação na síntese da hNF-PFL permitiram reduzir o tempo de incubação de 72 horas (meio estático a 25 °C) para apenas 20 minutos usando ultrassom, sem perdas no rendimento de imobilização (RI) ou atividade imobilizada (AI). Os valores otimizados de RI e AI para a hNF-PFL foram de 54 e 64 TBU%, respectivamente. A hNF-PFL mostrou alta estabilidade operacional mantendo praticamente os mesmos valores de rendimento de reação (RR) por 8 ciclos, um total de 192 h, e no 10º ciclo, total de 240 h, apresentou RR de 80 % em relação aos primeiros ciclos. A produção de FAIE utilizando ETL 2.0 com controle de umidade por peneira molecular nas condições de 39 e 9 % (relação massa de peneira molecular / massa de DDOS) atingiu valores de RR de 50 e 70 %, respectivamente. Quando a hNF-PFL foi utilizada para a síntese de FAIE, chegou-se ao RR de 64 % sem o uso de agentes de controle de humidade. Produtos com conversões parciais de DDOS em FAIE catalisados por ETL 2.0, com RR de 44 e 55 %, e por hNF-PFL, com RR de 56 e 57 %, apresentaram características físico-químicas similares a bases biolubrificantes comerciais. Assim, esta tese de doutorado tem potencial para contribuir economicamente para

o mercado de lubrificantes por meio de um processo enzimático ambientalmente amigável para a síntese de uma base estoque a partir de coprodutos da indústria nacional.

Palavras-chaves: DDOS, monoésteres isoamílicos de ácidos graxos, hybrid nanoflower, lipase de *Pseudomonas fluorescens*, Eversa.

ABSTRACT

Lubricants are among the many products whose manufacture is highly dependent on nonrenewable fossil resources, with high levels of production and a vast marketplace, so they are the focus of many environmental laws around the word. Currently, this market includes some biobased products, known as biolubricants, although they represent a very small fraction of this sector and have certain limitations. Studies concerning the development of new products, raw materials, and processes are essential for the expansion and commercial success of biolubricants. Therefore, the aim of this work was: evaluating the production of biolubricant base stocks such as fatty acid isoamyl esters (FAIEs) from soybean oil deodorizer distillate (SODD) as a fatty acids source, together with isoamyl alcohol (a byproduct from bioethanol fermentation and the main constituent of fusel oil), catalyzed by free Eversa Transform 2.0 lipase and *Pseudomonas fluorescens* lipase (PFL) immobilized by the hybrid nanoflower (hNF) method. Experimental design and response surface methodology were applied to define the parameters for PFL immobilization using hNFs (hNF-PFL), viz. protein concentration, metal concentration and immobilization pH, and for FAIEs production, viz. SODD/isoamyl alcohol molar ratio, reaction temperature, the enzyme mass and secant salt mass (for the reactions with hNF-PFL). Studies of the incubation step of the synthesis using hNF-PFL enabled the incubation time to be reduced from 72 h (static immobilization medium at 25 °C) to just 20 min using ultrasound, without losses of immobilization yield (IY) or immobilized activity (IA). The optimized IY and IA values for hNF-PFL were 54 and 64 TBU%, respectively. The hNF-PFL showed high operational stability, maintaining practically the same reaction yield (RY) values during 8 cycles, over a total of 192 h. At the 10^{th} cycle (total of 240 h), the material presented relative RY of 80%, compared to the earlier cycles. In the production of FAIEs using ETL 2.0 with molecular sieve (for moisture control) at 39 and 9 wt.% (molecular sieve mass / SODD mass), RY values of 50 and 70 wt.% were achieved, respectively. When hNF-PFL was employed in the FAIEs synthesis, RY of 64 wt.% was obtained, without the use of a moisture control agent. Products of partial conversion of SODD into FAIEs, catalyzed by ETL 2.0, with RY of 44 and 55 wt.%, and catalyzed by hNF-PFL, with RY of 56 and 57 wt.%, presented physicochemical characteristics similar to those of commercial biolubricant base stocks. Therefore, this doctoral thesis has the potential to contribute economically to the lubricant market through an environmentally friendly enzymatic process for the synthesis of a base stock from by-products of the national industry.

Keywords: SODD, fatty acid isoamyl monoesters, hybrid nanoflower, *Pseudomonas fluorescens* lipase, Eversa.

LIST OF TABLES

LIST OF FIGURES

TABLE OF CONTENTS

1 INTRODUCTION

1.1 Initial considerations

The structure of this work includes an introduction to the topics studied during a doctoral project, followed by a bibliographic review considering these topics in greater detail, together with a corresponding list of references. The sections providing the methodologies and the discussion of results are presented in the form of structured scientific articles (in English). At the end of this text, a summary is provided of the main findings of this work.

During the study, various ways of defining a biolubricant were encountered, including the following:

- Physiological lubricants applied to/in living beings;
- Industrial and automotive lubricants based on substances of mineral (petroleum) or biological origin, which present biodegradability;
- Industrial and automotive lubricants based exclusively on substances of biological origin, which present biodegradability and low toxicity.

For the purposes of the present work, the last definition of a biolubricant was adopted.

1.2 Introduction to the topic of biolubricants

Lubricant oils and greases are essential in human society, since they are required in applications ranging from simple tools to complex machinery. Their purpose is to facilitate the movement of components, reduce friction and wear, remove particles, exchange heat or avoid its generation, prevent corrosion, and provide electrical insulation. The origins of lubricants are unclear, although it is speculated that they date back to prehistory, taking the forms of sap, mud, or pastes of crushed plants. The invention of the wheel led to the first carts of prehistoric civilizations, which had wooden axles that at a certain time began to be lubricated with animal fats. The emergence of metallurgy, also in prehistory, led to the manufacture of metal materials, providing new solutions and at the same time new problems. The friction between the metallic parts was alleviated using animal and vegetable oils, which proved to be more satisfactory than animal fat. Crude petroleum was known to ancient civilizations such as the Assyrian and Egyptian. However, records of its use for lubricants are recent, dating from 1845 A.D. (Anderson, 1991). Since then, mineral lubricants have almost completely replaced those of biological origin. Bio-based oils now account for a minor portion of the lubricant market, with a relative value of only around 2%. This market, which has an estimated value of approximately US$ 160 billion, includes a diverse range of products specifically developed for use with a vast

spectrum of tools and machines (Luzuriaga, 2020; Markets and Markets, 2020; Tsagaraki et al., 2017).

Lubricants derived from biological sources are attractive due to their renewable characteristics, in addition to the fact that most are biodegradable, making them more environmentally friendly, compared to petroleum-based lubricants. However, the transition from petroleum-based to bio-based lubricants faces obstacles, the main one being the higher cost of the latter. Factors including raw material and processing costs (including catalysts) make biolubricants more expensive than traditional petroleum-based products. Studies aimed at reducing the costs of raw materials, identifying new sources, and developing processes and catalysts are essential for improving the competitiveness of biolubricants. This transition also requires statutory laws to protect the environment, in addition to economic incentives, before the production processes can become self-sustainable (Bart et al., 2013a, 2013b; Tsagaraki et al., 2017). Developed regions such as Europe and the United States (together accounting for the consumption of >75% of biolubricants globally) have implemented stricter environmental laws and targets (Tsagaraki et al., 2017). Such actions should be adopted by developing countries (or even be imposed on them), to ensure continuing access to major markets worldwide. These factors emphasize the importance of developing substitutes for petroleum derivatives that are sustainable, renewable, and nontoxic.

Biolubricant oil bases are essentially composed of esters that may be of natural or synthetic esters. There is a vast range of different types of esters that can be used for this purpose. Monoesters, diesters, glycerin esters, polyol esters, oligomeric esters, and complex esters, as well as mixtures of two or more types, can be employed as base for biolubricants. The great majority of natural esters are obtained from oleaginous plants, mainly in the form of triglycerides, while synthetic biolubricant esters are mainly obtained using reactions of fatty acids (in the free form or linked to glycerol molecules) obtained from natural oils with mono- or polyhydric alcohols, under chemical or enzymatic catalysis (Bart et al., 2013c). In an oleochemical and sugar-alcohol biorefinery, the integration of processes, together with a wide range of possible inputs, available in the form of products and byproducts from other processes, can enable the production of diverse biolubricants. This can also enable reductions of the operating and raw materials costs, making the products more competitive (Cherubini, 2010; Tsagaraki et al., 2017). The production of refined vegetable oils, biodiesel, glycerin and derivatives, sugar, and ethanol (1G and 2G) allows access to a wide variety of alcohols and polyols, which can be generated from glycerin and other byproducts of 1G and 2G ethanol

process steps, as well as fatty acid-rich byproducts generated during the refining of vegetable oils, enabling the availability of a wide range of substances suitable for producing lubricants (Cherubini, 2010; Schultz et al., 2014).

One of the byproducts of interest generated during the ethanol fermentation process is isoamyl alcohol, which is the main constituent of fusel oil, composed of a mixture of low molecular weight alcohols (Simsek and Ozdalyan, 2018). Fusel oil, obtained in the stage of distillation of the wine to separate ethanol, is mainly sent for combustion in the boiler or is incorporated into hydrated ethanol fuel[1]. Another byproduct of interest is oil deodorizer distillate (ODD), produced in the stages of deodorization of refined oils, which has a high content of fatty acids and may also contain significant amounts of sterols and tocopherols. In Brazil, soybean oil is the most widely produced edible vegetable oil (Corazza, 2021; dos Santos et al., 2022). During its industrial processing, soybean oil deodorizer distillate (SODD) is generated, which is mainly composed of linoleic acid and oleic acid, together with amounts of tocopherols. These tocopherols can act as natural additives, favoring the lubricating characteristics of the final product (Fox and Stachowiak, 2007; Gunawan et al., 2010; Khatoon et al., 2010; Sherazi et al., 2016).

Another issue for success in reducing process costs concerns the catalysts employed. Enzymatic catalysts usually function under milder operating conditions, compared to chemical catalysts, in addition to having greater substrate specificity and chemo-, enantio-, and regioselectivities. They present low or no toxicity and are biocompatible and biodegradable. These catalysts can contribute to reducing the costs associated with energy consumption, the maintenance of machinery and production lines, and the management, purification, and disposal of waste (Bart et al., 2013c; Jegannathan and Nielsen, 2013).

The base materials for synthetic biolubricants are generally obtained by esterification or transesterification reactions, which can be catalyzed by hydrolase class enzymes, specifically lipases, with commercial versions normally obtained from fungi or bacteria (Schultz et al., 2010; Türkay and Şahin-Yeşilçubuk, 2017). Enzymes tend to be more susceptible to inactivation under operational conditions and are usually more expensive, compared to chemical catalysts. Immobilization can be used to make enzymes more robust under operational

[1] Spoken information from a 2018 sugar and ethanol industrial site technical visit

conditions, promote greater catalytic activity, change their specificity and/or selectivity, and enable easy separation of the enzyme. These features allow greater control of the end of reactions, as well as enzyme reuse and expansion of possible reactor configurations (Souza et al., 2016). Many techniques using nanomaterials have been successfully explored for the immobilization of lipases, including the hybrid nanoflower (hNF) method (Zhong et al., 2020). Lipases immobilized by this technique have shown significant increases in activity, thermal stability, and stability at extreme pH values, in addition to presenting high porosity, good mechanical strength, long storage times, and the capacity for successive reuses without significant loss of activity (Cui et al., 2016; Fotiadou et al., 2019; Ke et al., 2016; Li et al., 2016; Li et al., 2018; Li et al., 2020; Zhang et al., 2016; Zhang et al., 2020).

There is expected to be a growing global demand for biolubricants in the next years. Consequently, research is needed to identify less expensive sources of raw materials that do not compete with food production and do not depend on expanding planted areas. There are several possible raw materials in the Brazilian productive chain that could attend those specifications. The use of SODD and isoamyl alcohol, as well as the development and application of more efficient enzymatic catalysts, such as lipases immobilized by the hNF technique, could open new possibilities to answer to the biolubricants challenges.

1.3 Objectives

The main objective of this work was to establish parameters for the synthesis of isoamyl esters of fatty acids with suitable characteristics for biolubricants, using renewable biomasses and enzymatic catalysis employing soluble and immobilized lipases.

In order to achieve this goal, it was necessary to determine the following:

- The viability of using SODD as a source of fatty acids (acyl donors);
- The lipase(s) to be employed in the synthesis of fatty acid isoamyl esters;
- The feasibility of catalyst immobilization using the hNF technique;
- The physicochemical characteristics of the produced crude fatty acid isoamyl esters.

2 BIBLIOGRAPHIC REVIEW

2.1 Biolubricants

Biolubricants are industrial or automotive lubricants based on substances that have natural and renewable origins, are biodegradable, and present low toxicity. These substances are typically esters derived from plants, in natural or synthetic forms. Biolubricants of natural esters are usually made from rapeseed (canola), soybean, sunflower, palm, or coconut oils (Bart et al., 2013a). Compared to mineral oils, natural oils tend to provide less wear on parts, lower coefficients of friction and volatility, and higher flash points, as well as better indices of viscosity, lubricity, shear stability, load capacity (pressure), detergency, and dispersion. In addition, the viscosity and surface tension of vegetable oils are similar to some petroleum-based lubricants employed in the steel industry. Since they are mainly composed of triglycerides, many of which consist of unsaturated fatty acids, the natural oils tend to have low thermo-oxidative stability, even at more moderate temperatures. These substances may also suffer from hydrolytic stress (Bart et al., 2013d; Reeves et al., 2017).

Synthetic biolubricant bases can be obtained by esterification or transesterification reactions of oils, fats, or free fatty acids (FFAs) from natural sources with mono- or polyhydric alcohols, generating different types of esters (Luther, 2014) (Figure 2.1-1). These synthetic esters can have physicochemical characteristics that are more favorable than those observed for natural oils, such as lower pour point and volatility temperatures, and higher flash points and thermo-oxidative stabilities (Reeves et al., 2017). However, the performance of biolubricant base stocks depends on factors related to the chains of the constituent molecules, such as the degree of unsaturation, carbon chain size, functional groups, and the effects of branching (Chan et al., 2018). The technical requirements and characteristics of a lubricant or biolubricant can vary greatly, depending on its purpose, given the wide range of possible applications (Bart et al., 2013e).

Figure 2.1-1. Scheme for the synthesis of synthetic esters from natural sources.

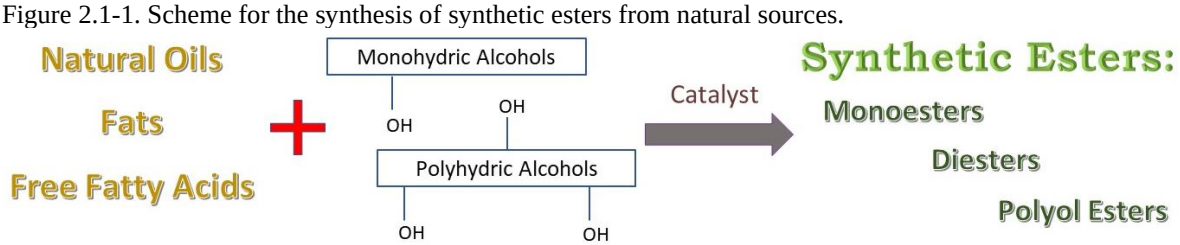

Source: Author.

Despite their advantages, biolubricants can have drawbacks such as temperature and viscosity limitations, unpleasant odor, low thermal and oxidative stabilities, and can promote the discoloration of metals (Bart et al., 2013d). These limitations can be overcome by chemical modification of the compounds in biolubricants, or the use of additives (Chan et al., 2018). Such additives are usually specific to biolubricants, since existing additives employed in mineral oils can prejudice the properties and performance of biolubricants, or be sufficiently toxic to hinder their biodegradation (Reeves et al., 2017).

2.2 Soybean oil residues and byproducts

Byproducts and residues containing high levels of fatty acid sources are produced throughout the lifecycle of edible soybean oil, since its production to its disposal. The neutralization, bleaching, and deodorization steps of the edible oil refining process result in the production of a soap (formed by the neutralization of FFAs), filter cake, and SODD, respectively, with high levels of fatty acids (Mandarino et al., 2015). In addition to fatty acids, these residues from the refining process contain significant concentrations of other natural compounds such as squalenes, sterols, and tocopherols, which have high commercial value after concentration and purification, so these refining residues become byproducts of interest to other industrial sectors (Hill and Höfer, 2009).

Edible oils are widely used in food frying processes, where they suffer degradations after prolonged use, forming compounds harmful to health, although they still contain FFAs and triglycerides in high concentrations (Avagyan and Singh, 2019; Hosseini et al., 2016; Zhang et al., 2019). In several countries, there is widespread the segregation of these used frying oils (from residential, commercial, and food industry sources) for reuse, such as to produce biodiesel. In China, biodiesel production almost entirely employs used frying oil (Avagyan and Singh, 2019).

2.2.1 SODD

SODD is generated during the deodorization step of soybean oil refining, when a flow of superheated steam (0.5 to 3.0% of steam, relative to the mass of oil), at a temperature of 160 to 260 °C (depending on the source of the oil), enters into contact with the oil in a deodorizer, under low pressure (1.5 to 5.0 mbar). The steam drags FFAs, glycerides (mono-, di-, and triglycerides), tocopherols, sterols, carotenoids, squalenes, aldehydes, and ketones, among other compounds. Figure 2.2.1-1 shows a flow diagram of a typical industrial deodorization

process. SODD typically contains high concentrations of FFAs, lower amounts of glycerides, 5-20% tocopherols, 6-23% sterols, 0.1-3.0% squalenes, and traces of other organic compounds. Certain process conditions can produce SODD with higher quantities of glycerides (Greyt, 2021; Mandarino et al., 2015).

Figure 2.2.1-1. Flow diagram of a soybean oil deodorization process.

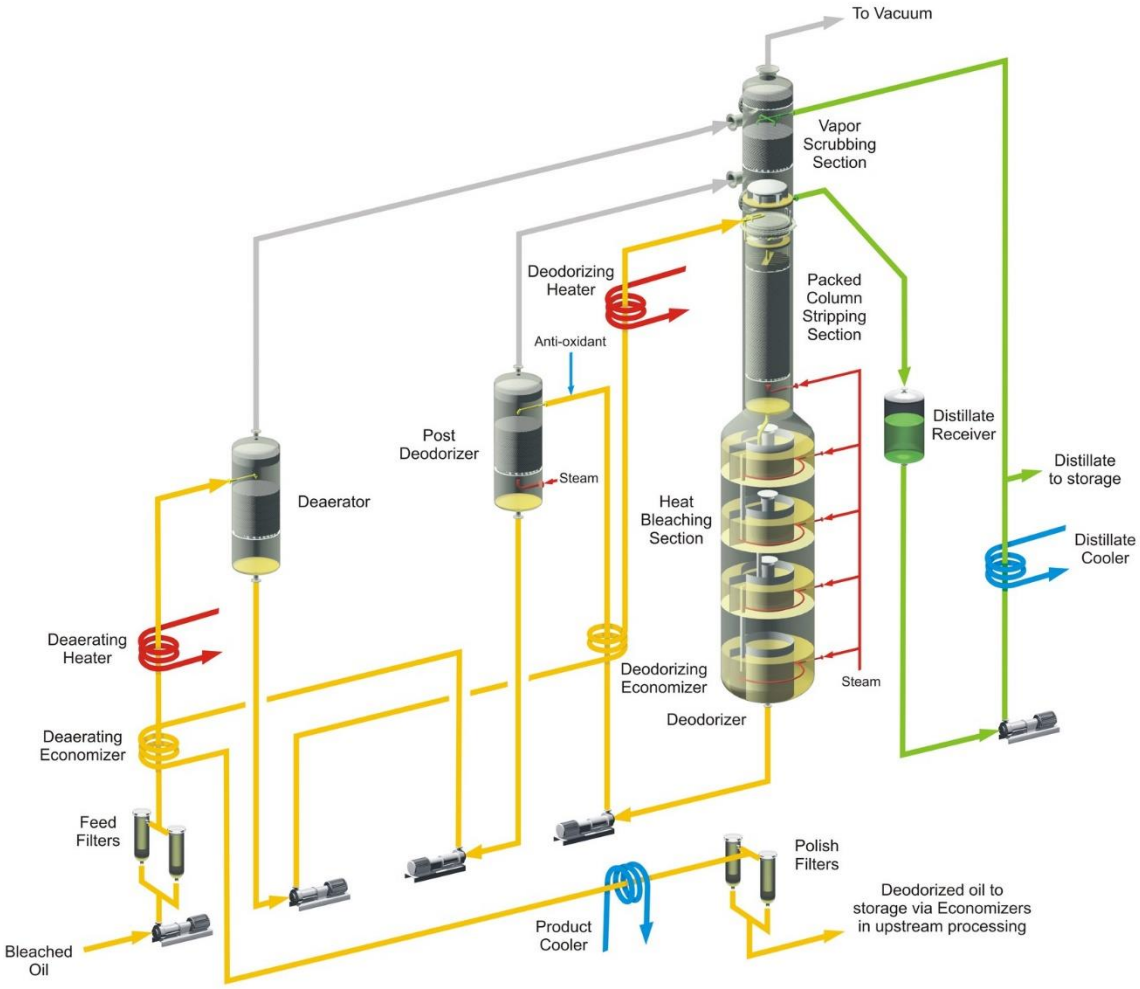

Source: Bragante, 2009.

Commercial interest in SODD is mainly due to its contents of tocopherols and sterols. Tocopherols are used as food supplements, in the form of α-tocopherol acetate (vitamin E) or as functional food additives. They act as natural antioxidants, preventing oils from going rancid and consequently increasing their shelf life. The SODD price is influenced to a greater degree by the tocopherols market, compared to the sterols market. When markets for these biocompounds are unfavorable, SODD can be sold as a source of fatty acids (FAs) for incorporation in animal feed. Otherwise, they become waste, creating problems of disposal, with the associated cost (Sherazi et al., 2016).

The viability of using SODD to produce biodiesel, whether composed of methyl esters (FAMEs) or ethyl esters (FAEEs), has been investigated in several studies (Aguieiras et al., 2013; Du et al., 2007; Lv et al., 2021; Panpipat et al., 2012; Souza et al., 2009; Vieira et al., 2021; Visioli et al., 2016; Yin et al., 2017; Zheng et al., 2020). In addition to its use for biodiesel production, SODD has also been used as a source of carbon in cultures of *Pseudomonas aeruginosa* MR01 for the production of biosurfactants (Partovi et al., 2013).

2.3 Fusel oil

Fusel oil is a byproduct obtained in the distillation step of ethanol production. It mainly consists of isoamyl alcohol (Figure 2.3-1a), but with significant amounts of other monohydric alcohols including amyl alcohol (Figure 2.3-1b), ethanol, isobutanol, and propanol, together with water (Ferreira et al., 2013). The fusel oil composition can vary considerably, depending on the type of carbon source used and factors related to the fermentation process. The amount produced depends on the pH of the fermentation must (Awad et al., 2018).

Figure 2.3-1. Chemical structures of (a) isoamyl alcohol and (b) amyl alcohol.

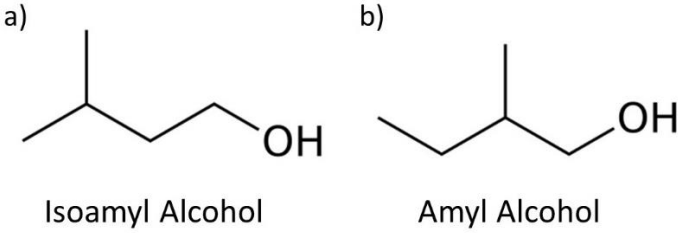

Source: Author.

In addition to being combusted in boilers or incorporated into fuel ethanol, fusel oil can be used in the chemical, food, and pharmaceutical industries. Alcohols of interest, such as isoamyl alcohol, can be separated for use in perfumes, aromatizers, and solvents for paints (Incauca S.A.S., 2018).

Some studies have investigated the use of fusel oil to synthesize esters with biolubricating properties, employing oleic acid, palm oil, and microalgae oil, together with fusel oil, under enzymatic catalysis (Cerón et al., 2018; Da Silva et al., 2020; Dörmő et al., 2004) or chemical catalysis (Özgülsün et al., 2000). In comparison to methyl esters (FAMEs), esters from fusel oil were shown to be a viable option for application as biodiesel (Monroe et al., 2020).

2.4 Lipases

Lipases are hydrolase enzymes (EC 3.1.1.3) that act on glycerides, other esters, and their constituents such as fatty acids and alcohols, promoting hydrolysis, esterification, transesterification, interesterification, and thioesterification reactions (Figure 2.4-1). These enzymes are present in all biological kingdoms, participating in metabolic cycles involving lipids (Aouf et al., 2014; Konwar and Sagar, 2018). They act both intra- and extracellularly, and the same single-celled organism can present more than one form of lipase. For example, the fungus *Candida rugosa* (formerly known as *Candida cylindracea*) possesses at least 7 genetically different extracellular lipases (de Maria et al., 2006). They can have high substrate specificity, stereospecificity, chemoselectivity, and regioselectivity, which can explain the variety of lipases produced by the same organism. They have folded α/β structures, characteristic of hydrolases, in many cases with an amphiphilic peptide sequence in the form of an α-helix, which behaves as a lid that opens in the presence of an organic phase (Figure 2.4-2). When the lid opens, access is provided to the active site composed of the 3 amino acids serine–aspartic acid–histidine or serine–glutamic acid–histidine (Ser–Asp/Glu–His). When solubilized in water, the enzymes can promote heterogeneous catalysis of oils and fats by interfacial reactions at the edges of polar/nonpolar systems. Although they can act in organic media, lipases require a minimum amount of moisture to maintain their conformation and, consequently, their activity (Aouf et al., 2014; Konwar and Sagar, 2018).

Figure 2.4-1. Reactions catalyzed by lipases.

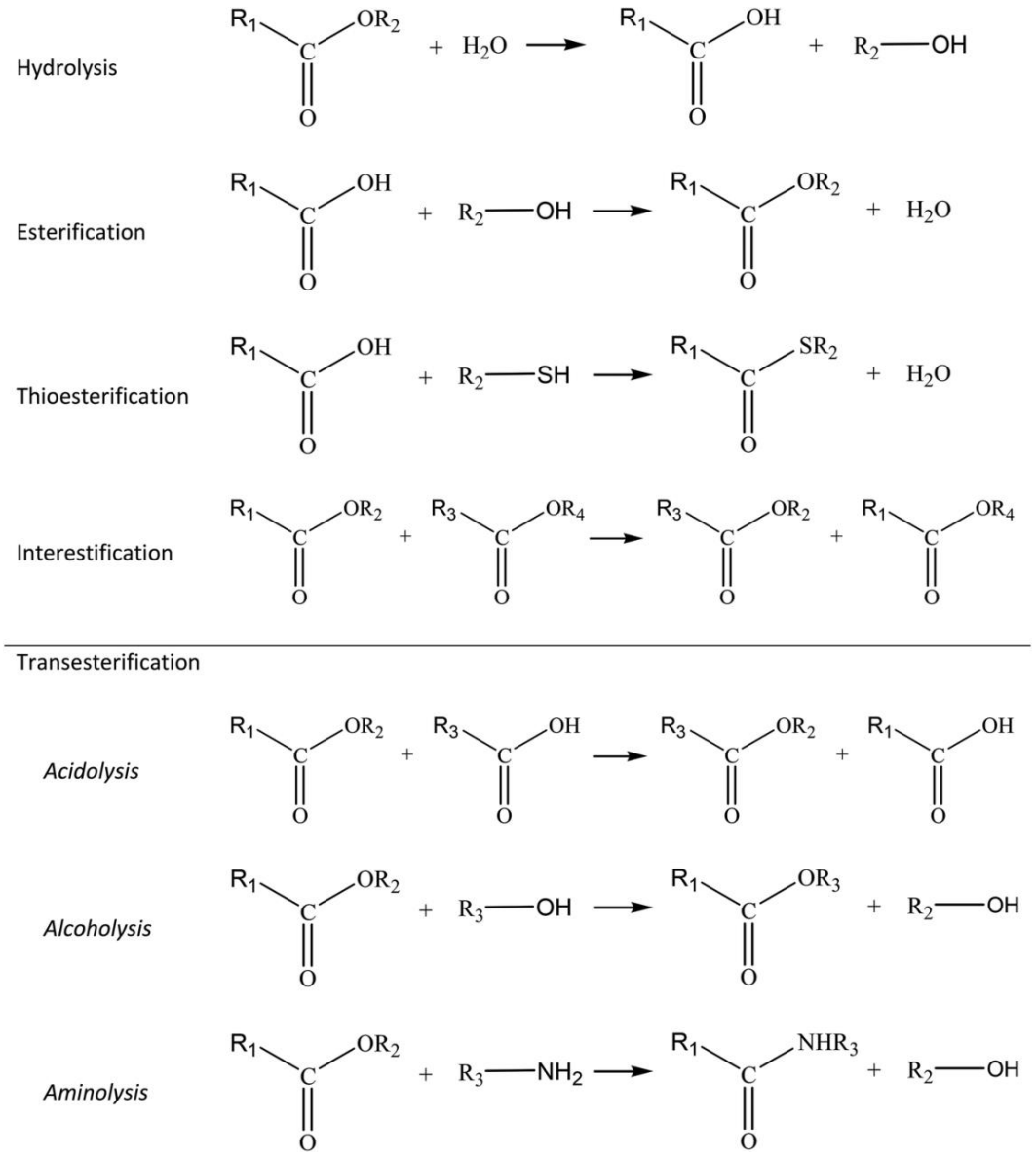

Source: Aouf et al., 2014.

Figure 2.4-2. Characteristic structure of lipases. Image of a lipase 3 from *Candida rugosa* with "closed lid" (purple section), represented as a ribbon (A) and a surface (B). The access tunnel to the catalytic site is represented by the reticulated structure. The protein residues corresponding to the catalytic site are shown at the center of the images.

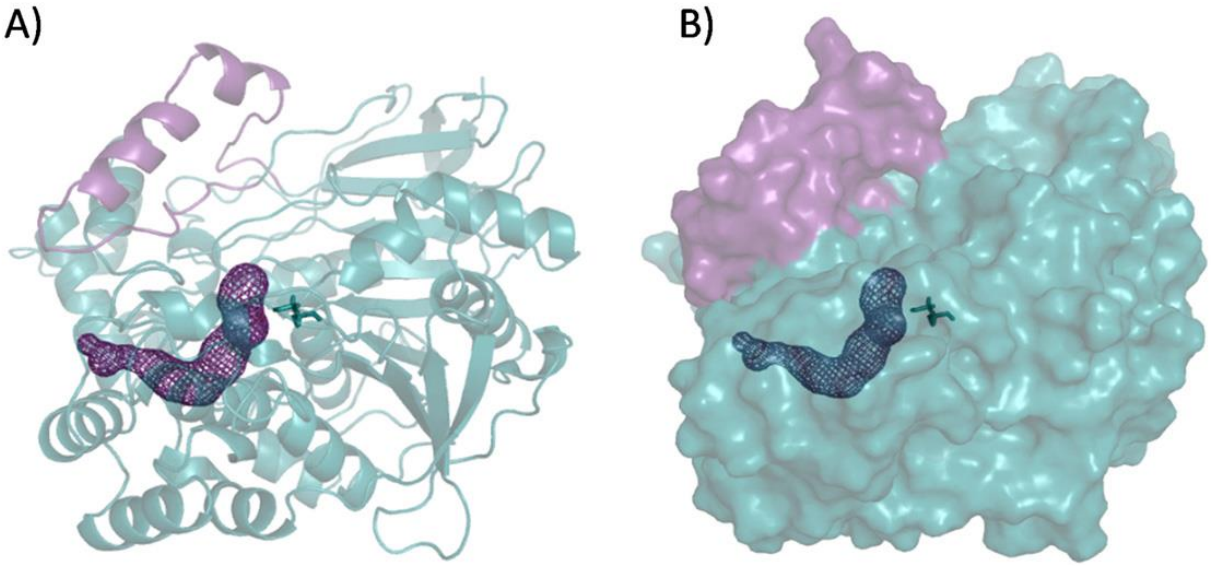

Source: Barriuso et al., 2016.

Lipases of microbial origin are naturally more stable towards operational conditions such as pH and temperature, besides acting in a wide range of lipid reactions and being easier to synthesize, so for these reasons they are more commonly used in industrial processes or final products (Aouf et al., 2014; Konwar and Sagar, 2018; Schultz et al., 2010; Türkay and Şahin-Yeşilçubuk, 2017). Many lipases have been studied for producing biodiesel (composed of FAMEs or FAEEs), using a wide variety of different sources of fatty acids, as reported in nearly 2000 papers published between the years 1990 and 2019 (Almeida et al., 2021; Cavalcante et al., 2021). There are fewer reports concerning the synthesis of biolubricants. Lipases from *Burkholderia cepacia* (BCL), *Candida antarctica* (lipase B – CALB), *Candida rugosa* (CRL), *Candida* sp. (CALA), Eversa Transform 2.0 (ETL 2.0, a variant of *Thermomyces lanuginosus* lipase), *Rhizopus arrhizus* (RAL), *Rhizomucor miehei* (RML), and *Thermomyces lanuginosus* (TLL), in free or immobilized forms, have been used in the production of different biolubricants (Bolina et al., 2021; Guimarães et al., 2021).

The presence of some surfactants (mainly nonionic) can increase lipase activity, due to the interactions of surfactants with the reaction medium, which decrease the size of micelles (or reverse micelles) and consequentially increases the aqueous-organic interfacial area where lipases act; and/or due interactions of surfactants with enzymes, favoring a more active and/or stable conformations (Delorme et al., 2011; Eckard et al., 2013; Weiss and Landfester, 2013).

2.5 Enzyme immobilization

The enzyme immobilization aims to make enzymes insoluble in the reaction medium and allow then to become more robust towards the operational conditions. It also enables easy separation of the biocatalysts from the reaction medium, consequently allowing greater control of the reaction endpoint and reuse of the biocatalyst, in addition to increasing the purity of the product. It also expands the range of possible regimes and reactors used for the reactions, such as the continuous fluidized bed regime (which would not be feasible using solubilized free enzymes). The greater robustness reduces the loss of enzyme activity during the processes, allowing operations to proceed for longer times, more numbers of reuses (in cases where it is possible to make a comparison with the use of free enzyme, such as in the production of biodiesel, where the free enzyme remains in the polar phase and the product of interest is found in the non-polar phase),and/or to operate under more extreme conditions, with shorter reaction times, or when the viscosity of the medium is a limiting factor (since the operation can be performed at higher temperature) (Melo et al., 2020; Zdarta et al., 2018).

After immobilization, enzymes can exhibit increases or decreases in their specificity, selectivity, and activity. One of the drawbacks of enzyme immobilization is that it creates additional process costs. For immobilization to be viable, the cost must be offset by the gains, such as the possibility of reuse without significant loss of activity in batch processes, or easy separation reducing the costs associated with product purification. Depending on the support used, the biocatalysts may occupy a significant volume of the reactor. There may also be diffusional problems, steric hindrance, rigidify or deformation of the enzymes, which can compromise their activity (Barbosa et al., 2015; Melo et al., 2020; Romero-Fernández and Paradisi, 2020; Santos et al., 2015; Sheldon and van Pelt, 2013; Zdarta et al., 2018).

Traditional immobilization techniques based on adsorption, covalent bonding, encapsulation, entrapment, and crosslinking have been extensively studied and continue to be used, although they are now applied to more modern and technological materials, at smaller scales and/or employing new compounds. Selection of the technique and material for immobilization depend on both the enzyme to be immobilized and the type and conditions of the catalytic process. It worth to mention that the selection of the most suitable immobilization material, whether as a support or for crosslinking, is a crucial challenge for success in obtaining a viable biocatalyst, since this can directly affect the biocatalytic system (Melo et al., 2020; Zdarta et al., 2018).

Current methods aim to immobilize enzymes on nanometric-scale supports, in order to reduce diffusional limitations and increase the loading by maximizing the functional surface area (Melo et al., 2020). New nanomaterials have distinct shapes, with the possibility of achieving greater control of the desired pore sizes. In addition, they can have highly variable amounts of different functional groups available for interactions with enzymes or for surface modifications, high chemical and thermal stabilities, and excellent mechanical properties. Many of these new nanomaterials are composites or hybrids of materials having organic and/or inorganic origins, with combinations of properties that maximize their performance (Zdarta et al., 2018). Magnetic nanoparticles coated with mesoporous silicas or other materials, metal-organic frameworks (MOFs), and hNFs are examples of these new nanomaterials used to immobilize different types of enzymes, including lipases (Bilal et al., 2018; Bilal and Iqbal, 2021; Giannakopoulou et al., 2020; Li et al., 2020; Ye et al., 2020; Zhong et al., 2020).

2.5.1 Hybrid nanoflowers (hNFs)

Hybrid nanoflowers, discovered by Ge et al. (2012), are composed of proteins and inorganic crystals (usually copper(II) phosphate trihydrate, $Cu_3(PO_4)_2 \cdot 3H_2O$), which combine to form microscopic structures that visually resemble flower shapes (Figure 2.5-1). They are obtained by mixing a protein solubilized in sodium phosphate-buffered saline (PBS) with an inorganic salt, usually copper(II) sulfate ($CuSO_4$). After mixing the components, the precipitation of $Cu_3(PO_4)_2 \cdot 3H_2O$, together with the protein amide groups (Figure 2.5-2a), forms precipitates on a nanometer scale (Figure 2.5-2b). There is then nucleation for crystal growth by complexation with chloride ions (Cl^-) present in the medium. The hNF structure results from agglomeration of the crystals formed, with their growth being anisotropic (Figures 2.5-2a, 2.5-2c and 2.5-2d) (Ge et al., 2012).

Figure 2.5-1. Comparison of the structures of flowers and hNFs produced with bovine serum albumin (BSA) at different concentrations.

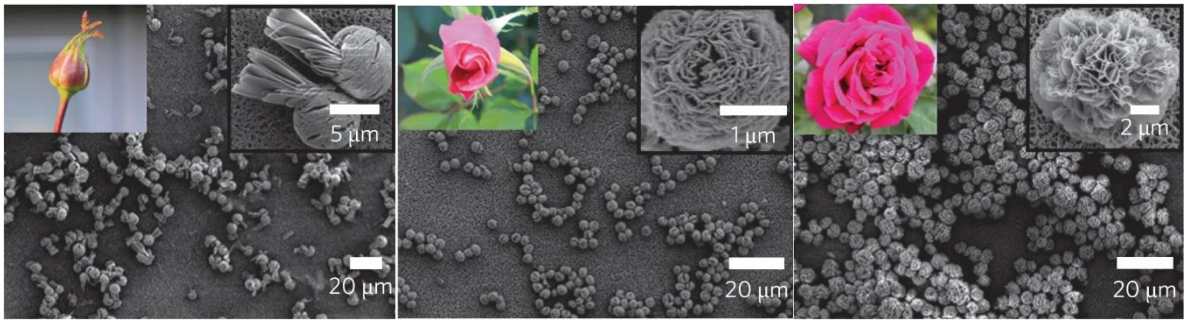

BSA 0.5 mg/mL BSA 0.1 mg/mL BSA 0.02 mg/mL

Source: Ge et al., 2012.

Figure 2.5-2. Formation of hNFs composed of BSA and $Cu_3(PO_4)_2 \cdot 3H_2O$. (a) Proposed mechanism, consisting of three steps: (1) nucleation and formation of crystals; (2) growth of the crystals; (3) formation of the nanoflowers. Yellow spheres indicate protein molecules. (b-d) Scanning electron microscopy (SEM) images acquired after 2 h, 12 h, and 3 days.

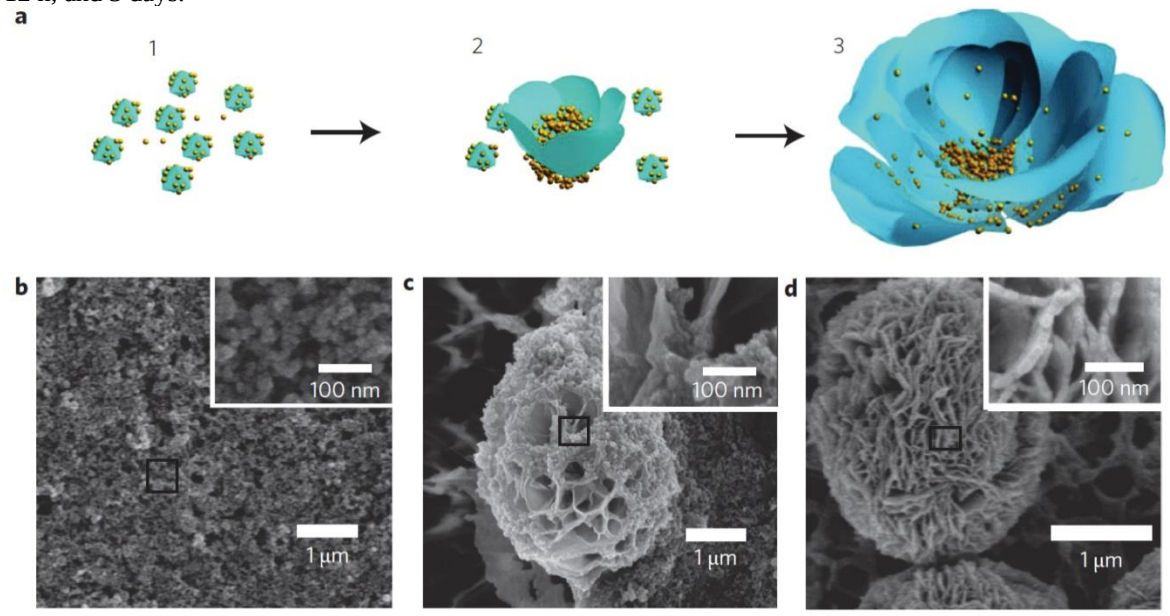

Source: Ge et al., 2012.

Besides $CuSO_4$, various other inorganic salts, the majority containing divalent cations, have also been used to produce hNFs. These cations include aluminum (Al^{3+}), calcium (Ca^{2+}), cobalt (Co^{2+}), iron(II) (Fe^{2+}), magnesium (Mg^{2+}), manganese (Mn^{2+}), nickel (Ni^{2+}), gold (Au^{3+}), silver (Ag^{+}), and zinc (Zn^{2+}) (Lin et al., 2020; Ocsoy et al., 2015; Sharma et al., 2017; Talens-Perales et al., 2020; Xin et al., 2020; Yin et al., 2015; Zhang et al., 2015; Zhang et al., 2016). Factors such as the concentrations of protein, PBS buffer, and inorganic salts, as well as medium pH, temperature, and incubation time, influence the success of obtaining hNFs (Ge et al., 2012; Li et al., 2016; Somturk et al., 2015; Somturk et al., 2016). Figure 2.5-1 shows the effect of varying the concentration of bovine serum albumin (BSA) protein on the shape and size of the

hNF structures. Various enzymes have been immobilized using this technique, usually resulting in significant increases in activity, compared to the free enzymes. Li et al. (2016) and Liang et al. (2015) synthesized hNFs using papain, obtaining activities of 7260% and 4510%, respectively, relative to the free enzyme. The difference between the results for the two immobilizations was related to the pH values employed, which were 9.0 and 7.4, respectively. Other features of enzymatic hNFs are improved stability and shelf life. Cui et al. (2016) immobilized bovine pancreas lipase type II (BPL tII), resulting in activity of 460%, compared to the free enzyme, together with high thermal stability, with 93% activity remaining after 10 h at 60 ºC, while the free enzyme showed activity close to zero, under the same conditions. Both Cui et al. (2016) and Somturk et al. (2016) reported over 95% activity of hNFs after 20 days of storage.

Lipases activated with surfactants and immobilized by the hNF technique have sometimes shown even greater increases in activity. Cui et al. (2016) compared the activities of BPL tII hNFs prepared without surfactant and other BPL tII hNFs prepared in the presence of different surfactants at varying concentrations. Use of hexadecyltrimethylammonium bromide (CTAB) at a concentration of 0.25 mM resulted in 200% higher activity of BPL tII-CTAB-hNF, compared to the activity found for the BPL tII-hNF biocatalyst without surfactant. However, such a positive effect was not always observed, since other CTAB concentrations led to BPL tII-CTAB-hNF with less substantial activity increases, as well as lower activities, compared to BPL tII-hNF. The same was observed for the other surfactants studied, with one of them reducing the activity to less than 20% (compared to the BPL tII-hNF biocatalyst) at any applied concentration. Li et al. (2020) immobilized *Aspergillus oryzae* lipase (AOL) by the hNF technique, obtaining AOL-hNFs with 75% and 170% activity, relative to free AOL, under conditions without surfactant and in the presence of Tween-80 (0.15 mM), respectively.

In recent years, the technique has undergone changes aiming at improving both the synthesis and its applications. Li et al. (2018) immobilized BCL on carbon nanotubes (CNTs), before applying the hNF technique (Figure 2.5-3). As a result, the esterification activity of the hNFs formed with Cu^{2+} was 68 times higher than observed for free BCL, and 51 times higher than for the BCL-hNF biocatalyst without CNTs. Zhong et al. (2021) produced magnetic hNFs (MhNFs) with AOL using Ca^{2+} ions and magnetic nanoparticles (MNPs). Two strategies were adopted for use of the MNPs, one with covalent binding of the enzymes to the MNPs and the other without binding them to the MNPs, prior to the synthesis of hNFs (Figure 2.5-4). In other studies, activated carbon fibers (Figure 2.5-5) and activated polyvinyl alcohol nanofibers

copolymerized with polyethylene (PVA-co-PE) (Figure 2.5-6) have been used for the *in situ* growth of hNFs (Li et al., 2016; Luo et al., 2020; Vo et al., 2020).

Figure 2.5-3. Comparative schematic illustrations of the synthesis of *Burkholderia cepacia* lipase hNFs, without (BCL-hNF) and with prior immobilization of BCL on carbon nanotubes (BCL-CNT-hNF).

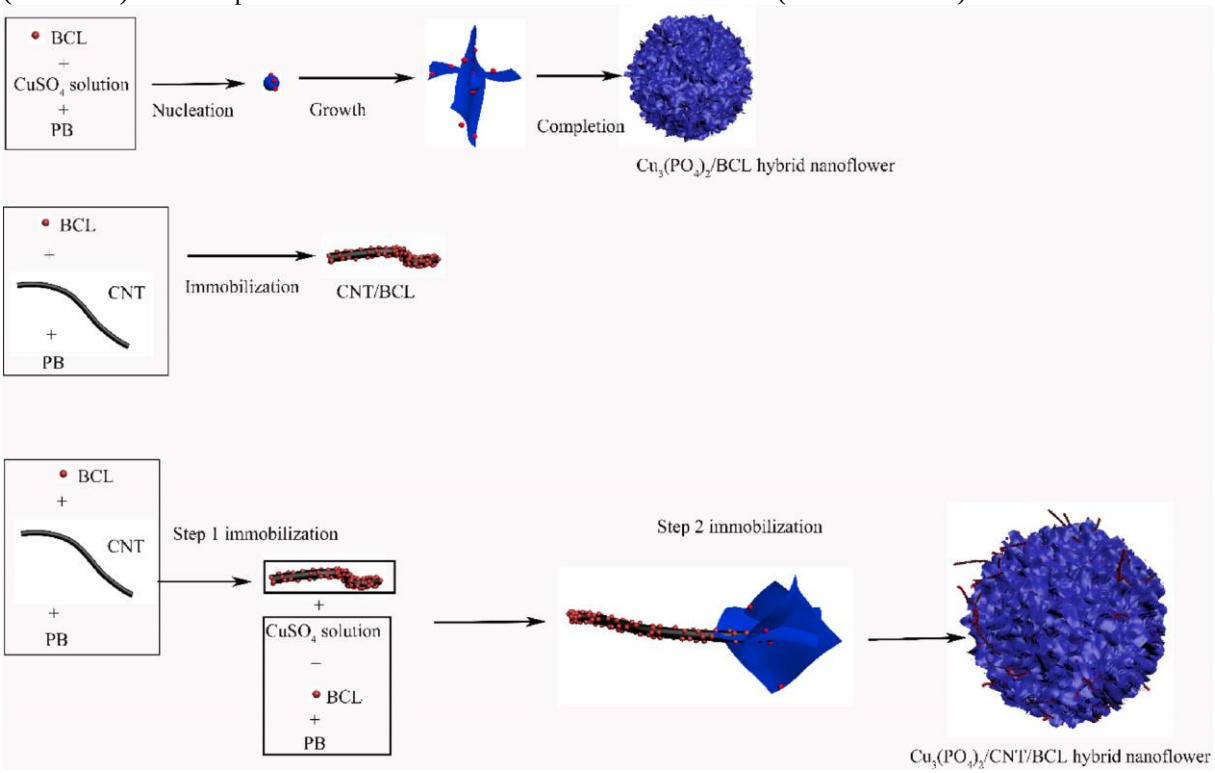

Source: Li et al., 2018.

Figure 2.5-4. Syntheses of hNFs and magnetic hNFs (MhNFs) containing *Aspergillus oryzae* lipase (AOL).

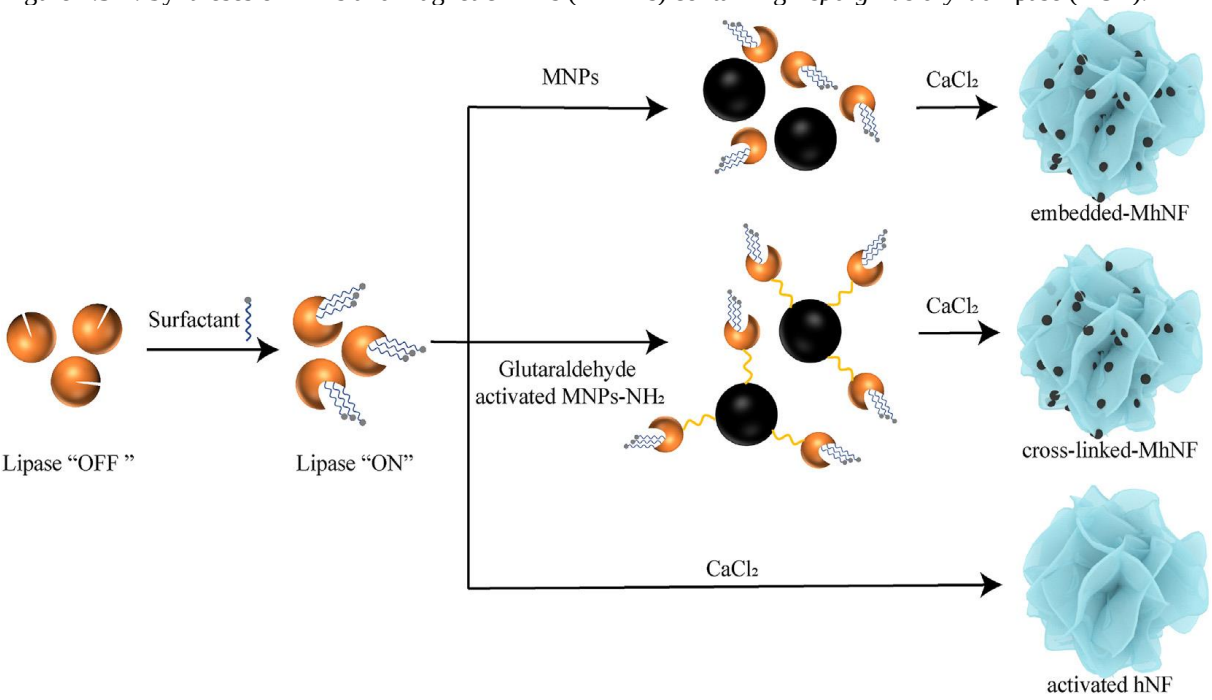

Source: Zhong et al., 2021.

Figure 2.5-5. *In situ* growth of hNFs on activated carbon fibers.

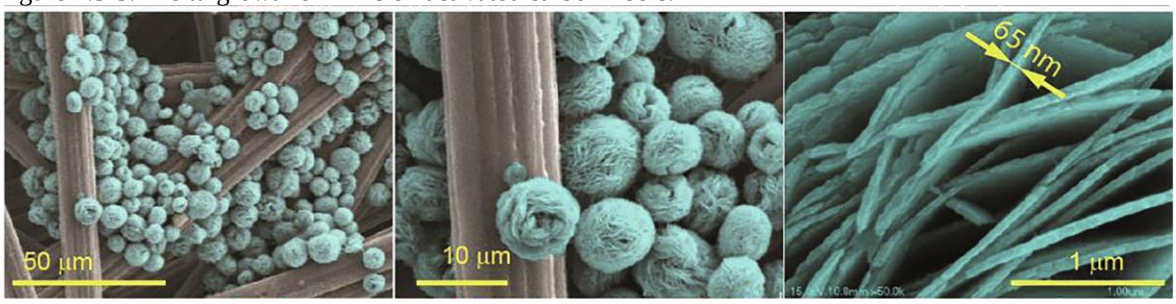

Source: Vo et al., 2020.

Figure 2.5-6. *In situ* growth of hNFs on PVA-co-PE nanofibers.

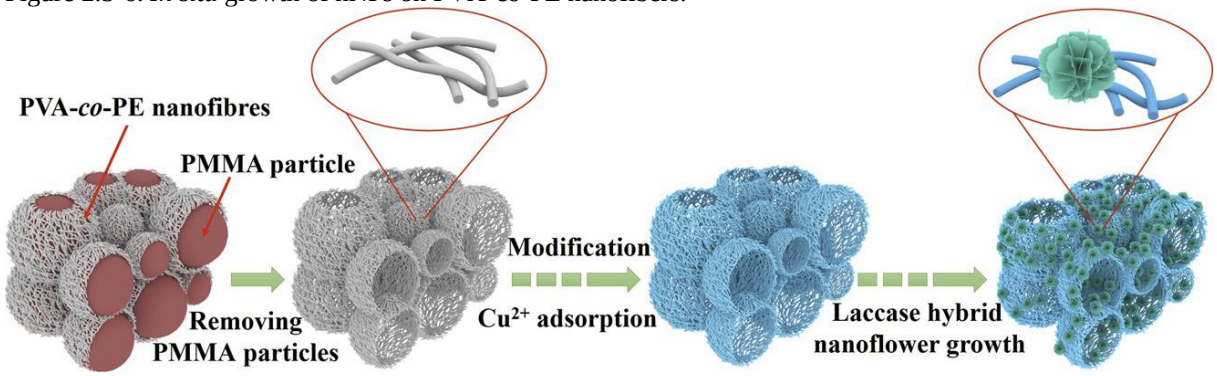

Source: Luo et al., 2020.

Other studies have reported the production of hNFs using more than one enzyme (Aydemir et al., 2020; Han et al., 2020; Mauryu et al., 2020a; Rai et al., 2020), two different cations (Wen et al., 2020), and even bones (Wang et al., 2020). Maurya et al. (2020b) reduced the hNFs synthesis time from 3 days to 6 h by using chitosan in the immobilization medium. Luo et al. (2020) were able to reduce the hNFs synthesis time even further, to 30 min, using a vortex flow system. Dwivedee et al. (2018) and Soni et al. (2018) reduced the hNFs synthesis time to only 10 min and 7.5 min, respectively, using an ultrasonication system. These studies show that the hNF technique can be highly versatile, with many possibilities still to be explored.

3 REFERENCES FOR THE INTRODUCTION AND THE BIBLIOGRAPHIC REVIEW

Aguieiras, E. C. G., Souza, S. L., & Langone, M. A. P. (2013). Estudo do comportamento da lipase comercial Lipozyme RM IM em reações de esterificação para obtenção de biodiesel. *Química Nova*, *36*(5), 646–650. https://doi.org/10.1590/S0100-40422013000500006

Almeida, F. L. C., Travália, B. M., Gonçalves, I. S., & Forte, M. B. S. (2021). Biodiesel production by lipase-catalyzed reactions: bibliometric analysis and study of trends. *Biofuels, Bioproducts and Biorefining*, bbb.2183. https://doi.org/10.1002/bbb.2183

Anderson, K. J. (1991). A History of Lubricants. *MRS Bulletin*, *16*(10), 69–69. https://doi.org/10.1557/S0883769400055895

Aouf, C., Durand, E., Lecomte, J., Figueroa-Espinoza, M.-C., Dubreucq, E., Fulcrand, H., & Villeneuve, P. (2014). The use of lipases as biocatalysts for the epoxidation of fatty acids and phenolic compounds. *Green Chem.*, *16*(4), 1740–1754. https://doi.org/10.1039/C3GC42143K

Avagyan, A. B., & Singh, B. (2019). Biodiesel from Plant Oil and Waste Cooking Oil. In A. B. Avagyan & B. Singh (Eds.), *Biodiesel: Feedstocks, Technologies, Economics and Barriers* (p. 137). Springer Singapore. https://doi.org/10.1007/978-981-13-5746-6

Awad, O. I., Ali, O. M., Hammid, A. T., & Mamat, R. (2018). Impact of fusel oil moisture reduction on the fuel properties and combustion characteristics of SI engine fueled with gasoline-fusel oil blends. *Renewable Energy*, *123*, 79–91. https://doi.org/10.1016/j.renene.2018.02.019

Aydemir, D., Gecili, F., Özdemir, N., & Nuray Ulusu, N. (2020). Synthesis and characterization of a triple enzyme-inorganic hybrid nanoflower (TrpE@ihNF) as a combination of three pancreatic digestive enzymes amylase, protease and lipase. *Journal of Bioscience and Bioengineering*, *129*(6), 679–686. https://doi.org/10.1016/j.jbiosc.2020.01.008

Barbosa, O., Ortiz, C., Berenguer-Murcia, Á., Torres, R., Rodrigues, R. C., & Fernandez-Lafuente, R. (2015). Strategies for the one-step immobilization–purification of enzymes as industrial biocatalysts. *Biotechnology Advances*, *33*(5), 435–456. https://doi.org/10.1016/j.biotechadv.2015.03.006

Barriuso, J., Vaquero, M. E., Prieto, A., & Martínez, M. J. (2016). Structural traits and catalytic versatility of the lipases from the Candida rugosa -like family: A review. *Biotechnology Advances*, *34*(5), 874–885. https://doi.org/10.1016/j.biotechadv.2016.05.004

Bart, J. C. J., Gucciardi, E., & Cavallaro, S. (2013a). Renewable lubricants. In J. C. J. Bart, E. Gucciardi, & S. Cavallaro (Eds.), *Biolubricants: Science and technology* (p. 944). Woodhead Publishing.

Bart, J. C. J., Gucciardi, E., & Cavallaro, S. (2013b). The transition from reliance on fossil resources to biomass valorisation. In J. C. J. Bart, E. Gucciardi, & S. Cavallaro (Eds.), *Biolubricants: Science and technology* (p. 944). Woodhead Publishing.

Bart, J. C. J., Gucciardi, E., & Cavallaro, S. (2013c). Chemical transformations of renewable lubricant feedstocks. In J. C. J. Bart, E. Gucciardi, & S. Cavallaro (Eds.), *Biolubricants: Science and technology* (p. 944). Woodhead Publishing.

Bart, J. C. J., Gucciardi, E., & Cavallaro, S. (2013d). Lubricants: properties and characteristics. In J. C. J. Bart, E. Gucciardi, & S. Cavallaro (Eds.), *Biolubricants: Science and technology* (p. 944). Woodhead Publishing.

Bart, J. C. J., Gucciardi, E., & Cavallaro, S. (2013e). Biolubricant product groups and technological applications. In J. C. J. Bart, E. Gucciardi, & S. Cavallaro (Eds.), *Biolubricants: Science and technology* (p. 944). Woodhead Publishing.

Bilal, M., & Iqbal, H. M. N. (2021). Armoring bio-catalysis via structural and functional coordination between nanostructured materials and lipases for tailored applications. *International Journal of Biological Macromolecules*, *166*, 818–838. https://doi.org/10.1016/j.ijbiomac.2020.10.239

Bilal, M., Zhao, Y., Rasheed, T., & Iqbal, H. M. N. (2018). Magnetic nanoparticles as versatile carriers for enzymes immobilization: A review. *International Journal of Biological Macromolecules*, *120*, 2530–2544. https://doi.org/10.1016/j.ijbiomac.2018.09.025

Bolina, I. C. A., Gomes, R. A. B., & Mendes, A. A. (2021). Biolubricant Production from Several Oleaginous Feedstocks Using Lipases as Catalysts: Current Scenario and Future Perspectives. *BioEnergy Research*. https://doi.org/10.1007/s12155-020-10242-4

Bragante, A. G. (2009). *Processo de Extração de Óleos Vegetais*. http://abgtecalim.yolasite.com/

Cavalcante, F. T. T., Neto, F. S., Rafael de Aguiar Falcão, I., Erick da Silva Souza, J., de Moura Junior, L. S., da Silva Sousa, P., Rocha, T. G., de Sousa, I. G., de Lima Gomes, P. H., de Souza, M. C. M., & dos Santos, J. C. S. (2021). Opportunities for improving biodiesel production via lipase catalysis. *Fuel*, *288*, 119577. https://doi.org/10.1016/j.fuel.2020.119577

Cerón, A. A., Vilas Boas, R. N., Biaggio, F. C., & de Castro, H. F. (2018). Synthesis of biolubricant by transesterification of palm kernel oil with simulated fusel oil: Batch and continuous processes. *Biomass and Bioenergy*, *119*, 166–172. https://doi.org/10.1016/j.biombioe.2018.09.013

Chan, C.-H., Tang, S. W., Mohd, N. K., Lim, W. H., Yeong, S. K., & Idris, Z. (2018). Tribological behavior of biolubricant base stocks and additives. *Renewable and Sustainable Energy Reviews*, *93*, 145–157. https://doi.org/10.1016/j.rser.2018.05.024

Cherubini, F. (2010). The biorefinery concept: Using biomass instead of oil for producing energy and chemicals. *Energy Conversion and Management*, *51*(7), 1412–1421. https://doi.org/10.1016/j.enconman.2010.01.015

Corazza, E. (2021). *Caderno Nº 006/2021 – Indústria de óleos vegetais*. https://corecondf.org.br/caderno-no-006-2021-industria-de-oleos-vegetais/

Cui, J., Zhao, Y., Liu, R., Zhong, C., & Jia, S. (2016). Surfactant-activated lipase hybrid nanoflowers with enhanced enzymatic performance. *Scientific Reports*, *6*(29), 1–13. https://doi.org/10.1038/srep27928

Da Silva, A. P. T., Bredda, E. H., de Castro, H. F., & Da Rós, P. C. M. (2020). Enzymatic catalysis: An environmentally friendly method to enhance the transesterification of microalgal oil with fusel oil for production of fatty acid esters with potential application as biolubricants. *Fuel*, *273*, 117786. https://doi.org/10.1016/j.fuel.2020.117786

De María, P. D., Sánchez-Montero, J. M., Sinisterra, J. V., & Alcántara, A. R. (2006). Understanding Candida rugosa lipases: An overview. *Biotechnology Advances*, *24*(2), 180–196. https://doi.org/10.1016/j.biotechadv.2005.09.003

Delorme, V., Dhouib, R., Canaan, S., Fotiadu, F., Carrière, F., & Cavalier, J.-F. (2011). Effects of Surfactants on Lipase Structure, Activity, and Inhibition. *Pharmaceutical Research*, *28*(8), 1831–1842. https://doi.org/10.1007/s11095-010-0362-9

Dörmő, N., Bélafi-Bakó, K., Bartha, L., Ehrenstein, U., & Gubicza, L. (2004). Manufacture of an environmental-safe biolubricant from fusel oil by enzymatic esterification in solvent-free system. *Biochemical Engineering Journal*, *21*(3), 229–234. https://doi.org/10.1016/j.bej.2004.06.011

dos Santos, A. C., Ferreira, P. M., Lopes, C. L., Braga, M., & Viana, N. M. (2022). *Estudo prospectivo de óleos vegetais*. https://www.infoteca.cnptia.embrapa.br/infoteca/bitstream/doc/1140622/1/-DOC41.pdfDu, W., Wang, L., & Liu, D. (2007). Improved methanol tolerance during Novozym435-mediated methanolysis of SODD for biodiesel production. *Green Chem.*, *9*(2), 173–176. https://doi.org/10.1039/B613704K

Dwivedee, B. P., Soni, S., Laha, J. K., & Banerjee, U. C. (2018). Self Assembly through Sonication: An Expeditious and Green Approach for the Synthesis of Organic-Inorganic Hybrid Nanopetals and their Application as Biocatalyst. *ChemNanoMat*, *4*(7), 670–681. https://doi.org/10.1002/cnma.201800110

Eckard, A., Muthukumarappan, K., & Gibbons, W. (2013). A Review of the Role of Amphiphiles in Biomass to Ethanol Conversion. *Applied Sciences*, *3*(2), 396–419. https://doi.org/10.3390/app3020396

Ferreira, M. C., Meirelles, A. J. A., & Batista, E. A. C. (2013). Study of the fusel oil distillation process. *Industrial and Engineering Chemistry Research*, *52*(6), 2336–2351. https://doi.org/10.1021/ie300665z

Fotiadou, R., Patila, M., Hammami, M. A., Enotiadis, A., Moschovas, D., Tsirka, K., Spyrou, K., Giannelis, E. P., Avgeropoulos, A., Paipetis, A., Gournis, D., & Stamatis, H. (2019). Development of Effective Lipase-Hybrid Nanoflowers Enriched with Carbon and Magnetic Nanomaterials for Biocatalytic Transformations. *Nanomaterials*, *9*(6), 808. https://doi.org/10.3390/nano9060808

Fox, N. J., & Stachowiak, G. W. (2007). Vegetable oil-based lubricants—A review of oxidation. *Tribology International*, *40*(7), 1035–1046. https://doi.org/10.1016/j.triboint.2006.10.001

Ge, J., Lei, J., & Zare, R. N. (2012). Protein-inorganic hybrid nanoflowers. *Nature Nanotechnology*, *7*(7), 428–432. https://doi.org/10.1038/nnano.2012.80

Giannakopoulou, A., Gkantzou, E., Polydera, A., & Stamatis, H. (2020). Multienzymatic Nanoassemblies: Recent Progress and Applications. *Trends in Biotechnology*, *38*(2), 202–216. https://doi.org/10.1016/j.tibtech.2019.07.010

Greyt, W. De. (n.d.). *Deodorization*. AOCS Lipid Library. Retrieved May 17, 2021, from https://lipidlibrary.aocs.org/edible-oil-processing/deodorization

Guimarães, J. R., Miranda, L. P., Fernandez-Lafuente, R., & Tardioli, P. W. (2021). Immobilization of Eversa® Transform via CLEA Technology Converts It in a Suitable Biocatalyst for Biolubricant Production Using Waste Cooking Oil. *Molecules*, *26*(1), 193. https://doi.org/10.3390/molecules26010193

Gunawan, S., Melwita, E., & Ju, Y.-H. (2010). Analysis of trans–cis fatty acids in fatty acid steryl esters isolated from soybean oil deodoriser distillate. *Food Chemistry*, *121*(3), 752–757. https://doi.org/10.1016/j.foodchem.2009.12.079

Han, J., Luo, P., Wang, L., Wu, J., Li, C., & Wang, Y. (2020). Construction of a Multienzymatic Cascade Reaction System of Coimmobilized Hybrid Nanoflowers for Efficient Conversion of Starch into Gluconic Acid. *ACS Applied Materials & Interfaces*, *12*(13), 15023–15033. https://doi.org/10.1021/acsami.9b21511

Hill, K., & Höfer, R. (2009). Natural Fats and Oils. In R. Höfer (Ed.), *Sustainable Solutions for Modern Economies* (p. 525). RSC Publishing.

Hosseini, H., Ghorbani, M., Meshginfar, N., & Mahoonak, A. S. (2016). A Review on Frying: Procedure, Fat, Deterioration Progress and Health Hazards. *Journal of the American Oil Chemists' Society*, *93*(4), 445–466. https://doi.org/10.1007/s11746-016-2791-z

Incauca S.A.S. (n.d.). *Fusel Oil*. Retrieved August 22, 2018, from http://www.incauca.com/en/producto/fusel-oil/

Jegannathan, K. R., & Nielsen, P. H. (2013). Environmental assessment of enzyme use in industrial production – a literature review. *Journal of Cleaner Production*, *42*, 228–240. https://doi.org/10.1016/j.jclepro.2012.11.005

Ke, C., Fan, Y., Chen, Y., Xu, L., & Yan, Y. (2016). A new lipase–inorganic hybrid nanoflower with enhanced enzyme activity. *RSC Advances*, *6*(23), 19413–19416. https://doi.org/10.1039/C6RA01564F

Khatoon, S., Raja Rajan, R. G., & Gopala Krishna, A. G. (2010). Physicochemical Characteristics and Composition of Indian Soybean Oil Deodorizer Distillate and the Recovery of Phytosterols. *Journal of the American Oil Chemists' Society*, *87*(3), 321–326. https://doi.org/10.1007/s11746-009-1499-8

Konwar, B. K., & Sagar, K. (2018). Introduction. In B. K. Konwar & K. Sagar (Eds.), *Lipase: An Industrial Enzyme Through Metagenomics* (p. 231). Apple Academic Press.

Li, C., Zhao, J., Zhang, Z., Jiang, Y., Bilal, M., Jiang, Y., Jia, S., & Cui, J. (2020). Self-assembly of activated lipase hybrid nanoflowers with superior activity and enhanced stability. *Biochemical Engineering Journal*, *158*, 107582. https://doi.org/10.1016/j.bej.2020.107582

Li, K., Wang, J., He, Y., Abdulrazaq, M. A., & Yan, Y. (2018). Carbon nanotube-lipase hybrid nanoflowers with enhanced enzyme activity and enantioselectivity. *Journal of Biotechnology*, *281*, 87–98. https://doi.org/10.1016/j.jbiotec.2018.06.344

Li, M., Luo, M., Li, F., Wang, W., Liu, K., Liu, Q., Wang, Y., Lu, Z., & Wang, D. (2016). Biomimetic Copper-Based Inorganic–Protein Nanoflower Assembly Constructed on the Nanoscale Fibrous Membrane with Enhanced Stability and Durability. *The Journal of Physical Chemistry C*, *120*(31), 17348–17356. https://doi.org/10.1021/acs.jpcc.6b03537

Li, Y., Fei, X., Liang, L., Tian, J., Xu, L., Wang, X., & Wang, Y. (2016). The influence of synthesis conditions on enzymatic activity of enzyme-inorganic hybrid nanoflowers. *Journal of Molecular Catalysis B: Enzymatic*, *133*, 92–97. https://doi.org/10.1016/j.molcatb.2016.08.001

Liang, L., Fei, X., Li, Y., Tian, J., Xu, L., Wang, X., Wang, Y., Xia, Y. N., & Lee, J. H. (2015). Hierarchical assembly of enzyme-inorganic composite materials with extremely high enzyme activity. *RSC Adv.*, *5*(117), 96997–97002. https://doi.org/10.1039/C5RA17754E

Lin, J., Zhong, C., Lu, Q., & Lin, Z. (2020). Room-Temperature Synthesis of Trypsin-Inorganic Hybrid Nanocomposites for Fast and Efficient Protein Digestion. *ChemistrySelect*, *5*(40), 12500–12504. https://doi.org/10.1002/slct.202002859

Liu, J., Ma, R.-T., & Shi, Y.-P. (2020). "Recent advances on support materials for lipase immobilization and applicability as biocatalysts in inhibitors screening methods"-A review. *Analytica Chimica Acta*, *1101*, 9–22. https://doi.org/10.1016/j.aca.2019.11.073

Luo, M., Li, M., Jiang, S., Shao, H., Razal, J., Wang, D., & Fang, J. (2020). Supported growth of inorganic-organic nanoflowers on 3D hierarchically porous nanofibrous membrane for enhanced enzymatic water treatment. *Journal of Hazardous Materials*, *381*, 120947. https://doi.org/10.1016/j.jhazmat.2019.120947

Luo, X., Mohammed Al-Antaki, A. H., Igder, A., Stubbs, K. A., Su, P., Zhang, W., Weiss, G. A., & Raston, C. L. (2020). Vortex Fluidic-Mediated Fabrication of Fast Gelated Silica Hydrogels with Embedded Laccase Nanoflowers for Real-Time Biosensing under Flow. *ACS Applied Materials & Interfaces*, *12*(46), 51999–52007. https://doi.org/10.1021/acsami.0c15669

Luther, R. (2014). Bio-Based and Biodegradable Base Oils. In T. Mang (Ed.), *Encyclopedia of Lubricants and Lubrication - Vol. 1* (p. 2413). Springer.

Luzuriaga, S. (2020). *Biolubricants market during COVID-19*. Society of Tribologists Abd Lubrication Engineers. https://www.stle.org/files/TLTArchives/2020/09_September/Market_Trends.aspx

Lv, W., Wu, C., Lin, S., Wang, X., & Wang, Y. (2021). Integrated Utilization Strategy for Soybean Oil Deodorizer Distillate: Synergically Synthesizing Biodiesel and Recovering Bioactive Compounds by a Combined Enzymatic Process and Molecular Distillation. *ACS Omega*, *6*(13), 9141–9152. https://doi.org/10.1021/acsomega.1c00333

Mandarino, J. M. G., Hirakuri, M. H., & Roessing, A. C. (2015). *Tecnologia para produção do óleo de soja: descrição das etapas, equipamentos, produtos e subprodutos*. https://ainfo.cnptia.embrapa.br/digital/bitstream/item/126080/1/Doc171-OL.pdf

Markets and Markets. (2020). *Lubricants Market by Base Oil (Mineral Oil, Synthetic Oil, Bio-based Oil), Product Type (Engine Oil, Hydraulic Fluid, Metalworking Fluid), Application (Transportation and Industrial lubricants), Region - Global Forecast to 2025*. https://www.marketsandmarkets.com/Market-Reports/lubricants-market-182046896.html?gclid=EAIaIQobChMIyqOy3LP27gIVBA-RCh0iYQCKEAAYASAAEgIj6_D_BwE

Maurya, S. S., Nadar, S. S., & Rathod, V. K. (2020a). Dual activity of laccase-lysine hybrid organic–inorganic nanoflowers for dye decolourization. *Environmental Technology & Innovation*, *19*, 100798. https://doi.org/10.1016/j.eti.2020.100798

Maurya, S. S., Nadar, S. S., & Rathod, V. K. (2020b). A rapid self-assembled hybrid bio-microflowers of alpha–amylase with enhanced activity. *Journal of Biotechnology*, *317*, 27–33. https://doi.org/10.1016/j.jbiotec.2020.04.010

Melo, J. S., Tripathi, A., Kumar, J., Mishra, A., Sandaka, B. P., & Bhainsa, K. C. (2020). Immobilization: Then and Now. In A. Tripathi & J. S. Melo (Eds.), *Immobilization Strategies: Biomedical, Bioengineering and Environmental Applications* (p. 665). Springer.

Monroe, E., Shinde, S., Carlson, J. S., Eckles, T. P., Liu, F., Varman, A. M., George, A., & Davis, R. W. (2020). Superior performance biodiesel from biomass-derived fusel alcohols and low grade oils: Fatty acid fusel esters (FAFE). *Fuel*, *268*, 117408. https://doi.org/10.1016/j.fuel.2020.117408

Novozymes. (2016). *Immobilized lipases for biocatalysis: for smarter chemical synthesis* (p. 6).

Ocsoy, I., Dogru, E., & Usta, S. (2015). A new generation of flowerlike horseradish peroxides as a nanobiocatalyst for superior enzymatic activity. *Enzyme and Microbial Technology*, *75–76*, 25–29. https://doi.org/10.1016/j.enzmictec.2015.04.010

Özgülsün, A., Karaosmanôglu, F., & Tüter, M. (2000). Esterification reaction of oleic acid with a fusel oil fraction for production of lubricating oil. *Journal of the American Oil Chemists' Society*, *77*(1), 105–109. https://doi.org/10.1007/s11746-000-0017-5

Panpipat, W., Xu, X., & Guo, Z. (2012). Towards a commercially potential process: Enzymatic recovery of phytosterols from plant oil deodoriser distillates mixture. *Process Biochemistry*, *47*(8), 1256–1262. https://doi.org/10.1016/j.procbio.2012.04.024

Partovi, M., Lotfabad, T. B., Roostaazad, R., Bahmaei, M., & Tayyebi, S. (2013). Management of soybean oil refinery wastes through recycling them for producing biosurfactant using Pseudomonas aeruginosa MR01. *World Journal of Microbiology and Biotechnology*, *29*(6), 1039–1047. https://doi.org/10.1007/s11274-013-1267-7

Rai, S. K., Kaur, H., Kauldhar, B. S., & Yadav, S. K. (2020). Dual-Enzyme Metal Hybrid Crystal for Direct Transformation of Whey Lactose into a High-Value Rare Sugar D-Tagatose: Synthesis, Characterization, and a Sustainable Process. *ACS Biomaterials Science & Engineering*, *6*(12), 6661–6670. https://doi.org/10.1021/acsbiomaterials.0c00841

Reeves, C. J., Siddaiah, A., & Menezes, P. L. (2017). A Review on the Science and Technology of Natural and Synthetic Biolubricants. *Journal of Bio- and Tribo-Corrosion*, *3*(1), 11. https://doi.org/10.1007/s40735-016-0069-5

Romero-Fernández, M., & Paradisi, F. (2020). General Overview on Immobilization Techniques of Enzymes for Biocatalysis. In M. Benaglia & A. Puglisi (Eds.), *Catalyst Immobilization: Methods and Applications* (p. 494). Wiley-VCH.

Santos, J. C. S. dos, Barbosa, O., Ortiz, C., Berenguer-Murcia, A., Rodrigues, R. C., & Fernandez-Lafuente, R. (2015). Importance of the Support Properties for Immobilization or Purification of Enzymes. *ChemCatChem*, *7*(16), 2413–2432. https://doi.org/10.1002/cctc.201500310

Schultz, A. K., Haas, M. J., & Banavali, R. (2010). Catalysis in Biodiesel Processing. In G. Knothe, J. Krahl, & J. Van Gerpen (Eds.), *The Biodiesel Handbook* (2nd ed., p. 524). AOCS Press.

Schultz, E. L., de Souza, D. T., & Damaso, M. C. T. (2014). The glycerol biorefinery: a purpose for Brazilian biodiesel production. *Chemical and Biological Technologies in Agriculture*, *1*(1), 7. https://doi.org/10.1186/s40538-014-0007-z

Scofield, L. (2022, April 20). Txai Suruí: "Não estão queimando só a Amazônia, estão queimando as pessoas de lá também." *Agência Pública*, 1. https://apublica.org/2022/04/txai-surui-nao-estao-queimando-so-a-amazonia-estao-queimando-as-pessoas-de-la-tambem/

Sharma, N., Parhizkar, M., Cong, W., Mateti, S., Kirkland, M. A., Puri, M., & Sutti, A. (2017). Metal ion type significantly affects the morphology but not the activity of lipase–metal–phosphate nanoflowers. *RSC Advances*, *7*(41), 25437–25443. https://doi.org/10.1039/C7RA00302A

Sheldon, R. A., & van Pelt, S. (2013). Enzyme immobilisation in biocatalysis: why, what and how. *Chem. Soc. Rev.*, *42*(15), 6223–6235. https://doi.org/10.1039/C3CS60075K

Sherazi, H. S. T., Mahesar, S. A., & Sirajuddin. (2016). Vegetable Oil Deodorizer Distillate: A Rich Source of the Natural Bioactive Components. *Journal of Oleo Science*, *65*(12), 957–966. https://doi.org/10.5650/jos.ess16125

Simsek, S., & Ozdalyan, B. (2018). Improvements to the Composition of Fusel Oil and Analysis of the Effects of Fusel Oil–Gasoline Blends on a Spark-Ignited (SI) Engine's Performance and Emissions. *Energies*, *11*(3), 625. https://doi.org/10.3390/en11030625

Somturk, B., Hancer, M., Ocsoy, I., & Özdemir, N. (2015). Synthesis of copper ion incorporated horseradish peroxidase-based hybrid nanoflowers for enhanced catalytic activity and stability. *Dalton Trans.*, *44*(31), 13845–13852. https://doi.org/10.1039/C5DT01250C

Somturk, B., Yilmaz, I., Altinkaynak, C., Karatepe, A., Özdemir, N., & Ocsoy, I. (2016). Synthesis of urease hybrid nanoflowers and their enhanced catalytic properties. *Enzyme and Microbial Technology*, *86*, 134–142. https://doi.org/10.1016/j.enzmictec.2015.09.005

Soni, S., Dwivedee, B. P., & Banerjee, U. C. (2018). An Ultrafast Sonochemical Strategy to Synthesize Lipase-Manganese Phosphate Hybrid Nanoflowers with Promoted Biocatalytic Performance in the Kinetic Resolution of β-Aryloxyalcohols. *ChemNanoMat*, *4*(9), 1007–1020. https://doi.org/10.1002/cnma.201800250

Souza, L. T. de A., Veríssimo, L. A. A., João, B. C. P., Santoro, M. M., Resende, R. R., & Mendes, A. A. (2016). Imobilização Enzimática: Princípios Fundamentais e Tipos de Suporte. In R. R. Resende (Ed.), *Biotecnologia Aplicada à Agro&iIdústria: Fundamentos e Aplicações – Vol. 4* (p. 1070). Edgard Blücher LTDA.

Souza, M. S., Aguieiras, E. C. G., da Silva, M. A. P., & Langone, M. A. P. (2009). Biodiesel Synthesis via Esterification of Feedstock with High Content of Free Fatty Acids. *Applied Biochemistry and Biotechnology*, *154*(1–3), 74–88. https://doi.org/10.1007/s12010-008-8444-4

Talens-Perales, D., Fabra, M. J., Martínez-Argente, L., Marín-Navarro, J., & Polaina, J. (2020). Recyclable thermophilic hybrid protein-inorganic nanoflowers for the hydrolysis of milk lactose. *International Journal of Biological Macromolecules*, *151*, 602–608. https://doi.org/10.1016/j.ijbiomac.2020.02.115

Tsagaraki, E., Karachaliou, E., Delioglanis, I., & Kouzi, E. (2017). *Bio-based products and applications potential*. https://www.bioways.eu/download.php?f=150&l=en&key=441a4e6a27f83a8e828b802c37adc6e1

Türkay, S., & Şahin-Yeşilçubuk, N. (2017). Processing and Modification Technologies for Edible Oils and Fats. In C. C. Akoh (Ed.), *Food Lipids : Chemistry, Nutrition, and Biotechnology* (4th ed., p. 1048). CRC Press.

UOL. (2020, July 6). Marina culpa governo por fuga de investimentos: “estamos indo na contramão.” *UOL Economia*. https://economia.uol.com.br/noticias/redacao/2020/07/06/marina-culpa-governo-por-fuga-de-investimentos-estamos-indo-na-contramao.htm

Vieira, A. C., Cansian, A. B. M., Guimarães, J. R., Vieira, A. M. S., Fernandez-Lafuente, R., & Tardioli, P. W. (2021). Performance of Liquid Eversa on Fatty Acid Ethyl Esters Production by Simultaneous Esterification/Transesterification of Low-to-High Acidity Feedstocks. *Catalysts*, *11*(12), 1486. https://doi.org/10.3390/catal11121486

Visioli, L. J., de Castilhos, F., Cardozo-Filho, L., de Mello, B. T. F., & da Silva, C. (2016). Production of esters from soybean oil deodorizer distillate in pressurized ethanol. *Fuel Processing Technology*, *149*, 326–331. https://doi.org/10.1016/j.fuproc.2016.04.038

Vo, T. N., Tran, T. D., Nguyen, H. K., Kong, D. Y., Kim, M. Il, & Kim, I. T. (2020). In situ growth of hybrid nanoflowers on activated carbon fibers as electrodes for mediatorless enzymatic biofuel cells. *Materials Letters*, *281*, 128662. https://doi.org/10.1016/j.matlet.2020.128662

Wang, A., Chen, X., Yu, J., Li, N., Li, H., Yin, Y., Xie, T., & Wu, S. G. (2020). Green preparation of lipase@Ca3(PO4)2 hybrid nanoflowers using bone waste from food production for efficient synthesis of clindamycin palmitate. *Journal of Industrial and Engineering Chemistry*, *89*, 383–391. https://doi.org/10.1016/j.jiec.2020.06.007

Weiss, C., & Landfester, K. (2013). Enzymatic Catalysis at Interfaces—Heterophase Systems as Substrates for Enzymatic Action. *Catalysts*, *3*(2), 401–417. https://doi.org/10.3390/catal3020401

Wen, H., Zhang, L., Du, Y., Wang, Z., Jiang, Y., Bian, H., Cui, J., & Jia, S. (2020). Bimetal based inorganic-carbonic anhydrase hybrid hydrogel membrane for CO2 capture. *Journal of CO2 Utilization*, *39*, 101171. https://doi.org/10.1016/j.jcou.2020.101171

Xin, Y., Gao, Q., Gu, Y., Hao, M., Fan, G., & Zhang, L. (2020). Self-assembly of metal-cholesterol oxidase hybrid nanostructures and application in bioconversion of steroids derivatives. *Frontiers of Chemical Science and Engineering*. https://doi.org/10.1007/s11705-020-1989-7

Ye, N., Kou, X., Shen, J., Huang, S., Chen, G., & Ouyang, G. (2020). Metal-Organic Frameworks: A New Platform for Enzyme Immobilization. *ChemBioChem*, *21*(18), 2585–2590. https://doi.org/10.1002/cbic.202000095

Yin, X., Zhang, X., Wan, M., Duan, X., You, Q., Zhang, J., & Li, S. (2017). Intensification of biodiesel production using dual-frequency counter-current pulsed ultrasound. *Ultrasonics Sonochemistry*, *37*, 136–143. https://doi.org/10.1016/j.ultsonch.2016.12.036

Yin, Y., Xiao, Y., Lin, G., Xiao, Q., Lin, Z., & Cai, Z. (2015). An enzyme–inorganic hybrid nanoflower based immobilized enzyme reactor with enhanced enzymatic activity. *J. Mater. Chem. B*, *3*(11), 2295–2300. https://doi.org/10.1039/C4TB01697A

Zdarta, J., Meyer, A., Jesionowski, T., & Pinelo, M. (2018). A General Overview of Support Materials for Enzyme Immobilization: Characteristics, Properties, Practical Utility. *Catalysts*, *8*(2), 92. https://doi.org/10.3390/catal8020092

Zhang, B., Li, P., Zhang, H., Wang, H., Li, X., Tian, L., Ali, N., Ali, Z., & Zhang, Q. (2016). Preparation of lipase/Zn3(PO4)2 hybrid nanoflower and its catalytic performance as an immobilized enzyme. *Chemical Engineering Journal*, *291*, 287–297. https://doi.org/10.1016/j.cej.2016.01.104

Zhang, D.-C., Liu, J.-J., Jia, L.-Z., Wang, P., & Han, X. (2019). Speciation of VOCs in the cooking fumes from five edible oils and their corresponding health risk assessments. *Atmospheric Environment*, *211*, 6–17. https://doi.org/10.1016/j.atmosenv.2019.04.043

Zhang, Y., Sun, W., Elfeky, N. M., Wang, Y., Zhao, D., Zhou, H., Wang, J., & Bao, Y. (2020). Self-assembly of lipase hybrid nanoflowers with bifunctional Ca2+ for improved activity and stability. *Enzyme and Microbial Technology*, *132*, 109408. https://doi.org/10.1016/j.enzmictec.2019.109408

Zhang, Z., Zhang, Y., He, L., Yang, Y., Liu, S., Wang, M., Fang, S., & Fu, G. (2015). A feasible synthesis of Mn3(PO4)2@BSA nanoflowers and its application as the support nanomaterial for Pt catalyst. *Journal of Power Sources*, *284*, 170–177. https://doi.org/10.1016/j.jpowsour.2015.03.011

Zheng, J., Wei, W., Wang, S., Li, X., Zhang, Y., & Wang, Z. (2020). Immobilization of Lipozyme TL 100L for methyl esterification of soybean oil deodorizer distillate. *3 Biotech*, *10*(2), 51. https://doi.org/10.1007/s13205-019-2028-6

Zhong, L., Feng, Y., Wang, G., Wang, Z., Bilal, M., Lv, H., Jia, S., & Cui, J. (2020). Production and use of immobilized lipases in/on nanomaterials: A review from the waste to biodiesel production. *International Journal of Biological Macromolecules*, *152*, 207–222. https://doi.org/10.1016/j.ijbiomac.2020.02.258

Zhong, L., Jiao, X., Hu, H., Shen, X., Zhao, J., Feng, Y., Li, C., Du, Y., Cui, J., & Jia, S. (2021). Activated magnetic lipase-inorganic hybrid nanoflowers: A highly active and recyclable nanobiocatalyst for biodiesel production. *Renewable Energy*, *171*, 825–832. https://doi.org/10.1016/j.renene.2021.02.155

4 RESULTS AND DISCUSSION IN THE FORM OF ARTICLES

As described in the initial considerations (Section 1.1), the parts related to the methodologies, results, discussion, and conclusions are arranged in the form of structured articles in English, with titles, abstracts, introductions, and separate references.

Section 4.1 presents the results related to the use of soybean oil deodorizer distillate (SODD) in the synthesis of fatty acid isoamyl esters (FAIEs) catalyzed by Eversa Transform 2.0 (ETL 2.0) in its free form. Section 4.2 presents the results related to the immobilization of *Pseudomonas fluorescens* lipase (PFL) by the hybrid nanoflower (hNF) technique, and its application in the synthesis of FAIEs using SODD as a source of fatty acids.

Preliminary evaluations of the hNF technique were performed, in an attempt to reproduce the immobilizations reported in the literature, as well as to immobilize different enzymes using the method described by Ge et al. (2012). These results are provided in the form of an appendix (Appendix A) at the end of the text.

4.1 Structured article on the feasibility of using SODD as a source of fatty acids for the synthesis of FAIEs and application as base stock for biolubricant

This section provides the full reproduction of an article produced from the results obtained during the doctoral research. It was published in online format and with free access in the journal Molecules (MDPI Publishers), on 04/22/2022, under DOI number 10.3390/molecules27092692. Its total or partial reproduction is permitted by the journal. The text below has been formatted in the same style as the rest of this document.

Title: **Enzymatic Synthesis of Fatty Acid Isoamyl Monoesters from Soybean Oil Deodorizer Distillate: A Renewable and Ecofriendly Base Stock for Lubricant Industries**

4.1.1 Abstract

In this study, soybean oil deodorizer distillate (SODD), a mixture of free fatty acids and acylglycerides, and isoamyl alcohol were evaluated as substrates in the synthesis of fatty acid isoamyl monoesters catalyzed by Eversa (a liquid formulation of *Thermomyces lanuginosus* lipase). SODD and the products were characterized by the chemical and physical properties of lubricant base stocks. The optimal conditions to produce isoamyl fatty acid esters were determined by response surface methodology (RSM) using rotational central composite design (RCCD, 2^3 factorial + 6 axial points + 5 replications at the central point); they were 1 mol of fatty acids (based on the SODD saponifiable index) to 2.5 mol isoamyl alcohol, 45 °C, and 6 wt.% enzymes (enzyme mass/SODD mass). The effect of the water content of the reactional medium was also studied, with two conditions of molecular sieve ratio (molecular sieve mass/SODD mass) selected as 39 wt.% (almost anhydrous reaction medium) and 9 wt.%. Ester yields of around 50 wt.% and 70 wt.% were reached after 50 h reaction, respectively. The reaction products containing 43.7 wt.% and 55.2 wt.% FAIE exhibited viscosity indices of 175 and 163.8, pour points of −6 °C and −9 °C, flash points of 178 and 104 °C, and low oxidative stability, respectively. Their properties (mainly very high viscosity indices) make them suitable to be used as base stocks in lubricant formulation industries.

4.1.2 Introduction

Synthetic base stocks from bio-based sources produced by chemical modifications of natural oils are promising candidates to formulate environmentally friendly lubricants (Afifah et al., 2021; Cecilia et al., 2020; Erhan et al., 2008). Although vegetable oils have some good lubricant properties, their poor oxidative stability and cold temperature properties (e.g., high pour point) must be corrected (Cecilia et al., 2020; Erhan et al., 2008; Zainal et al., 2018). Several routes can be adopted to chemically (or enzymatically) modified natural oils, such as epoxidation, hydrogenation, estolide formation (branched esters formed by linking the carboxyl group of one fatty acid to a site of unsaturation of another fatty acid), and transesterification/esterification or to obtain straight or branched-chain monoesters, diesters, triesters, and polyol esters (Afifah et al., 2021; Angulo et al., 2018; Borugadda and Goud, 2016; Cecilia et al., 2020; Erhan et al., 2008; Prasannakumar et al., 2022; Reeves, Siddaiah and Menezes, 2017; Zainal et al., 2018). Organic esters can solve some of the oil limitations, (Cecilia et al., 2020; ExxonMobil, 2017; Zainal et al., 2018). According to American Petroleum Institute (API), the esters are utilized as standalone base stocks or as blend components (ExxonMobil, 2017).

Ester-based base stocks for lubricant formulations can be synthesized by transesterification of oils or fats or esterification of free fatty acids (FFAs), with monohydroxy or polyhydroxy alcohols, catalyzed by homogenous or heterogeneous inorganic catalysts or enzymes (Angulo et al., 2018; Bart et al., 2013a; Bolina et al., 2021; Borugadda and Goud, 2016; Cecilia et al., 2020; Devi et al., 2016). The high pour points, low viscosities, and oxidation stabilities make them useful in metalworking (Boyde and Randles, 2013). To be considered as biolubricant, the ester-based blend must be biodegradable (Salih, 2021) and present low human and environmental toxicity, besides obviously performing its desired function, such as decreasing friction and heat, protecting against corrosion and wear, or transmitting energy (Bart et al., 2013c; Cecilia et al., 2020; Zainal et al., 2018). Monoester-based biolubricants are frequently applied as hydraulic fluid or lubricant additives; on the other hand, polyolester-based biolubricants also have possibilities to be used in transport, food industries, and greases (BASF, 2016).

Currently, biolubricants are a small fraction (about 2%) of the global lubricant market Markets and Markets, 2020), but this small market share has a solid potential to grow (Luzuriaga, 2020; Markets and Markets, 2020; Tsagaraki et al., 2017).

Despite the environmental benefits of bio-based lubricants compared with mineral oils, the use of edible vegetable oils as raw material in the biolubricant manufacture is of

particular concern (Cecilia et al., 2020). For example, soybean, as well as its oil, is widely used in food and feed industries (Byerlee et al., 2017). Using soybean oil as raw material in energy industries to produce biodiesel could impact its availability and price, generating social problems (Avagyan and Singh, 2019). To circumvent this problem, fatty acid sources from non-food biomass, wastes, or low-value byproducts could be viable options (Bart et al., 2013d cap 4; Prasannakumar et al., 2022; Syahir et al., 2017; Tsagaraki et al., 2017).

Soybean oil deodorizer distillate (SODD) is a byproduct of the edible soybean oil refinement process, rich in FFA and acylglycerols (17 to 47 wt.% and 9 to ~70 wt.%, respectively) and with considerable amounts of tocopherols (1.8 to 20 wt.%), a natural antioxidant (Greyt, 2020; Gunawan et al., 2008; Sherazi and Mahesar, 2016; Vieira et al., 2021). Its use as raw material for biodiesel production has been widely reported in the scientific literature (Aguieiras, Souza and Langone, 2013; Du, Wang and Liu, 2007; Panpipat, Xu and Guo, 2012; Souza et al., 2009; Vieira et al., 2021; Visioli et al., 2016; Yin et al., 2015; Yin et al., 2016; Yin et al., 2017; Yun, Ling and Yunjun, 2010; Zheng et al., 2020), but its exploitation to produce ester base stocks for the lubricant market is scarce, and even less in terms of enzymatic routes (Fernandes et al., 2021). Lately, Fernandes et al. (2021) investigated the esterification of FFA obtained from acidulation of soapstock of the soybean fatty acid distillate with trimethylolpropane (TMP) and neopentyl glycol (NPG) to produce biolubricant base stocks catalyzed by *Candida rugosa* lipase (CRL)s (Fernandes et al., 2021).

Linear or non-linear monohydroxy alcohols (e.g., methanol and 2-ethylhexanol) are commonly used to produce monoester base stocks, depending on the tribological properties required for the desired application (BASF, 2016; Boyde and Randles, 2013). Fusel oil, a byproduct of the bioethanol distillation (Ferreira et al., 2013) could be a source of alcohols to be applied in perfume fixers, essences, or paints (Incauca S.A.S., n.d.), but in many instances, they usually are burned in the plant boiler or incorporated in the ethanol combustive. Fusel oil has low costs (Pérez, Cardoso and Franco, 2001) and a high content of isoamyl alcohol. This has been utilized in the synthesis of esters using palm kernel oil (constituted by high amounts of lauric acid) (Cerón et al., 2018) and oleic acid (Dörmő et al., 2004) as acyl donors with high conversions but low kinematic viscosities at 40 °C.

Despite being cheaper, chemical catalysts are less selective (producing many by-products) and need harsher reactional conditions than enzymatic catalysts Falkeborg,

Berton-Carabin and Cheong, 2016). Many vegetable oils and esters may be damaged under these conditions, (Raof et al., 2019; Reeves, Siddaiah and Menezes, 2017), making lipases a good alternative for this application. Lipases are non-toxic and environmentally friendly biocatalysts, capable of promoting both esterification and transesterification reactions between FFAs and oils or fats as acyl donors, respectively, and alcohols as acyl acceptors under mild conditions (Konwar and Sagar, 2018; Monteiro et al., 2021; Parkin, 2017; Paul and Fernández, 2016; Vieira et al., 2021; Zhong et al., 2020). Lipases usually have high organic solvent stability, wide substrate specificity, and high enantioselectivity, and do not need cofactors (Konwar and Sagar, 2018; Parkin, 2017; Silva and Freire, 2016). Among the commercially available lipase, Eversa Transform 2.0 (a liquid formulation of an industrial variant of the lipase from *Thermomyces lanuginosus*) has been launched as a biocatalyst suitable for the synthesis of biodiesel in its liquid form, although some authors have shown the possibility of improving this feature after immobilization (Martínez-Sanchez et al., 2020; Miranda et al., 2020; Monteiro et al., 2021; Remonatto et al., 2018; Vieira et al., 2021). This enzyme has shown reaction rates comparable to transesterification of glycerides and esterification of FFA with methanol to produce fatty acid methyl ester (FAME) (Mibielli et al., 2019; Remonatto et al., 2016). Eversa Transform 2.0 (ETL 2.0) is more thermostable and has higher specific activity than their previous version (Mibielli et al., 2019; Remonatto et al., 2016; Novozymes A/S, n.d.), and is also more stable than the original lipase from *Thermomyces lanuginosus* (TLL) (Arana-Peña et al., 2018). Despite its several advantages in the use of immobilized lipases (Rodrigues et al., 2013; Rodrigues et al. 2021), in the case of simultaneous esterification/transesterification of free-fatty-acid-rich feedstocks, the water generated throughout the esterification reaction and accumulated within the biocatalyst particles could be a drawback (Marty, Dossat and Condoret, 1997). Although there are alternatives to circumvent this problem, such as the use of ultrasound (Alves et al., 2014; Martins et al., 2013; Paludo et al., 2015) and highly hydrophobic supports (Lima et al., 2015; Martins et al., 2013; Poppe et al., 2013; Séverac et al., 2011; Vescovi et al., 2016; Vescovi et al., 2017), the use of lipase in its free form is an appealing alternative because the water problem in the bulk can be easily circumvented using molecular sieves (Colombié et al., 1998; Vieira et al., 2021; Wang et al., 2006). Liquid Eversa formulations are highly active (low concentrations of different Eversa versions were required to achieve more than 95% of FAME yield in 16 h reaction under mild temperatures (Adewale et al., 2017; Mibielli

et al., 2019; Remonatto et al., 2016), operationally stable, and cheaper than other commercial lipases (Mibielli et al., 2019; Remonatto et al., 2016; Novozymes A/S, n.d.).

In this context, this study aimed to evaluate the production of fatty acid isoamyl esters (FAIE) from crude SODD, catalyzed by liquid Eversa formulation. Considering the higher value of biolubricant compared with biodiesel, if the use of Eversa is feasible in biodiesel production, we can expect that it can be in biolubricant base stock production. A design of experiments was performed to select some independent variables (temperature, acyl donor (as saponifiable matter)/alcohol molar ratio, and percentage of enzyme mass regarding the mass of crude SODD) capable of enhancing the FAIE through esterification/transesterification of SODD with isoamyl alcohol. The control of water concentration in the initial reaction medium and throughout the reaction was also investigated. A small amount of water in the reaction medium is required to maintain the enzyme 3D structure, thus preserving its active site polarity and protein stability adequate to the catalysis. However, a large amount of water can negatively affect the esterification equilibrium toward the hydrolysis reaction of the newly formed ester (Yahya, Anderson and Moo-Young, 1998). For ETL-2.0, in particular, Novozymes (Novozymes A/S, n.d.) recommends a reactional medium with 2% water for the best performance of enzyme in the synthesis of biodiesel using methanol as an acyl acceptor. The use of a molecular sieve (MS) in the reaction medium permits the capture of the excess water formed during the esterification reaction, increasing the esterification yield (Nott et al., 2012; Omar, Nishio and Nagai, 1988; Paludo et al., 2015). Finally, the products (isoamyl esters) obtained under the optimal conditions were characterized determining some of their physicochemical properties (viscosities at 40 °C and 100 °C, viscosity indices, pour points, flash points, oxidative stability, and copper corrosiveness).

4.1.3 Materials and Methods

4.1.3.1 Materials

Eversa Transform 2.0 (ETL 2.0, 1.2 g/mL density, 25 mg/mL protein, and 5425 Tributyrin Unit (TBU)/mg specific activity) and methyl heptadecanoate were purchased from Sigma-Aldrich (St. Louis, MO, USA), molecular sieve (MS) rods (1/16 in, 3 Å pore size, and water capacity of 0.20–0.23 g of water per gram of MS) were supplied by Fluka (Charlotte, NC, USA), isoamyl alcohol was from Êxodo Científica (Sumaré, SP, Brazil), and soybean oil deodorizer distillate (SODD) was kindly donated by COCAMAR

(Maringá, PR, Brazil). All other chemicals and solvents were of analytical or HPLC grade, and they were used as received.

4.1.3.2 Rotational Central Composite Design (RCCD)

The assays were carried out in sealed bottles with MS rods to provide a reaction medium near anhydrous conditions (32.7–56.7 wt.%, depending on the initial water content). The bottles were incubated in a shaker incubator (Marconi, MA832/H) at a 250 rpm stirring speed for 12 h. In the end, the reaction media were washed with boiling distilled water in a volume ratio of 1:1 (water:SODD), centrifuged at 10,400 rcf (9645 rpm) for 10 min at 25 °C, and the polar phase was discarded (this washing procedure was repeated 3 times). The samples were dried on a lab stove at 50-60 °C for approximately 24 h, and the reaction mass yields were calculated from the FID–GC results.

The independent variables SODD saponifiable ($SODD_{Sap}$)/isoamyl alcohol molar ratio ($R_{isoamyl}$, 1:0.318 to 1:3.682), reaction temperature (T, 19.8 to 70.2 °C), and enzyme mass in the reactor per SODD mass (m_{enz}, 1 to 13.1%) were chosen to carry out the RCCD (2^3 factorial with 6 axial points and with 5 repetitions at the central point) totaling 19 trials (Table 4.1-1) to evaluate the effects of these variables on the FAIE yields. Data were analyzed by Statistic Software, and a third-order model was obtained and evaluated statistically by analysis of variance (ANOVA).

Table 4.1-1. Values of independent variables used in the RCCD for enzymatic synthesis of fatty acid isoamyl esters for 12 h reaction.

Factors	−1.68	−1	0	+1	+1.68
$SODD_{Sap}$:isoamyl alcohol molar ratio ($R_{isoamyl}$) (x_1)	1:0.318	1:1	1:2	1:3	1:3.682
Temperature (°C) (T) (x_2)	19.8	30	45	60	70.2
Enzyme mass/SODD mass, wt.% (m_{enz}) (x_3)	0	1	5.5	10	13.1

After model validation and using the reaction conditions that yielded the highest ester yield, the water initial content of the reaction medium ranged from 1 wt.% to 6 wt.% (based on the MS capability to adsorb 0.20 g of water per gram of MS), adding the MS to adjust the initial water content in the reaction medium or adding water (without MS). The reactions were performed in sealed bottles (with plugs and caps) incubated in a shaker incubator (Marconi, MA832/H) at 250 rpm stirring speed for 12 h. In the end, the reaction

media were treated as described above to quantify the FAIE yields by gas chromatography.

4.1.3.3 Reaction Courses

The reaction courses were studied under the operational conditions previously selected (Section 4.1.3.2). The reaction was conducted in a jacketed reactor (80 × 35 mm, H × Di) with mechanical stirring with a straight paddle impeller (25 × 7 mm, L × H). Samples were withdrawn at regular time spans, washed with boiling distilled water, and dried, as described in Section 4.1.3.2, before being analyzed by gas chromatography (Section 4.1.3.4).

4.1.3.4 Chromatographic Analysis

4.1.3.4.1 Ester Analysis

FAIE were quantified by gas chromatography according to EN 14103 standard (Duvekot, 2011), with modifications. A mass of 50 mg of dry reaction sample was weighted in a vial and solubilized in 1.0 mL of a methyl heptadecanoate solution (1.0 mg/mL in heptane) as the internal standard. The analyses were carried out in a 7890-A Agilent chromatograph (Agilent Technologies, Santa Clara, CA, USA) using an Rtx-Wax capillary column (30 m × 0.25 mm × 0.25 μm, Restek Co., Bellefonte, PA, USA), injector temperature of 250 °C, and helium as carrier gas (19.91 psi, flow rate of 54 mL/min and split rate of 50:1). A volume of 1 μL of the sample was injected into the device, with the oven and FID detector set at 210 °C and 250 °C, respectively, and hydrogen, synthetic air, and nitrogen flow rates of 30, 400, and 25 mL/min, respectively.

The reaction yield (Y, in wt.%) for each sample was calculated by Equation (1),

$$Y\ [wt.\%] = 100 \cdot \frac{\sum A_i}{A_{standard}} \cdot \frac{C_{standard} \cdot V_{standard}}{m_{sample}} \quad (1)$$

where A_i is the sum of chromatography areas of the chromatogram peaks at the retention time of isoamyl esters, $A_{standard}$ is the area of methyl heptadecanoate peak, $C_{standard}$ is the mass concentration of methyl heptadecanoate solution in heptane, $V_{standard}$ is the volume of methyl heptadecanoate solution (1 mL, in heptane), and m_{sample} is the mass of reaction sample (~50 mg).

4.1.3.4.2 Analysis of Acylglycerides and Glycerin

Total monoglycerides, diglycerides, triglycerides, and glycerin were quantified by gas chromatography according to the ASTM D6584 standard (McCurry and Wang, 2007), with modifications. The analyses were carried out in a 7890-A Agilent chromatograph (Agilent Technologies, Santa Clara, CA, USA)) using a Select Biodiesel column (glycerides, UM + 2 m RG, 15 m × 0.32 mm × 0.1 μm, Agilent Technologies, Santa Clara, CA, USA), injector with a pressure of 7.52 psi, and 3 mL/min helium (carrier gas) flow rate. A volume of 1 μL of the sample was injected into the column, and the analysis was run under the following oven temperature ramp, with an initial temperature at 50 °C, followed by heating rates of 15, 7, and 30 °C/min to reach 180, 230 and 380 °C, respectively; the FID detector was set at 300 °C with hydrogen, synthetic air, and nitrogen flow rates of 30, 400 and 25 mL/min, respectively.

4.1.3.5 Chemical and Physicochemical Characterizations of the Reaction Products

Water content was quantified according to the Karl Fisher method (American Oil Chemists' Society, 2004a Ca 2e-84), and acid value and saponification value were determined according to AOCS Cd 3d-63 (American Oil Chemists' Society, 2004b Cd 3d-63) and Cd 3-25 (American Oil Chemists' Society, 2004c Cd 3-25) standards, respectively. Viscosities at 40 and 100 °C, viscosity index (VI), density, corrosiveness to copper, pour point, flash point, and oxidation stability (by rotatory pressured vessel oxidation test-RPVOT) were determined by ASTM standards D445, D2270, D1298, D130, D97, D93, and D2272, respectively, at the laboratories Lubrin Tribological Analyses (São Paulo, SP, Brazil) and SENAI (São Paulo, SP Brazil). Samples were washed three times with boiling point water, and the organic phase was dried in an oven at 60 °C until constant weight.

4.1.4 Results

4.1.4.1 Physicochemical Characterization of Soybean Oil Deodorizer Distillate (SODD)

The saponifiable composition and physicochemical proprieties of crude SODD are shown in Table 4.1-2. The crude SODD is saponifiable-rich biomass (>90 wt.%) composed mainly of triglycerides (~70 wt.%) and free fatty acids (18.5 wt.%).

In general, a good lubricant base stock should have high viscosity index, high flash point, low pour point, good corrosivity resistance, and high oxidation stability (Zainal et

al., 2018). The crude SODD exhibited physicochemical properties suitable to be used as (bio)lubricant base stock, such as a very high viscosity index, ~192 (the higher the viscosity index, the smaller the changes in viscosity over a broader temperature range) and high flash point, at 210 °C (desirable to warrant secure operation at high temperatures) (Cecilia et al., 2020; Reeves, Siddaiah and Menezes, 2017), as well as being non-corrosive to copper (Table 4.1-2). Although the crude SODD already has interesting properties as lubricant bases, its free acidity (~18 wt.%) and pour point (−3 °C) are high, and its oxidative stability is low, but the esterification/transesterification of their saponifiable matter could improve these parameters and increase the range of applications in lubricant formulation industry.

Table 4.1-2. Saponifiable composition and physicochemical properties of soybean oil deodorizer distillate (SODD) from Cocamar (Maringá, PR, Brazil), collected in June 2019.

Parameter	Value
Saponification value (mg $_{KOH}$/g)	186.75 ± 4.25
Saponification value (wt.%)	93.84 ± 2.13
Acid value (mg $_{KOH}$/g)	36.85 ± 0.07
Acid value (wt.%)	18.52 ± 0.03
Moisture (wt.%)	0.18
Relative density	0.921
Viscosity at 40 °C (mm^2/s)	33.5
Viscosity at 100 °C (mm^2/s)	7.3
Viscosity index	191.6
Pour point (°C)	−3.0
Flash point (°C)	210
Oxidation stability (min)	43
Corrosiveness to copper	1A [(a)]
Free glycerol (wt.%)	0.003
Monoglycerides (wt.%)	1.38
Diglycerides (wt.%)	4.39
Triglycerides (wt.%)	69.5

[(a)] The rating of 1A is given for appearance of freshly polished copper coupons with slight discoloration but barely noticeable.

4.1.4.2 Rotational Central Composite Design (RCCD) and Analysis by Response Surface Methodology (RSM)

From the results shown in Table 4.1-3, the regression coefficients of a third-order model of the type $y = a_0 + b_i x_j + c_i x_j x_k + d_i {x_j}^2 + e_i {x_j}^3$ were calculated, and a mathematical model using Equation (1) was built for the response FAIE yield only using significant terms (p-value < 0.05). ANOVA was used to evaluate the accuracy of the fitted

model (Table 4.1-4). The FAIE yields (Table 4.1-3) varied from 1.22 wt.% to 48.62 wt.%, and the R^2 and calculated F-value (Table 4.1-4) were suitable to obtain a third-order model using Equation (2), allowing the evaluation of the FAIE yield as a function of $R_{isoamyl}$ (x_1) and m_{enz} (x_3), within the range studied. The third-order model was chosen based on the literature recommendation when a second-order model is not capable of accurately describing the experimental results (Box, Hunter and Hunter, 2005).

The mathematical model was built using the coded variables with statistically significant parameters (at a 5% significance level; the temperature was not statistically significant in the evaluated range), according to the measured values for the response, defined by Equation (2).

$$Y[wt.\%] = 41.21 + 3.46x_1 + 6.74x_1x_3 - 4.21x_1^2 - 16.12x_3^2 + 10.30x_3^3 \quad (2)$$

where x_1 and x_3 are the independent variables coded for $R_{isoamyl}$ and m_{enz}, respectively.

Table 4.1-3. RCCD matrix for esterification/transesterification of SODD with isoamyl alcohol catalyzed by Eversa Transform 2.0 in almost anhydrous media (incubated in shaker at 250 rpm stirring for 12 h reaction) with experimental results for fatty acid isoamyl ester yield (Y).

Run	$SODD_{Sap}$: Isoamyl Alcohol Molar Ratio ($R_{isoamyl}$, x_1)	Temperature (°C) (T, x_2)	Enzyme Mass (wt.%) (m_{enz}, x_3)	Reaction Yield (wt.%) (Y)
1	1:1 (−1)	30.0 (−1)	1.0 (−1)	14.63
2	1:1 (−1)	30.0 (−1)	10.0 (+1)	20.00
3	1:1 (−1)	60.0 (+1)	1.0 (−1)	8.71
4	1:1 (−1)	60.0 (+1)	10.0 (+1)	14.81
5	1:3 (+1)	30.0 (−1)	1.0 (−1)	11.79
6	1:3 (+1)	30.0 (−1)	10.0 (+1)	33.76
7	1:3 (+1)	60.0 (+1)	1.0 (−1)	4.56
8	1:3 (+1)	60.0 (+1)	10.0 (+1)	47.96
9	1:2 (0)	45.0 (0)	5.5 (0)	39.79
10	1:2 (0)	45.0 (0)	5.5 (0)	41.45
11	1:2 (0)	45.0 (0)	5.5 (0)	43.29
12	1:2 (0)	45.0 (0)	5.5 (0)	42.83
13	1:2 (0)	45.0 (0)	5.5 (0)	48.62
14	1:0.318 (−1.68)	45.0 (0)	5.5 (0)	29.09
15	1:2 (0)	19.8 (−1.68)	5.5 (0)	38.74
16	1:2 (0)	45.0 (0)	0 (−1.22)	1.22
17	1:3.682 (+1.68)	4)5.0 (0)	5.5 (0)	33.33
18	1:2 (0)	70.2 (+1.68)	5.5 (0)	35.57
19	1:2 (0)	45.0 (0)	13.1 (+1.68)	46.92

Table 4.1-4. Analysis of variance (ANOVA) for the experimental design of the esterification/transesterification of SODD with isoamyl alcohol catalyzed by Eversa Transform 2.0.

Source of Variation	SS [a]	DF [b]	MS [c]	$F_{calculated}$	$F_{tabulated}$
Regression	4129.56	5	825.91	31.09	3.02
Residue	345.37	13	26.57		
Lack of fit	86.04	3	28.68	1.11	3.71
Pure error	259.32	10	25.93		
Total	4474.92	18	248.61		

[a] Sum of squares; [b] Degree of freedom; [c] Mean squares. R^2 = 92.28% at 5% significance level.

Equation (2) was used to generate the response surface for the FAIE yield (Figure 4.1-1), which showed a fast growth of Y between the range of 0 wt.% and 6 wt.% of m_{enz}. From 6 wt.% of m_{enz} upward, the Y growth was less pronounced. Aiming to combine ester productivity and enzyme consumption, it was established that the first turning point observed in the response surface would be the best operating condition for $R_{isoamyl}$ and m_{enz}, i.e., 1:2.5 wt.% and 6.0 wt.%, respectively. The reaction temperature was set at 45 °C, the level zero condition for this variable of the experimental design, for the further assays, due to this value being reported as a secure operational temperature for ETL 2.0 (Mibielli et al., 2019; Novozymes A/S, n.d.).

To validate the model, an experimental assay (in triplicate) was carried out under the designed optimal conditions ($R_{isoamyl}$ of 1:2.5, m_{enz} of 6.0 wt.%, 45 °C, and stirring at 250 rpm in a shaker incubator) gave a reaction yield of 35.0 ± 2.5 wt.%, while the model Equation (2) predicted a reaction yield of 41.9 ± 6.8 wt.% (a relative error between experimental and predicted value less than 20%). This result shows that the model could satisfactorily predict the real behavior of this complex reaction system.

Figure 4.1-1. Response surface showing the effects of independent variables on the yield of fatty acid isoamyl ester constructed from model Equation (2).

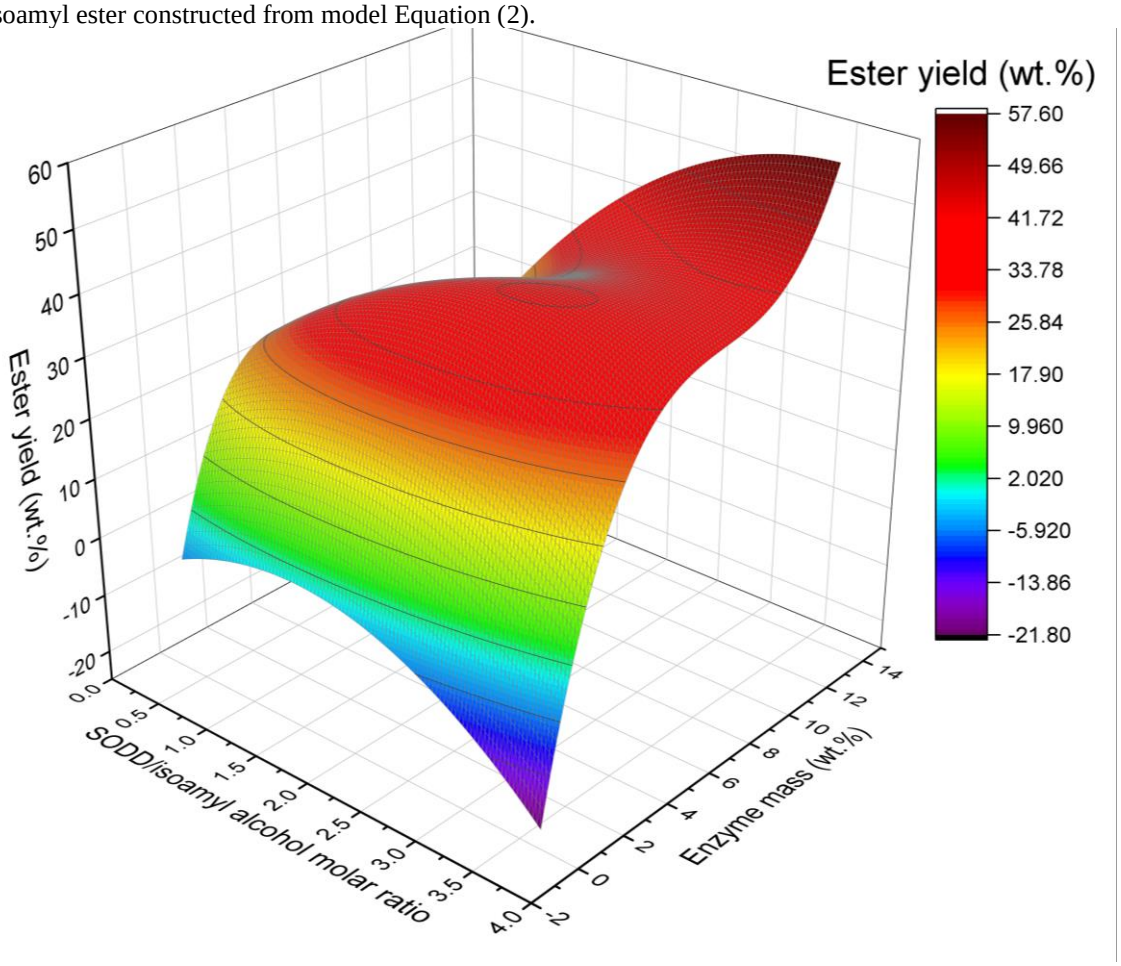

As previously discussed in the introduction section, the content of water in the reaction medium is an important parameter to be controlled aiming to retain the enzyme activity and prevent the hydrolysis of the formed ester. Based on the adsorption capacity of MS informed by the manufacturer (0.20 g of water per gram of MS), the addition of 4 wt.% and 9 wt.% of MS in the reaction medium was enough to reach around 2 wt.% and 1 wt.% water at the beginning of the reaction, respectively. The addition of 39 wt.% MS should be enough to guarantee an almost anhydrous medium throughout the reaction. Therefore, the presence of 4, 9, and 39 wt.% MS (MS mass/SODD mass), and the addition of additional water to the reaction medium (without MS), ranging from 2.8 wt.% (percentage of water already contained in the reagents and enzyme) to 6 wt.%, were evaluated to determine the influence of water on the reaction yield. Figure 4.1-2 shows the reaction yields (Y) with (Figure 4.1-2a) and without (Figure 4.1-2b) MS.

Figure 4.1-2. Reaction yields (Y, wt.%) of esterification/transesterification of SODD with isoamyl alcohol (molar ratio of 1:2.5, 6.0 wt.% of ETL 2.0, 45 °C, and stirring at 250 rpm in a shaker incubator for 12 h) as a function of water content in the reaction medium: (a) without added water and using molecular sieve (MS); (b) without MS and adding water at the beginning of the reaction. [a] Almost anhydrous condition throughout the reaction. [b] Only water content already contained in the reagents and enzyme (without molecular sieve or addition of water).

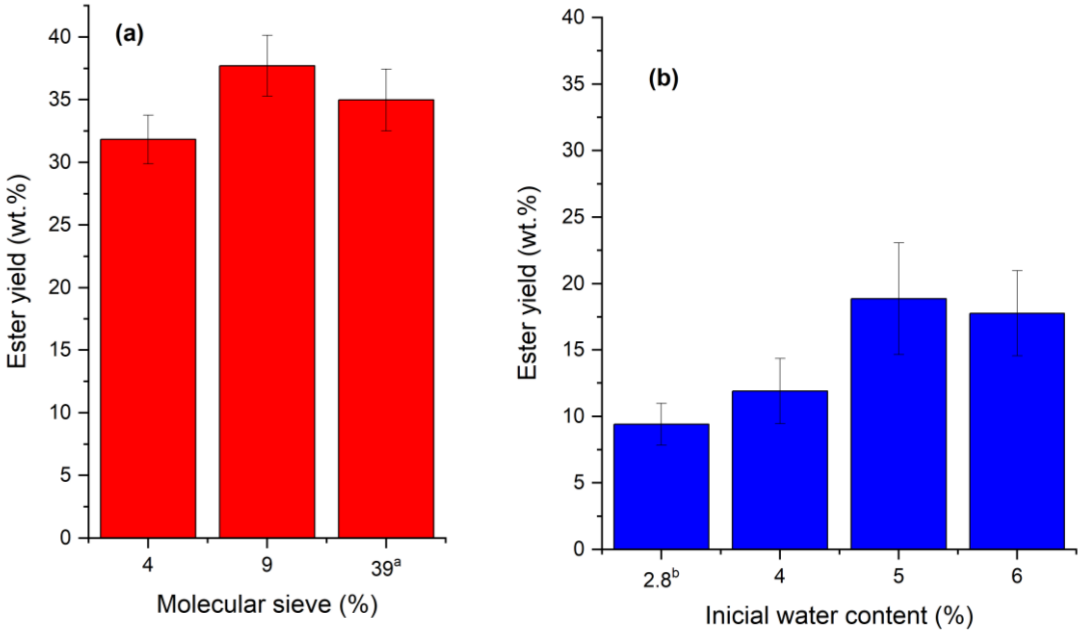

The ester synthesis had better performance in a water-controlled medium (Figure 4.1-2a), resulting in an ester yield almost twofold higher than that in a medium where the water content was only adjusted at the beginning of the reaction (Figure 4.1-2b). The water control during the reaction could favor the displacement of the equilibrium of the reaction towards the product while maintaining a water amount necessary to the enzyme catalysis (Marty, Dossat and Condoret, 1997). Differently, Remonatto et al. (Remonatto et al., 2016) reported better performance of Eversa in the esterification/transesterification of oleic acid/soybean oil (mass ratio of 1:1) with methanol (97% conversion after 16 h reaction) with 2.5% added water. In this case, the addition of water was necessary because methanol can drastically inactivate the enzyme due to the removal of the enzyme water layer required for the catalysis (Cavalcante et al., 2021; Lv et al., 2021).

4.1.4.3 Reaction Course under Optimal Conditions

Under optimal reaction conditions ($SODD_{Sap}$:isoamyl alcohol molar ratio of 1:2.5, 45 °C and 6.0 wt.% ETL 2.0 (enzyme mass/SODD mass), the esterification/transesterification reaction of SODD with isoamyl alcohol was carried out for two distinct MS conditions—9 wt.% and 39 wt.%—monitoring the reaction yield (Y)

with the time reaction. Figure 4.1-3 shows a better global evolution of the reaction using 9 wt.% MS, reaching almost 70 wt.% yield (ester mass/product mass) after 50.5 h reaction, but when using 39 wt.% MS, the reaction stopped after 12 h reaction, at around 50 wt.% yield. Although the lack of water using 39 wt.% MS favored the reaction for the first 12 h, this result suggests that, at this time span, the lack of water probably inactivated the enzyme. Moreover, it should be considered that this is a solvent-free reaction. This means that the composition of the medium is changing along the process, initially, the medium properties are defined by those of the substrate mixture, while at the end, the medium features are influenced by the isoamyl ester (Sousa et al., 2021). These dynamic changes may affect the role of water activity in the performance of the enzyme. Therefore, a small amount of water resulting from the use of 9 wt.% MS could be essential to preserve catalyst activity when there is a high ester concentration in the medium and, consequently, keeping going on the reaction (Adlercreutz, 2013; Han, Walde and Luisi 1990), even though it may not be so relevant in the initial steps.

Figure 4.1-3. Profiles of ester mass yield vs. reaction time for esterification/transesterification of SODD with isoamyl alcohol in presence of two MS concentration (9 wt% (●) and 39 wt% (■)). Reaction conditions: $SODD_{Sap}$/isoamyl alcohol molar ratio of 1:2.5, 6.0 wt.% Eversa Transform 2.0 (enzyme mass/SODD mass) and 45 °C.

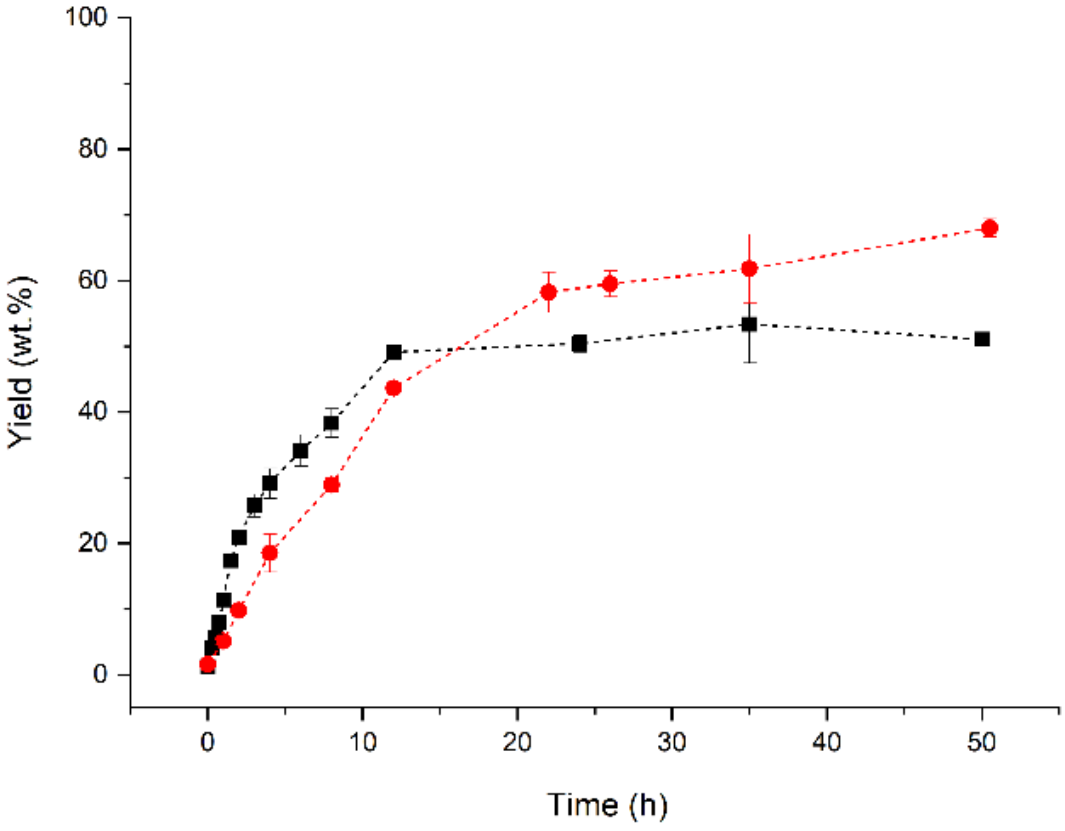

4.1.4.4 Chemical Composition and Some Physicochemical Properties of the Products

SODD and reaction products with 12 and 22 h reaction times (product 1 containing 43.7 wt.% FAIE and product 2 containing 55.3 wt.% FAIE, respectively) were characterized regarding their physicochemical properties and chemical compositions (Table 4.1-5).

As shown in Table 4.1-2 and discussed in Section 4.1.4.1, crude SODD has some interesting properties to be used as lubricant base stocks (results are listed again in Table 4.1-5 only for comparison purposes). Probably, due to the high triglyceride amount (more than 70 wt.%), SODD exhibited some physicochemical properties similar to those of refined soybean oil (Syahir et al., 2017). However, some properties shown in Table 4.1-2 were improved after the transesterification/esterification reaction. In general, Table 4.1-5 shows that the higher the content of isoamyl esters in the reaction products, the smaller the viscosities at 40 °C and 100 °C, the viscosity index, relative density, and the pour and flash points, but the higher the oxidative stability. In general, based on the physicochemical properties (viscosities at 40 and 100 °C, viscosity index, and flash point), both synthesized lubricant base stocks could serve to formulate hydraulic fluids (BASF, 2016; ExxonMobil, 2017; Petro-Canada, 2017; Shell, 2019).

A high viscosity index is an essential characteristic of a good lubricant base stock since it is an indication that the lubricant can be used over a wide range of temperatures by maintaining the thickness of the oil film (Zainal et al., 2018). SODD and products 1 and 2 had viscosity index similar to those of commercial synthetic lubricant base stocks according to the BASF Esters–Base Stocks Selection Guide for Lubricants and Metalworking Fluids (BASF, 2016). A high viscosity index (>160) could be associated with the polyunsaturated fatty acids chains of the soybean oil because it is reported that branched biolubricant (in the alcohol or in the carboxylic acid) favors a lower viscosity index (Cecilia et al., 2020).

The flash point is greatly impacted by the ester amount in the product but is high enough to ensure safe operations at moderate temperatures. The flash point of product 2 was lower than that of product 1, which could be related to the remaining amount of isoamyl alcohol (~1 wt.%, determined by gas chromatography) after drying. On the other hand, the pour point decreased until 6 °C, with the increase of the concentration (in wt.%) of isoamyl esters in the products, probably because the branched groups of isoamyl alcohol did hamper the acyl chains to come close for easy stacking because of steric interactions, thus inhibiting crystallization, resulting in a lower pour point (Erhan et al.,

2008). However, all products had poor pour points to work at low temperatures (Zainal et al., 2018), as cloudy conditions, precipitates, and solidification could not be avoided upon long-term exposure to cold temperatures, resulting in poor flow and pumpability (Zainal et al., 2018). Meanwhile, this problem, as well as some others, can be easily solved in the lubricant formulation by adding certain additives (e.g., pour point depressants, antioxidants, and viscosity modifiers) and diluents (e.g., 2-ethylhexyl oleate, isobutyl oleate, dibutyl adipate, di-isodecyl adipate, high oleic vegetable oils) or functional fluids in order to fulfill the requirements of a specific application (Cecilia et al., 2020; Erhan et al., 2008; Reeves, Siddaiah and Menezes, 2017; Zainal et al., 2018). For example, the addition of a 1% pour point depressant (e.g., Lubrizol TM 7670 made from sunflower and mineral oils) reduced the pour point of soybean-oil-based lubricant from −9 °C to −45 °C (Zainal et al., 2018).

Table 4.1-5. Physicochemical properties and chemical composition of the SODD and the esterification/transesterification reaction products containing different content of fatty acid isoamyl esters (FAIE).

Parameters	SODD	Product 1 [a]	Product 2 [b]	Unity	Standard
FAIE content	0	43.7	55.3	wt.%	
Viscosity at 40 °C	33.5	20.5	13.5	cSt	ASTM D445
Viscosity at 100 °C	7.3	4.9	3.6	cSt	ASTM D445
Viscosity index	191.6	175.0	163.8	-	ASTM 2270
Relative density	0.921	0.911	0.899	-	ASTM D1298
Pour point	−3.0	−6.0	−9.0	°C	ASTM D97
Flash point	210	178	104	°C	ASTM D93
Oxidative stability	43	37	53	min	ASTM D2272
Corrosiveness to copper [c]	1A	-	1B	-	ASTM D130
Saponification value	186.75 ± 4.25	153.3 ± 11.4	152.2 ± 0.46	mg_{KOH}/g	AOCS Cd 3-25
Acid values	36.85 ± 0.07	9.78 ± 0.04	15.45 ± 0.08	mg_{KOH}/g	AOCS Cd 3d-63
Free glycerol	0.003	0.25	0.50	wt.%	ASTM D6584
Monoglycerides	1.38	4.36	7.96	wt.%	ASTM D6584
Diglycerides	4.39	9.04	8.38	wt.%	ASTM D6584
Triglycerides	69.5	3.05	1.40	wt.%	ASTM D6584

[a] Product 1 was synthesized in presence of 39 wt.% molecular sieves for 12 h reaction, and [b] Product 2 was synthesized in presence of 9 wt.% molecular sieves for 22 h reaction, both using 1:2.5 (mol:mol) SODD: isoamyl alcohol, 6.0 wt.% (m_{enzyme}/m_{SODD}) Eversa Transform 2.0 and 45 °C; [c] The rating of 1A is given for appearance of freshly polished copper coupons with slight discoloration but barely noticeable; 1B indicates slight tarnish, and the ratings proceed further down the scale as corrosion staining of the test coupon increases, with 4C being the worst, typically appearing as severely corroded, blackened, and pitted coupon.

The oxidative stability was not expected to improve greatly because the unsaturated nature of fatty acids in soybean oil makes them prone to rapid oxidation (mainly linolenic and linoleic acids) (Perez, Rudnick and Erhan, 2013; Zainal et al., 2018) and, in turn, the SODD and their isoamyl esters. The oxidative stability of product 2 increased by 10 min, compared with SODD, most likely due to the elimination of the β-CH group of the acylglycerol structure, highly susceptible to thermal instability (Zainal et al., 2018). As discussed above, this parameter can be improved by adding antioxidants in the lubricant formulation depending on the desired application. The presence of tocopherols, a natural antioxidant, is reported to improve the oxidative stability of unrefined vegetable oils, compared with refined ones (Bart et al., 2013b; Sathwik Chatra, Jayadas and Kailas, 2012). In fact, naturally occurring antioxidants such as tocopherol, L-ascorbic acid, esters of gallic acid, citric acid derivatives, or EDTA derivatives have been reported to serve as synthetic metal scavengers and provide viable alternatives to the currently used toxic antioxidants (Reeves, Siddaiah and Menezes, 2017). However, the low content of tocopherols in the SODD (Vieira et al., 2021), and thus in the reaction products, was not enough and/or inefficient to reach high oxidative stability at harsh assay conditions (measured by RPVOT method in a sealed cell pressurized with oxygen and submitted to a temperature of 150 °C). Thus, the improvement of this parameter requires the use of suitable antioxidants or even a chemical modification of acyl moieties double bonds of the isoamyl esters, depending on the desired applications (Reeves, Siddaiah and Menezes, 2017).

The acid value of crude SODD was greatly reduced with the reaction, but when using only 9 wt.% MS, this decrease was not enough. The presence of some water could permit the glycerides hydrolysis, probably impacting the product viscosity. On the other hand, the presence of water avoided lipase inactivation, allowing a reaction yield to be reached that is higher than that achieved using 39 wt.% molecular sieves. However, FFAs and monoglycerides (higher in product 2 than product 1), such as glycerol monooleate, are known as friction modifiers, with high tribological appeal (Kenbeck and Bunemann, 2017; Luther, 2014).

Synthetic esters-based lubricants still display several limitations to compete with mineral lubricants, since chemical modification raises the price of the lubricant, slightly increases the volatility and toxicity, and diminishes the friction tolerance, and the esters do not work well with mineral oils in comparison to unmodified vegetable oils (Thangaraj et al., 2019). Resources regarding the improvement of some properties must continue,

mainly regarding the improvement of oxidative stability and pour point. Besides the use of additives mentioned above, modification of unsaturated acyl chains by chemical processes (epoxidation followed by ring opening) is a promising alternative to improve oxidative stability (Borugadda and Goud, 2016; Cecilia et al., 2020; Prasannakumar et al., 2022; Zainal et al., 2018). On the other hand, the goals for environmental protection are essential to change this scenario. Beyond that, vegetable oil products are ideally suited for applications such as lubrication of sawmill blades or chain drives, whereby the lubricant is used on a single-use basis (Zainal et al., 2018). However, to reach a final decision, a complete tribological study (study of friction, lubrication, and wear) must be carried out.

4.1.5 Conclusion

The soybean oil distillate deodorizer (SODD) showed to be a promising source of acyl donor to produce isoamyl esters via enzymatic catalysis. The partial conversion of the fatty acids (in form of free fatty acids or glycerides) from the SODD produced base stocks with some interesting lubricant properties, mainly high viscosity index (>160). The synthesized lubricant base stocks have suitable properties to be used as hydraulic fluid or as biolubricant additive. Nevertheless, for use in other specific applications, its physicochemical properties must be adjusted.

4.1.6 Funding

This work was funded by São Paulo Research Foundation (FAPESP, grant 2016/10636-8), Conselho Nacional de Desenvolvimento Científico e Tecnológico (CNPq, grant 308212/2017-7), and in part by the Coordenação de Aperfeiçoamento de Pessoal de Nível Superior – Brasil (CAPES) – Finance Code 001.

4.1.7 Acknowledgments

The authors thank COCAMAR (Maringá, PR, Brazil) for supplying the soybean oil deodorizer distillate (SODD).

4.1.8 References

Adewale, P., Vithanage, L. N., & Christopher, L. (2017). Optimization of enzyme-catalyzed biodiesel production from crude tall oil using Taguchi method. *Energy*

Conversion and Management, *154*, 81–91. https://doi.org/10.1016/j.enconman.2017.10.045

Adlercreutz, P. (2013). Immobilisation and application of lipases in organic media. *Chemical Society Reviews*, *42*(15), 6406. https://doi.org/10.1039/c3cs35446f

Afifah, A. N., Syahrullail, S., Wan Azlee, N. I., & Rohah, A. M. (2021). Synthesis and tribological studies of epoxidized palm stearin methyl ester as a green lubricant. *Journal of Cleaner Production*, *280*, 124320. https://doi.org/10.1016/j.jclepro.2020.124320

Aguieiras, E. C. G., Souza, S. L., & Langone, M. A. P. (2013). Estudo do comportamento da lipase comercial Lipozyme RM IM em reações de esterificação para obtenção de biodiesel. *Química Nova*, *36*(5), 646–650. https://doi.org/10.1590/S0100-40422013000500006

Alves, J., Garcia-Galan, C., Schein, M., Silva, A., Barbosa, O., Ayub, M., Fernandez-Lafuente, R., & Rodrigues, R. (2014). Combined Effects of Ultrasound and Immobilization Protocol on Butyl Acetate Synthesis Catalyzed by CALB. *Molecules*, *19*(7), 9562–9576. https://doi.org/10.3390/molecules19079562

American Oil Chemists' Society. (2004). AOCS Official Method Cd 3d-63. Acid value. In D. Firestone (Ed.), *Official Methods and Recommended Practices of the AOCS* (p. 2). AOCS Press.

American Oil Chemists' Society. (2004). AOCS Official Method Ca 2e-84. Moisture Karl Fischer reagent. In D. Firestone (Ed.), *Official Methods and Recommended Practices of the AOCS* (p. 2).

American Oil Chemists' Society. (2004). AOCS Official Method Cd 3-25. Saponification value. In D. Firestone (Ed.), *Official Methods and Recommended Practices of the AOCS* (p. 2). AOCS Press.

Angulo, B., Fraile, J. M., Gil, L., & Herrerías, C. I. (2018). Bio-lubricants production from fish oil residue by transesterification with trimethylolpropane. *Journal of Cleaner Production*, *202*, 81–87. https://doi.org/10.1016/j.jclepro.2018.07.260

Arana-Peña, S., Lokha, Y., & Fernández-Lafuente, R. (2018). Immobilization of Eversa Lipase on Octyl Agarose Beads and Preliminary Characterization of Stability and Activity Features. *Catalysts*, *8*(11), 511. https://doi.org/10.3390/catal8110511

Avagyan, A. B., & Singh, B. (2019). Biodiesel from Plant Oil and Waste Cooking Oil. In A. B. Avagyan & B. Singh (Eds.), *Biodiesel: Feedstocks, Technologies, Economics and Barriers* (p. 137). Springer Singapore. https://doi.org/10.1007/978-981-13-5746-6

Bart, J. C. J., Gucciardi, E., & Cavallaro, S. (2013a). Chemical transformations of renewable lubricant feedstocks. In J. C. J. Bart, E. Gucciardi, & S. Cavallaro (Eds.), *Biolubricants: Science and technology* (p. 944). Woodhead Publishing.

Bart, J. C. J., Gucciardi, E., & Cavallaro, S. (2013b). Renewable feedstocks for lubricant production. In J. C. J. Bart, E. Gucciardi, & S. Cavallaro (Eds.), *Biolubricants: Science and technology* (p. 944). Woodhead Publishing.

Bart, J. C. J., Gucciardi, E., & Cavallaro, S. (2013c). Renewable lubricants. In J. C. J. Bart, E. Gucciardi, & S. Cavallaro (Eds.), *Biolubricants: Science and technology* (p. 944). Woodhead Publishing.

Bart, J. C. J., Gucciardi, E., & Cavallaro, S. (2013d). The transition from reliance on fossil resources to biomass valorisation. In J. C. J. Bart, E. Gucciardi, & S. Cavallaro (Eds.), *Biolubricants: Science and technology* (p. 944). Woodhead Publishing.

BASF. (2016). *Esters – Base Stocks Selection Guide for Lubricants and Metalworking Fluids* (p. 2). https://www.btc-europe.com/fileadmin/user_upload/Downloads/Pdf_s/Industries/Brochure_Selection-Guide-Base-Stocks-Esters.pdf

Bolina, I. C. A., Gomes, R. A. B., & Mendes, A. A. (2021). Biolubricant Production from Several Oleaginous Feedstocks Using Lipases as Catalysts: Current Scenario and Future Perspectives. *BioEnergy Research*. https://doi.org/10.1007/s12155-020-10242-4

Borugadda, V. B., & Goud, V. V. (2016). Improved thermo-oxidative stability of structurally modified waste cooking oil methyl esters for bio-lubricant application. *Journal of Cleaner Production*, *112*, 4515–4524. https://doi.org/10.1016/j.jclepro.2015.06.046

Box, G. E. P., Hunter, J. S., & Hunter, W. G. (2005). *Statistics for Experiments: Design, Innovation, and Discovery* (2nd ed.). John Wiley & Sons.

Boyde, S., & Randles, S. J. (2013). Esters. In L. R. Rudnick (Ed.), *SYNTHETICS, MINERAL OILS, and BIO-BASED LUBRICANTS: Chemistry and Technology* (2nd ed., p. 1018). CRC Press.

Byerlee, D., Falcon, W. P., & Naylor, R. L. (2017). Soybean Production and Supply Chains in the Tropics. In D. Byerlee, W. P. Falcon, & R. L. Naylor (Eds.), *The Tropical Oil Crop Revolution: Food, Feed, Fuel, and Forests* (p. 305). Oxford University Press.

Cavalcante, F. T. T., Neto, F. S., Rafael de Aguiar Falcão, I., Erick da Silva Souza, J., de Moura Junior, L. S., da Silva Sousa, P., Rocha, T. G., de Sousa, I. G., de Lima Gomes, P. H., de Souza, M. C. M., & dos Santos, J. C. S. (2021). Opportunities for improving biodiesel production via lipase catalysis. *Fuel*, *288*, 119577. https://doi.org/10.1016/j.fuel.2020.119577

Cecilia, J. A., Ballesteros Plata, D., Alves Saboya, R. M., Tavares de Luna, F. M., Cavalcante, C. L., & Rodríguez-Castellón, E. (2020). An Overview of the Biolubricant Production Process: Challenges and Future Perspectives. *Processes*, *8*(3), 257. https://doi.org/10.3390/pr8030257

Cerón, A. A., Vilas Boas, R. N., Biaggio, F. C., & de Castro, H. F. (2018). Synthesis of biolubricant by transesterification of palm kernel oil with simulated fusel oil: Batch and continuous processes. *Biomass and Bioenergy*, *119*, 166–172. https://doi.org/10.1016/j.biombioe.2018.09.013

Colombié, S., Tweddell, R. J., Condoret, J.-S., & Marty, A. (1998). Water activity control: A way to improve the efficiency of continuous lipase esterification. *Biotechnology and Bioengineering*, *60*(3), 362–368. https://doi.org/10.1002/(SICI)1097-0290(19981105)60:3<362::AID-BIT13>3.0.CO;2-O

Da Silva, J. A. C., & Freire, D. M. G. (2016). Produção de Biolubrificantes Catalisada por Lipases: Fundamentos e Aplicações. In R. R. Resende (Ed.), *Biotecnologia Aplicada à Agro&Indústria - Volume 4* (p. 1070). Edgard Blücher LTDA.

Devi, B. L. A. P., Reddy, T. V. K., & Yusoff, M. F. M. (2016). Ionic Liquids in the Production of Biodiesel and Other Oleochemicals. In X. Xu, Z. Guo, & L.-Z. Cheong (Eds.), *Ionic Liquids in Lipid Processing and Analysis: Opportunities and Challenges* (p. 486). Academic Press & AOCS Press.

Dörmő, N., Bélafi-Bakó, K., Bartha, L., Ehrenstein, U., & Gubicza, L. (2004). Manufacture of an environmental-safe biolubricant from fusel oil by enzymatic esterification in solvent-free system. *Biochemical Engineering Journal*, *21*(3), 229–234. https://doi.org/10.1016/j.bej.2004.06.011

Du, W., Wang, L., & Liu, D. (2007). Improved methanol tolerance during Novozym435-mediated methanolysis of SODD for biodiesel production. *Green Chem.*, *9*(2), 173–176. https://doi.org/10.1039/B613704K

Duvekot, C. (2011). *Determination of total FAME and linolenic acid methyl esters in biodiesel according to EN-14103* (Publication Part Number: 5990-8983EN). Agilent Technologies Inc.

Erhan, S. Z., Sharma, B. K., Liu, Z., & Adhvaryu, A. (2008). Lubricant Base Stock Potential of Chemically Modified Vegetable Oils. *Journal of Agricultural and Food Chemistry*, *56*(19), 8919–8925. https://doi.org/10.1021/jf801463d

ExxonMobil. (2017). *Synthetic lubricant base stocks formulations guide* (p. 136). https://www.exxonmobilchemical.com/-/media/project/wep/exxonmobil-chemicals/chemicals/low-viscosity-polyalphaolefins/synthetic_lubricant_base_stocks_formulations_guide_en_2017pdf.pdf

Falkeborg, M., Berton-Carabin, C. C., & Cheong, L.-Z. (2016). Ionic Liquids in the Synthesis of Antioxidant Targeted Compounds. In X. Xu, Z. Guo, & L.-Z. Cheong (Eds.), *Ionic Liquids in Lipid Processing and Analysis: Opportunities and Challenges* (p. 486). AOCS Press.

Fernandes, K. V., Cavalcanti, E. D. C., Cipolatti, E. P., Aguieiras, E. C. G., Pinto, M. C. C., Tavares, F. A., da Silva, P. R., Fernandez-Lafuente, R., Arana-Peña, S., Pinto,

J. C., Assunção, C. L. B., da Silva, J. A. C., & Freire, D. M. G. (2021). Enzymatic synthesis of biolubricants from by-product of soybean oil processing catalyzed by different biocatalysts of *Candida rugosa* lipase. *Catalysis Today*, *362*, 122–129. https://doi.org/10.1016/j.cattod.2020.03.060

Ferreira, M. C., Meirelles, A. J. A., & Batista, E. A. C. (2013). Study of the fusel oil distillation process. *Industrial and Engineering Chemistry Research*, *52*(6), 2336–2351. https://doi.org/10.1021/ie300665z

Greyt, W. De. (n.d.). *Deodorization*. AOCS Lipid Library. Retrieved May 17, 2021, from https://lipidlibrary.aocs.org/edible-oil-processing/deodorization

Gunawan, S., Fabian, C., & Ju, Y.-H. (2008). Isolation and Purification of Fatty Acid Steryl Esters from Soybean Oil Deodorizer Distillate. *Industrial & Engineering Chemistry Research*, *47*(18), 7013–7018. https://doi.org/10.1021/ie800346x

Han, D., Walde, P., & Luisi, P. L. (1990). Dependence of Lipase Activity on Water Content and Enzyme Concentration in Reverse Micelles. *Biocatalysis*, *4*(2–3), 153–161. https://doi.org/10.3109/10242429008992087

Incauca S.A.S. (n.d.). *Fusel Oil*. Retrieved August 22, 2018, from http://www.incauca.com/en/producto/fusel-oil/

Kenbeck, D., & Bunemann, T. F. (2017). Organic Friction Modifiers. In L. R. Rudnick (Ed.), *Lubricant Additives: Chemistry and Applications* (3rd ed., p. 709). CRC Press.

Konwar, B. K., & Sagar, K. (2018). Introduction. In B. K. Konwar & K. Sagar (Eds.), *Lipase : an industrial enzyme through metagenomics* (p. 231). Apple Academic Press.

Lima, L. N., Oliveira, G. C., Rojas, M. J., Castro, H. F., Da Rós, P. C. M., Mendes, A. A., Giordano, R. L. C., & Tardioli, P. W. (2015). Immobilization of *Pseudomonas fluorescens* lipase on hydrophobic supports and application in biodiesel synthesis by transesterification of vegetable oils in solvent-free systems. *Journal of Industrial Microbiology & Biotechnology*, *42*(4), 523–535. https://doi.org/10.1007/s10295-015-1586-9

Luther, R. (2014). Bio-Based and Biodegradable Base Oils. In T. Mang (Ed.), *Encyclopedia of Lubricants and Lubrication - Vol. 1* (p. 2413). Springer.

Luzuriaga, S. (2020). *Biolubricants market during COVID-19*. Society of Tribologists Abd Lubrication Engineers. https://www.stle.org/files/TLTArchives/2020/09_September/Market_Trends.aspx

Lv, L., Dai, L., Du, W., & Liu, D. (2021). Progress in Enzymatic Biodiesel Production and Commercialization. *Processes*, *9*(2), 355. https://doi.org/10.3390/pr9020355

Markets and Markets. (2020). *Lubricants Market by Base Oil (Mineral Oil, Synthetic Oil, Bio-based Oil), Product Type (Engine Oil, Hydraulic Fluid, Metalworking*

Fluid), Application (Transportation and Industrial lubricants), Region - Global Forecast to 2025. https://www.marketsandmarkets.com/Market-Reports/lubricants-market-182046896.html?gclid=EAIaIQobChMIyqOy3LP27gIVBA-RCh0iYQCKEAAYASAAEgIj6_D_BwE

Martínez-Sanchez, J. A., Arana-Peña, S., Carballares, D., Yates, M., Otero, C., & Fernandez-Lafuente, R. (2020). Immobilized Biocatalysts of Eversa® Transform 2.0 and Lipase from *Thermomyces Lanuginosus*: Comparison of Some Properties and Performance in Biodiesel Production. *Catalysts*, *10*(7), 738. https://doi.org/10.3390/catal10070738

Martins, A. B., Friedrich, J. L. R., Cavalheiro, J. C., Garcia-Galan, C., Barbosa, O., Ayub, M. A. Z., Fernandez-Lafuente, R., & Rodrigues, R. C. (2013). Improved production of butyl butyrate with lipase from *Thermomyces lanuginosus* immobilized on styrene–divinylbenzene beads. *Bioresource Technology*, *134*, 417–422. https://doi.org/10.1016/j.biortech.2013.02.052

Martins, A. B., Schein, M. F., Friedrich, J. L. R., Fernandez-Lafuente, R., Ayub, M. A. Z., & Rodrigues, R. C. (2013). Ultrasound-assisted butyl acetate synthesis catalyzed by Novozym 435: Enhanced activity and operational stability. *Ultrasonics Sonochemistry*, *20*(5), 1155–1160. https://doi.org/10.1016/j.ultsonch.2013.01.018

Marty, A., Dossat, V., & Condoret, J.-S. (1997). Continuous operation of lipase-catalyzed reactions in nonaqueous solvents: Influence of the production of hydrophilic compounds. *Biotechnology and Bioengineering*, *56*(2), 232–237. https://doi.org/10.1002/(SICI)1097-0290(19971020)56:2<232::AID-BIT12>3.0.CO;2-I

McCurry, J. D., & Wang, C.-X. (2007). *Analysis of glycerin and glycerides in biodiesel (B100) using ASTM D6584 and EN14105*. Agilent Technologies, Inc.

Mibielli, G. M., Fagundes, A. P., Bender, J. P., & Vladimir Oliveira, J. (2019). Lab and pilot plant FAME production through enzyme-catalyzed reaction of low-cost feedstocks. *Bioresource Technology Reports*, *5*, 150–156. https://doi.org/10.1016/j.biteb.2019.01.013

Miranda, L. P., Guimarães, J. R., Giordano, R. C., Fernandez-Lafuente, R., & Tardioli, P. W. (2020). Composites of Crosslinked Aggregates of Eversa® Transform and Magnetic Nanoparticles. Performance in the Ethanolysis of Soybean Oil. *Catalysts*, *10*(8), 817. https://doi.org/10.3390/catal10080817

Monteiro, R. R. C., Arana-Peña, S., da Rocha, T. N., Miranda, L. P., Berenguer-Murcia, Á., Tardioli, P. W., dos Santos, J. C. S., & Fernandez-Lafuente, R. (2021). Liquid lipase preparations designed for industrial production of biodiesel. Is it really an optimal solution? *Renewable Energy*, *164*, 1566–1587. https://doi.org/10.1016/j.renene.2020.10.071

Nott, K., Brognaux, A., Richard, G., Laurent, P., Favrelle, A., Jérôme, C., Blecker, C., Wathelet, J.-P., Paquot, M., & Deleu, M. (2012). (Trans)esterification of mannose catalyzed by lipase b from *Candida antarctica* in an improved reaction medium using co-solvents and molecular sieve. *Preparative Biochemistry and Biotechnology*, *42*(4), 348–363. https://doi.org/10.1080/10826068.2011.622330

Novozymes. (2016). *The Novozymes enzymatic biodiesel handbook* (p. 90). http://lp.novozymes.com/Biodiesel-HandbookForm_01-DairyApplicationSheet-LP.html

Omar, I. C., Nishio, N., & Nagai, S. (1988). The role of water on the equilibrium of esterification by immobilized lipase packed-bed column reactor. *Biotechnology Letters*, *10*(11), 799–804. https://doi.org/10.1007/BF01027576

Paludo, N., Alves, J. S., Altmann, C., Ayub, M. A. Z., Fernandez-Lafuente, R., & Rodrigues, R. C. (2015). The combined use of ultrasound and molecular sieves improves the synthesis of ethyl butyrate catalyzed by immobilized Thermomyces lanuginosus lipase. *Ultrasonics Sonochemistry*, *22*, 89–94. https://doi.org/10.1016/j.ultsonch.2014.05.004

Panpipat, W., Xu, X., & Guo, Z. (2012). Towards a commercially potential process: Enzymatic recovery of phytosterols from plant oil deodoriser distillates mixture. *Process Biochemistry*, *47*(8), 1256–1262. https://doi.org/10.1016/j.procbio.2012.04.024

Parkin, K. L. (2017). Enzymes. In S. Damodaran & K. L. Parkin (Eds.), *Fennema's Food Chemistry* (5th ed., p. 1125). CRC Press.

Paul, C. E., & Fernández, V. G. (2016). Biocatalysis and Biotransformation in Ionic Liquids. In X. Xu, Z. Guo, & L.-Z. Cheong (Eds.), *Ionic Liquids in Lipid Processing and Analysis* (p. 486). Academic Press & AOCS Press.

Pérez, E. R., Cardoso, D. R., & Franco, D. W. (2001). Análise dos álcoois, ésteres e compostos carbonílicos em amostras de óleo fúsel. *Química Nova*, *24*(1), 10–12. https://doi.org/10.1590/S0100-40422001000100003

Perez, J. M., Rudnick, L. R., & Erhan, S. Z. (2013). Natural Oils as Lubricants. In L. R. Rudnick (Ed.), *Synthetics, Mineral Oils, and Bio-Based Lubricants: Chemistry and Technology* (2nd ed., p. 1018). CRC Press.

Petro-Canada. (2017). *Petro-Canada Lubricants Handbook 2017* (p. 228). file:///C:/Users/Rafael/AppData/Local/Temp/PCL-Handbook-2017-LUB1007E.pdf

Poppe, J. K., Garcia-Galan, C., Matte, C. R., Fernandez-Lafuente, R., Rodrigues, R. C., & Ayub, M. A. Z. (2013). Optimization of synthesis of fatty acid methyl esters catalyzed by lipase B from *Candida antarctica* immobilized on hydrophobic supports. *Journal of Molecular Catalysis B: Enzymatic*, *94*, 51–56. https://doi.org/10.1016/j.molcatb.2013.05.010

Prasannakumar, P., Edla, S., Thampi, A. D., Arif, M., & Santhakumari, R. (2022). A comparative study on the lubricant properties of chemically modified *Calophyllum inophyllum* oils for bio-lubricant applications. *Journal of Cleaner Production*, *339*, 130733. https://doi.org/10.1016/j.jclepro.2022.130733

Raof, N. A., Yunus, R., Rashid, U., Azis, N., & Yaakub, Z. (2019). Effect of molecular structure on oxidative degradation of ester based transformer oil. *Tribology International*, *140*, 105852. https://doi.org/10.1016/j.triboint.2019.105852

Reeves, C. J., Siddaiah, A., & Menezes, P. L. (2017). A Review on the Science and Technology of Natural and Synthetic Biolubricants. *Journal of Bio- and Tribo-Corrosion*, *3*(1), 11. https://doi.org/10.1007/s40735-016-0069-5

Remonatto, D., de Oliveira, J. V., Manuel Guisan, J., de Oliveira, D., Ninow, J., & Fernandez-Lorente, G. (2018). Production of FAME and FAEE via Alcoholysis of Sunflower Oil by Eversa Lipases Immobilized on Hydrophobic Supports. *Applied Biochemistry and Biotechnology*, *185*(3), 705–716. https://doi.org/10.1007/s12010-017-2683-1

Remonatto, D., Santin, C. M. T., de Oliveira, D., Di Luccio, M., & de Oliveira, J. V. (2016). FAME Production from Waste Oils Through Commercial Soluble Lipase Eversa ® Catalysis. *Industrial Biotechnology*, *12*(4), 254–262. https://doi.org/10.1089/ind.2016.0002

Rodrigues, R. C., Berenguer-Murcia, Á., Carballares, D., Morellon-Sterling, R., & Fernandez-Lafuente, R. (2021). Stabilization of enzymes via immobilization: Multipoint covalent attachment and other stabilization strategies. *Biotechnology Advances*, *52*, 107821. https://doi.org/10.1016/j.biotechadv.2021.107821

Rodrigues, R. C., Ortiz, C., Berenguer-Murcia, Á., Torres, R., & Fernández-Lafuente, R. (2013). Modifying enzyme activity and selectivity by immobilization. *Chem. Soc. Rev.*, *42*(15), 6290–6307. https://doi.org/10.1039/C2CS35231A

Salih, N. (2021). A Review on New Trends, Challenges and Prospects of Ecofriendly Friendly Green Food-Grade Biolubricants. *Biointerface Research in Applied Chemistry*, *12*(1), 1185–1207. https://doi.org/10.33263/briac121.11851207

Sathwik Chatra, K. R., Jayadas, N. H., & Kailas, S. V. (2012). Natural Oil-Based Lubricants. In M. Nosonovsky & B. Bhushan (Eds.), *Green Tribology - Biomimetics, Energy Conservation and Sustainability* (p. 647). Springer.

Séverac, E., Galy, O., Turon, F., Pantel, C. A., Condoret, J.-S., Monsan, P., & Marty, A. (2011). Selection of CalB immobilization method to be used in continuous oil transesterification: Analysis of the economical impact. *Enzyme and Microbial Technology*, *48*(1), 61–70. https://doi.org/10.1016/j.enzmictec.2010.09.008

Shell. (2019). *Lubricants for Marine Applications* (p. 8). https://www.shell.com/business-customers/marine/brochures-and-communication-materials/_jcr_content/par/tabbedcontent/tab_1407999154/textimage.stream/15862

62283450/b3720e3a879d04da294e770506f9e7552e6ad303/product-catalogue-voct-2019.pdf

Sherazi, H. S. T., Mahesar, S. A., & Sirajuddin. (2016). Vegetable Oil Deodorizer Distillate: A Rich Source of the Natural Bioactive Components. *Journal of Oleo Science*, *65*(12), 957–966. https://doi.org/10.5650/jos.ess16125

Sousa, R. R., Silva, A. S., Fernandez-Lafuente, R., & Ferreira-Leitão, V. S. (2021). Solvent-free esterifications mediated by immobilized lipases: a review from thermodynamic and kinetic perspectives. *Catalysis Science & Technology*, *11*(17), 5696–5711. https://doi.org/10.1039/D1CY00696G

Souza, M. S., Aguieiras, E. C. G., da Silva, M. A. P., & Langone, M. A. P. (2009). Biodiesel Synthesis via Esterification of Feedstock with High Content of Free Fatty Acids. *Applied Biochemistry and Biotechnology*, *154*(1–3), 74–88. https://doi.org/10.1007/s12010-008-8444-4

Syahir, A. Z., Zulkifli, N. W. M., Masjuki, H. H., Kalam, M. A., Alabdulkarem, A., Gulzar, M., Khuong, L. S., & Harith, M. H. (2017). A review on bio-based lubricants and their applications. *Journal of Cleaner Production*, *168*, 997–1016. https://doi.org/10.1016/j.jclepro.2017.09.106

Thangaraj, B., Solomon, P. R., Muniyandi, B., Ranganathan, S., & Lin, L. (2019). Catalysis in biodiesel production—a review. *Clean Energy*, *3*(1), 2–23. https://doi.org/10.1093/ce/zky020

Tsagaraki, E., Karachaliou, E., Delioglanis, I., & Kouzi, E. (2017). *Bio-based products and applications potential*. https://www.bioways.eu/download.php?f=150&l=en&key=441a4e6a27f83a8e828b802c37adc6e1

Vescovi, V., Giordano, R., Mendes, A., & Tardioli, P. (2017). Immobilized Lipases on Functionalized Silica Particles as Potential Biocatalysts for the Synthesis of Fructose Oleate in an Organic Solvent/Water System. *Molecules*, *22*(2), 212. https://doi.org/10.3390/molecules22020212

Vescovi, V., Kopp, W., Guisán, J. M., Giordano, R. L. C., Mendes, A. A., & Tardioli, P. W. (2016). Improved catalytic properties of *Candida antarctica* lipase B multi-attached on tailor-made hydrophobic silica containing octyl and multifunctional amino- glutaraldehyde spacer arms. *Process Biochemistry*, *51*(12), 2055–2066. https://doi.org/10.1016/j.procbio.2016.09.016

Vieira, A. C., Cansian, A. B. M., Guimarães, J. R., Vieira, A. M. S., Fernandez-Lafuente, R., & Tardioli, P. W. (2021). Performance of Liquid Eversa on Fatty Acid Ethyl Esters Production by Simultaneous Esterification/Transesterification of Low-to-High Acidity Feedstocks. *Catalysts*, *11*(12), 1486. https://doi.org/10.3390/catal11121486

Visioli, L. J., de Castilhos, F., Cardozo-Filho, L., de Mello, B. T. F., & da Silva, C. (2016). Production of esters from soybean oil deodorizer distillate in pressurized

ethanol. *Fuel Processing Technology*, *149*, 326–331. https://doi.org/10.1016/j.fuproc.2016.04.038

Wang, L., Du, W., Liu, D., Li, L., & Dai, N. (2006). Lipase-catalyzed biodiesel production from soybean oil deodorizer distillate with absorbent present in tert-butanol system. *Journal of Molecular Catalysis B: Enzymatic*, *43*(1–4), 29–32. https://doi.org/10.1016/j.molcatb.2006.03.005

Yahya, A. R. ., Anderson, W. A., & Moo-Young, M. (1998). Ester synthesis in lipase-catalyzed reactions. *Enzyme and Microbial Technology*, *23*(7–8), 438–450. https://doi.org/10.1016/S0141-0229(98)00065-9

Yin, X., Duan, X., You, Q., Dai, C., Tan, Z., & Zhu, X. (2016). Biodiesel production from soybean oil deodorizer distillate usingcalcined duck eggshell as catalyst. *Energy Conversion and Management*, *112*, 199–207. https://doi.org/10.1016/j.enconman.2016.01.026

Yin, X., You, Q., Ma, H., Dai, C., Zhang, H., Li, K., & Li, Y. (2015). Biodiesel production from soybean oil deodorizer distillate enhanced by counter-current pulsed ultrasound. *Ultrasonics Sonochemistry*, *23*, 53–58. https://doi.org/10.1016/j.ultsonch.2014.08.020

Yin, X., Zhang, X., Wan, M., Duan, X., You, Q., Zhang, J., & Li, S. (2017). Intensification of biodiesel production using dual-frequency counter-current pulsed ultrasound. *Ultrasonics Sonochemistry*, *37*, 136–143. https://doi.org/10.1016/j.ultsonch.2016.12.036

Yun, L., Ling, W., & Yunjun, Y. (2010). Cogeneration of biodiesel and tocopherols by combining pretreatment with supercritical carbon dioxide extraction from soybean oil deodorizer distillate. *Chemistry and Technology of Fuels and Oils*, *46*(2), 79–86. https://doi.org/10.1007/s10553-010-0191-x

Zainal, N. A., Zulkifli, N. W. M., Gulzar, M., & Masjuki, H. H. (2018). A review on the chemistry, production, and technological potential of bio-based lubricants. *Renewable and Sustainable Energy Reviews*, *82*, 80–102. https://doi.org/10.1016/j.rser.2017.09.004

Zheng, J., Wei, W., Wang, S., Li, X., Zhang, Y., & Wang, Z. (2020). Immobilization of Lipozyme TL 100L for methyl esterification of soybean oil deodorizer distillate. *3 Biotech*, *10*(2), 51. https://doi.org/10.1007/s13205-019-2028-6

Zhong, L., Feng, Y., Wang, G., Wang, Z., Bilal, M., Lv, H., Jia, S., & Cui, J. (2020). Production and use of immobilized lipases in/on nanomaterials: A review from the waste to biodiesel production. *International Journal of Biological Macromolecules*, *152*, 207–222. https://doi.org/10.1016/j.ijbiomac.2020.02.258

4.2 Structured article on the application of *Pseudomonas fluorescens* lipase (PFL) immobilized by the hybrid nanoflower (hNF) technique in synthesis of FAIEs from SODD

This section presents the results for immobilization of PFL by the hNF technique and its application in the synthesis of FAIEs from SODD and isoamyl alcohol, using a drying salt to control free moisture in the reaction medium. This material has not yet been published or submitted for publication in any scientific journal.

Title: **Application of *Pseudomonas fluorescens* lipase immobilized by the hybrid nanoflower method in the synthesis of fatty acid isoamyl esters from soybean oil deodorizer distillate**

4.2.1 Abstract

The application of lipases immobilized using the hybrid nanoflower (hNF) technique is usually restricted to the hydrolysis of para-nitrophenol esters, with little exploration for other reactions. Few works have applied lipase hNFs in organic systems for esterification or transesterification reactions. After an initial screening of six lipases to identify the most appropriate lipase for esterification of oleic acid and transesterification of soybean oil with isoamyl alcohol, *Pseudomonas fluorescens* lipase (PFL) immobilized by the hNF method was selected for the synthesis of fatty acid isoamyl esters (FAIEs) from soybean oil deodorizer distillate (SODD) and isoamyl alcohol. Experimental design and response surface methodology were used to identify significant variables and trends, as well as for optimization of the PFL immobilization and the FAIEs synthesis parameters. Improvements in the hNF-PFL incubation were studied, with the use of ultrasound enabling the incubation time to be reduced from 72 h to only 20 min. The immobilized activity of hNF-PFL reached 64 TBU%, with a well-defined hNF structure. During the FAIEs synthesis, it was observed that the desiccant salt (sodium sulfate) employed to control the moisture in the reaction medium could damage the hNF-PFL structure. Synthesis of FAIEs using hNF-PFL achieved a maximum reaction yield (RY) of 64 wt.%, without use of a moisture control agent. The hNF-PFL showed high operational stability, maintaining practically the same RY during 8 cycles (totaling 192 h of operation), with 80% of the initial RY obtained in the 10^{th} cycle (after 240 h of operation). Partially converted SODD, with FAIEs content of 57 wt.%, was submitted to chemical and physicochemical characterization, before and after caustic polishing, with

the physicochemical characteristics of the materials being very similar and analogous to those of commercial biolubricant base stocks.

4.2.2 Introduction

The hybrid nanoflower (hNF) immobilization technique is a very simple method of enzyme immobilization that can provide a microscale material with high surface area (usually resembling flowers), composed of an insoluble inorganic phosphate salt (from phosphate-buffered saline, PBS) and a metal (copper is most commonly employed, although other metals that can be used include aluminum, gold, calcium, iron(II), magnesium, manganese, nickel, silver, and zinc), combined with the enzyme protein (Ge et al., 2012; Lin et al., 2020; Ocsoy et al., 2015; Sharma et al., 2017; Talens-Perales et al., 2020; Xin et al., 2020; Yin et al., 2015; Zhang et al., 2015; Zhang et al., 2016). The nitrogen present in protein amide groups and some amino acid residues of the polypeptide chain of the enzyme, such as histidine, are linked with the metal by complexation, with the complexed metal then being linked to phosphate, creating a complex network of inorganic/organic material (Ge et al., 2012). The mechanism of hNF immobilization consists of three steps: nucleation of the organic-inorganic structures; agglomeration of these structures and formation of primary crystals; and anisotropic growth of the crystals, resulting in branched structures resembling flowers (Ge et al., 2012). The agglomeration and anisotropic growth are mediated by chloride ion complexes (Somturk et al., 2016) present in PBS. Enzymes immobilized by this method are frequently reported to achieve hyperactivation, with improvements in stability also being common. Li et al. (2016) found that hNFs with papain presented immobilized activity of 7260%, compared to the free enzyme. Cui et al. (2016) observed high thermal stability of a lipase type II from bovine pancreas (BPL tII), after hNF immobilization. After 10 h at 60 °C, the hNF-BPL tII maintained 93% of the initial activity, while the free BPL tII had almost no activity. In addition, a 200% increase of the hNF-BPL tII activity was observed when 0.25 mM of cetyl trimethyl ammonium bromide (CTAB) surfactant was used during the immobilization, reaching an immobilized activity of 460%, compared to the free lipase. Modifications of the hNF immobilization procedure could lead to further improvements. Soni et al. (2018) found that the application of ultrasound during the incubation of a *Burkholderia cepacia* lipase hNF increased the immobilized activity from 399% to 423%, while the immobilization time was reduced from 3 days to only 7.5 min. Ultrasound was also applied for 10 min to form a cobalt hNF with *Pseudomonas fluorescens* lipase (PFL),

with the immobilized activity increasing by 89%, when compared to static incubation at 25 °C for 3 days (Dwivedee et al., 2018).

The protein concentration, metal concentration, incubation time, pH, and temperature of the immobilization medium can significantly influence hNF size, shape, and immobilized enzyme activity. Somturk et al. (2016) and Li et al. (2016) studied the effects of enzyme concentration and PBS pH on the activity of hNFs at two different temperatures. Somturk et al. (2016) immobilized urease and obtained a maximum activity of 3990% (compared to the free enzyme), using 0.02 mg/mL of urease, PBS at pH 7.4, and 0.8 mM of Cu^{2+}, at ambient temperature of 20 °C for 3 days. Li et al. (2016) immobilized papain and porcine pancreas lipase type II (PPL tII), obtaining maximum activities of 7260% and 876% (compared to the free enzyme), respectively, using 0.25 mg/mL of papain, PBS at pH 9.0, and 0.8 mM of Cu^{2+}, at 25 °C for 3 days, and using 0.25 mg/mL of PPL tII, PBS at pH 6.0, and 0.8 mM of Cu^{2+}, at ambient temperature of 25 °C for 3 days. Horseradish peroxidase (HRP) was immobilized by the hNF method using two different metals, Cu^{2+} and Fe^{2+}, reaching immobilized activities of 300% using 0.02 mg of HRP, PBS at pH 7.4, and 0.8 mM of Cu^{2+}, at 4 °C for 3 days (Somturk et al., 2015), and 710% using 0.10 mg of HRP, PBS at pH 7.4, and 0.8 mM of Fe^{2+}, at 4 °C for 3 days (Ocsoy et al., 2015).

Lipases are among the various enzymes that have been successfully immobilized using the hNF technique, including those from *Alcaligenes* sp. (lipase QLM) (Liu et al., 2021), *Aspergillus oryzae* (AOL) (Li et al., 2020; Zhong et al., 2021), *Bacillus subtilis* (BSL) (Wu et al., 2014), bovine pancreas (BPL tII) (Cui et al., 2016), *Burkholderia cepacia* (BCL) (Ke et al., 2016; Li et al., 2018; Sharma et al., 2017; Soni et al., 2018), *Candida antarctica* (Ge et al., 2012), *Candida antarctica* (lipase B, CALB) (Hua et al., 2016; Yu et al., 2018; Zhang et al., 2018), *Candida rugosa* (CRL) (Lee et al., 2017), *Enterobacter* sp. MG10 (Mohammadi-Mahani et al., 2021), porcine pancreas (PPL) (Altinkaynak et al., 2020; Jiang et al., 2018; Yu et al., 2018; Zhang et al., 2016), porcine pancreas (PPL tII) (Li et al., 2016), *Pseudomonas fluorescens* (PFL) (Dwivedee et al., 2018), *Pseudozyma antarctica* (lipase B, PALB) (Fotiadou et al., 2019), *Psychrobacter* sp. (lipase ZC12) (Zhang et al., 2020), and *Thermomyces lanuginosus* (TLL) (Yu et al., 2018; Wang et al., 2020). However, the applications of these immobilized enzymes have still not been fully explored. The use of hNF lipases has been restricted to the synthesis of fatty acid methyl esters (FAMEs) (Jiang et al., 2018; Mohammadi-Mahani et al., 2021; Zhong et al., 2021), tyrosol esters (Fotiadou et al., 2019), clindamycin palmitate (Yu et

al., 2018; Wang et al., 2020), and fructose lauric ester (Zhang et al., 2020), in addition to the epoxidation of alkenes (Hua et al., 2016; Zhang et al., 2018) and enzymatic kinetic resolution of racemates (Dwivedee et al., 2018; Ke et al., 2016; Li et al., 2018; Soni et al., 2018; Wu et al., 2014).

A potential application of immobilized lipases is in the synthesis of long chain esters that could be applied as biolubricants or biolubricant components (base stocks or additives), due to the urgent need to reduce petroleum dependency, decelerate climatic changes, and diminish environmental degradation and hazards (European Environmental Agency, 2020; Nowak et al., 2019; Tsagaraki et al., 2017).

Biolubricants are natural or synthetic bio-based compounds that are biodegradable, with low human and environmental toxicity, employed as lubricants for corrosion and wear protection, reduction of friction and heat, and in energy transmission (Bart et al., 2013; Cecilia et al., 2020; Zainal et al., 2018). The various classes of biolubricant compounds include monoesters (Luther, 2014), which are easily obtained from the reaction of fatty acids and monohydroxy alcohols in the presence of lipases (Parkin, 2017). Araujo-Silva et al. (2022) obtained fatty acid isoamyl esters (FAIEs) from soybean oil deodorizer distillate (SODD) and isoamyl alcohol, catalyzed by Eversa Transform 2.0 (ETL 2.0), obtaining products with biolubricant base stock characteristics. SODD, a byproduct from the edible soybean oil production process, is a rich source of free fatty acids (FFAs, 17-47 wt.%) and glycerides (9-70 wt.%) (Araujo-Silva et al., 2022; Gunawan et al., 2008; Sherazi et al., 2016). Isoamyl alcohol is a byproduct from bioethanol production, which can be extracted and purified from fusel oil (Ferreira et al., 2013).

Over the last few years, many studies of hNF lipases have focused on the immobilization process and characterization of the catalysts formed, but few have explored their applicability. Therefore, this study investigated the use of a lipase immobilized by the hNF technique in the synthesis of FAIEs from SODD and isoamyl alcohol. Firstly, an appropriate lipase for the FAIEs synthesis was selected. A study of immobilization of the selected lipase by the hNF method was performed, using experimental design and response surface methodology. This enabled identification of the most significant variables, elucidation of trends, and optimization of the immobilization conditions. It was also possible to propose enhancements in the incubation step of the immobilization and the use of surfactants. The best condition for obtaining lipase hNFs was determined considering the immobilization yield (IY) and

immobilized activity (IA), together with image and elemental composition analyses, before employing the catalyst in FAIEs synthesis. Experimental design with response surface methodology was used to identify the significant variables and trends, in order to optimize the FAIEs reaction yield (RY). Reaction course curves were plotted to identify the maximum conversions, with the products being characterized by chemical and physicochemical analyses.

4.2.3 Materials and Methods

4.2.3.1 Materials

CRL, ETL 2.0, PFL, *Rhizopus niveus* lipase (RNL), TLL, tributyrin, methyl heptadecanoate, and standard solutions for ASTM D6584 analysis were purchased from Sigma-Aldrich (St. Louis, MO, USA). Isoamyl alcohol was purchased from Êxodo Científica (Sumaré, SP, Brazil), CALB was kindly donated by Novozymes Latin America (Araucária, PR, Brazil), and soybean oil deodorizer distillate (SODD) was kindly donated by COCAMAR (Maringá, PR, Brazil). All other chemicals and solvents were of analytical or HPLC grade.

4.2.3.2 Lipase screening

Six lipases (CALB, CRL, ETL 2.0, PFL, RNL, and TLL) were investigated for the esterification of oleic acid and the transesterification of soybean oil with isoamyl alcohol, in order to select the best lipase for production of isoamyl esters. Triplicate reactions were conducted in sealed bottles with plugs and caps, incubated in a shaker for 12 h at 37.5 °C and 250 rpm. The reaction media had the stoichiometric compositions of 1:1 mol of oleic acid per mol of alcohol, or 1:3 mol of soybean oil triglycerides per mol of alcohol, together with 600 tributyrin hydrolysis units (TBU) per g of acyl donor (oleic acid or soybean oil), and sufficient molecular sieve to provide an anhydrous medium condition. At the end of the reactions, the liquid phases were transferred to 15 mL Falcon tubes, washed with 3 mL of boiling water, centrifuged at 10707 rpm and 25 °C for 5 min, and the polar phase was discarded. The washing and centrifugation processes were repeated one more time, followed by separation of the nonpolar phases in 2 mL Eppendorf tubes and drying in an oven at 60 °C for one day. The reaction yields were determined by GC-FID analysis.

4.2.3.3 Lipase hybrid nanoflower immobilization

Screening of the lipases showed that PFL provided good esterification and transesterification yields, so it was chosen as a viable lipase for application in the production of isoamyl ester from SODD (which is composed by long chain fatty acids and glycerides). The hNF immobilization of PFL used Cu^{2+} (from $CuSO_4$ reagent) as the metal ion to compose the inorganic portion of the hNF-PFL. The immobilization was optimized using experimental design, as described below. The performance of the hNF-PFL formation process was quantified in terms of immobilization yield (IY) and immobilized activity (IA), according to Equations 1 and 2, respectively:

$$IY\ [\%TBU] = 100 \cdot \frac{A_{hNFsusp}}{A_{offered}} \quad (1)$$

$$IA\ [\%TBU] = 100 \cdot \frac{A_{hNFsusp}}{A_{offered} - A_{supernat}} \quad (2)$$

where, $A_{hNFsusp}$, $A_{offered}$, and $A_{supernat}$ are the total activity in the hNF-PFL suspension, the activity initially offered, and the activity in the supernatant, respectively.

4.2.3.3.1 Determination of trends and ranges for basic variables of the hNF immobilization process (protein concentration, metal concentration, and pH), using experimental design and response surface methodology

This experiment used an adaptation of the hNF immobilization procedure described by Ge et al. (2012), employing an experimental design to evaluate three variables important for the success of hNF immobilization, namely the enzymatic protein concentration (C_{prot}), the $CuSO_4$ concentration (C_{CuSO_4}), and the pH of the phosphate-buffered saline (PBS). Mixtures were prepared in 5 mL Eppendorf tubes, using 3 mL of PBS at different pH values, a volume of 2 mg_{prot}/mL PFL solution solubilized in ultrapure water (sufficient to achieve the C_{prot} concentration), and a volume of 120 mM $CuSO_4$ solution solubilized in ultrapure water (sufficient to achieve the C_{CuSO_4} concentration). The immobilization medium was homogenized by vortex agitation after each addition. The Eppendorf tubes were incubated in a thermostatic bath at 25 °C for 3 days, followed by separation of the solids from the supernatant by centrifugation at 7000 rpm and 25 °C for 5 min, washing with 3 mL of distilled water at room temperature, separation by centrifugation at 7000 rpm and 25 °C for 5 min (repeating the washing process 2 times), and resuspending to 3 mL with distilled water. The hydrolytic activities of the supernatant and the resuspended hNF-PFL were measured using the tributyrin method with a pHstat instrument. PFL protein content was determined by Bradford method (Bradford, 1976).

Table 4.2-01 shows the conditions of the different experiments of the experimental design for the variables PBS pH, C_{prot}, and C_{CuSO_4}.

Table 4.2-01. Different conditions for the hNF-PFL experimental design using three variables (C_{prot}, C_{CuSO_4}, and PBS pH). Incubation at 25 °C for 3 days.

Exp.	C_{prot} (mg_{prot}/mL)		C_{CuSO_4} (mM)		PBS pH	
1	0.21	(1)	2.0	(1)	7.0	(0)
2	0.21	(1)	0.8	(-1)	7.0	(0)
3	0.21	(1)	1.4	(0)	8.0	(1)
4	0.21	(1)	1.4	(0)	6.0	(-1)
5	0.11	(0)	2.0	(1)	8.0	(1)
6	0.11	(0)	2.0	(1)	6.0	(-1)
7	0.11	(0)	0.8	(-1)	8.0	(1)
8	0.11	(0)	0.8	(-1)	6.0	(-1)
9	0.01	(-1)	2.0	(1)	7.0	(0)
10	0.01	(-1)	0.8	(-1)	7.0	(0)
11	0.01	(-1)	1.4	(0)	8.0	(1)
12	0.01	(-1)	1.4	(0)	6.0	(-1)
13	0.11	(0)	1.4	(0)	7.0	(0)
14	0.11	(0)	1.4	(0)	7.0	(0)
15	0.11	(0)	1.4	(0)	7.0	(0)
16	0.11	(0)	1.4	(0)	7.0	(0)

4.2.3.3.2 Improvements in the hNF methodology and optimization of variables for maximization of the immobilization yield.

The results of the first experimental design revealed the need for improvement with respect to the level of C_{CuSO_4}. Therefore, assays were performed according to the procedure described in Section 4.2.3.3.1, under the best conditions of PBS pH and C_{prot} (pH 8.0 and 0.14 mg_{prot}/mL, respectively), increasing the value of C_{CuSO_4} until a peak of the immobilization yield was observed.

The influence of different incubation methods was also explored, using a reaction medium composed of 3 mL of PBS pH 8.0, 0.14 mg_{prot}/mL of PFL, and 7.04 mM $CuSO_4$. The medium was submitted to the following procedures: (i) ultrasonication in an ultrasonic bath (Maxi Clean 1450, Unique); (ii) incubation at 35 °C for 3 days; (iii) ultrasonication followed by incubation at 25 °C for 3 days; (iv) agitation at 8 rpm and 25 °C for 3 days, using a blood roller mixer (model K45-8020, Kasvi) (low speed agitation

condition); (v) agitation at 45 rpm and 25 °C for 3 days (medium speed agitation condition); (vi) no incubation, with the steps of supernatant separation, washing, and resuspension performed immediately after the addition of $CuSO_4$.

Investigation was also made of the use and concentration of different surfactants. For this, 5 mL Eppendorf tubes were prepared with 3 mL of PBS (pH 8.0), 0.14 mg_{prot}/mL of PFL, 7.04 mM $CuSO_4$, and 0.001, 0.01, 0.1, or 1.0% (v/v) of Triton X-100, Tween 20, or Tween 80. The tubes were ultrasonicated for 20 min, followed by separation of the supernatant, washing, and resuspension of the hNF-PFL, as described in Section 4.2.3.3.1.

Having defined a new range of C_{CuSO_4} and a new incubation method, optimization of the variables C_{prot} and C_{CuSO_4} by experimental design was performed using 5 mL Eppendorf tubes containing 3.0 mL of immobilization medium composed of PBS pH 8.0 and different concentrations of C_{prot} and C_{CuSO_4}, as described in Table 4.2-02.

Table 4.2-02. Concentrations of protein and copper sulfate for the second experimental design to determine the best conditions for hNF-PFL immobilization.

Exp.	C_{prot} (mg_{prot}/mL)		C_{CuSO_4} (mM)	
1	0.180	(1)	7.60	(1)
2	0.180	(1)	6.40	(-1)
3	0.100	(-1)	7.60	(1)
4	0.100	(-1)	6.40	(-1)
5	0.140	(0)	6.15	(-1.41)
6	0.083	(-1.41)	7.00	(0)
7	0.140	(0)	7.85	(1.41)
8	0.197	(1.41)	7.00	(0)
9	0.140	(0)	7.00	(0)
10	0.140	(0)	7.00	(0)
11	0.140	(0)	7.00	(0)

4.2.3.4 Use of experimental design and surface response methodology to establish the reaction conditions for the synthesis of SODD isoamyl esters using hNF-PFL as catalyst

In this step, an initial screening was firstly performed of the variables of interest, using experimental design. A study was then performed with different values for each of the variables. Finally, fine tuning using experimental design was applied to determine the best operational conditions for the synthesis of SODD isoamyl esters using hNF-PFL as catalyst.

4.2.3.4.1 Screening to determine the values of the variables of interest using experimental design and surface response methodology

Optimization of synthesis of the SODD FAIEs catalyzed by hNF-PFL considered the following three variables: molar ratio of saponifiable SODD and isoamyl alcohol ($SODD_{Sap}$/isoamyl alcohol, $R_{isoamyl}$, mol saponifiable SODD/mol of isoamyl alcohol), reaction temperature (T, ºC), and mass of anhydrous Na_2SO_4 desiccant ($m_{desiccant\ salt}$, desiccant salt/SODD mass percentage). A first screening using experimental design and response surface methodology for a quadratic model was used to evaluate the effects of these variables, considering their values, ranges, and trends. The initial ranges applied, shown in Table 4.2-03, were based on a previous study of SODD isoamyl esters synthesis (Araujo-Silva et al., 2022). The experimental points were obtained for assays performed in sealed bottles (with plugs and caps), with 100 TBU of hNF-PFL per mL of SODD and incubation in a shaker incubator (MA832/H, Marconi) at 250 rpm for 24 h. The nonpolar liquid phase was drained from the bottles, washed with water at boiling point (water/SODD ratio of 3:1 v/v), and centrifuged at 10707 rpm for 2 min, followed by draining of the polar phase (repeating the washing process two times). The samples were dried in an oven at 60-65 °C for 2 days, followed by GC-FID analysis to determine the reaction yield.

Table 4.2-03. Conditions of reagents molar ratio, temperature and desiccant salt mass for the experimental design of the screening step.

Exp.	$SODD_{Sap}$: Isoamyl alcohol molar ratio, mol:mol ($R_{isoamyl}$)				Temperature, °C (T)		Desiccant salt mass/SODD mass, wt.% ($m_{drying\ salt}$)	
	SODD		Isoamyl alcohol					
1	1	:	2	(-1)	35	(-1)	1	(-1)
2	1	:	2	(-1)	35	(-1)	2	(+1)
3	1	:	2	(-1)	45	(+1)	1	(-1)
4	1	:	2	(-1)	45	(+1)	2	(+1)
5	1	:	4	(+1)	35	(-1)	1	(-1)
6	1	:	4	(+1)	35	(-1)	2	(+1)
7	1	:	4	(+1)	45	(+1)	1	(-1)
8	1	:	4	(+1)	45	(+1)	2	1
9	1	:	3	(0)	40	(0)	1.5	(0)
10	1	:	3	(0)	40	(0)	1.5	(0)
11	1	:	3	(0)	40	(0)	1.5	(0)
12	1	:	3	(0)	40	(0)	1.5	(0)
13	1	:	3	(0)	40	(0)	1.5	(0)
14	1	:	1.32	(-1.68)	40	(0)	1.5	(0)
15	1	:	3	(0)	31.6	(-1.68)	1.5	(0)
16	1	:	3	(0)	40	(0)	0.659	(-1.68)
17	1	:	4.68	(+1.68)	40	(0)	1.5	(0)
18	1	:	3	(0)	48.4	(+1.68)	1.5	(0)
19	1	:	3	(0)	40	(0)	2.341	(+1.68)

4.2.3.4.2 Influence of desiccant salt mass concentration on reaction yield

The influence of the desiccant salt mass concentration in the synthesis of isoamyl esters was evaluated using $m_{desiccant\ salt}$ values from 2 to 16%. The procedure was the same as described in Section 4.2.3.4.1, using the best conditions of $R_{isoamyl}$ and T obtained from the experimental design of the screening assays (1 mol of $SODD_{Sap}$ to 2.3 mol of isoamyl alcohol, 40 °C).

4.2.3.4.3 Refining of the isoamyl esters synthesis using experimental design

A final refining for the variables $R_{isoamyl}$ and $m_{desiccant\ salt}$ was performed using experimental design and response surface methodology to establish the optimum conditions. The experimental procedure was the same as described in Section 4.2.3.4.1, with T of 40 °C for all experiments. Table 4.2-04 provides the experimental conditions for the variables $R_{isoamyl}$ and $m_{desiccant\ salt}$.

Table 4.2-04. Conditions of reagents molar ratio and desiccant salt mass for the experimental design of the refining step.

Exp.	$SODD_{Sap}$: Isoamyl alcohol molar ratio, mol:mol ($R_{isoamyl}$)				Desiccant salt mass/SODD mass, wt.% ($m_{desiccant\ salt}$)	
	SODD		Isoamyl alcohol			
1	1	:	2	(-1)	12	(-1)
2	1	:	2	(-1)	18	(+1)
3	1	:	4	(+1)	12	(-1)
4	1	:	4	(+1)	18	(+1)
5	1	:	1.59	(-1.41)	15	(0)
6	1	:	4.41	(+1.41)	15	(0)
7	1	:	3	(0)	10.76	(-1.41)
8	1	:	3	(0)	19.24	(+1.41)
9	1	:	3	(0)	15	(0)
10	1	:	3	(0)	15	(0)
11	1	:	3	(0)	15	(0)

4.2.3.5 FAIEs reaction course

Monitoring of the reaction for synthesis of the isoamyl esters was performed during assays performed in a jacketed reactor at 40 °C, with 350 TBU of enzyme (free or hNF-PFL) for each 1 mL of SODD, 1.0 mol $SODD_{Sap}$: 3.51 mol isoamyl alcohol, and 15% of desiccant salt (desiccant salt mass/SODD mass), under mechanical stirring at 1250 rpm with a straight blade impeller. Samples were collected at different time intervals and were washed as described in Section 4.2.3.4.1, prior to quantification of FAIEs by GC-FID. Monitoring was also performed of the reaction for synthesis of FAIEs in the absence of the desiccant salt, using 500 TBU of hNF-PFL for each 1 mL of SODD (the other conditions and procedures were kept the same).

4.2.3.6 Assay of hNF-PFL reuse test

The hNF-PFL reuse assay was performed using a jacketed reactor at 40 °C, in the absence of desiccant salt, with 500 TBU of hNF-PFL for each 1 mL of SODD, 1.0 mol $SODD_{Sap}$: 3.51 mol isoamyl alcohol, and mechanical stirring at 1250 rpm with a straight blade impeller. After 24 h, the reaction medium was centrifuged at 10707 rpm and 25 °C for 5 min, a sample of the liquid phase was withdrawn, the rest of the liquid phase was discarded, and the hNF-PFL (solid phase) was resuspended in SODD and isoamyl alcohol for a new cycle. The sample was washed as described in Section 4.2.3.4.1, prior to quantification of the FAIEs by GC-FID.

4.2.3.7 Hydrolytic activity determination

The hydrolytic activity of the PFL (free or immobilized) was measured by the tributyrin hydrolysis method, using a pHstat instrument (Ramos et al. 2018), in order to determine the initial reaction rate and, therefore, the hydrolytic activity. The PFL samples were transferred to a jacketed reactor containing 22.5 mL of 26.67 mM sodium phosphate buffer pH 7.5 and 1.5 mL of tributyrin, at 37 °C, under mechanical stirring at 900 rpm. The butyric acid released in the medium was neutralized using 20 mM potassium hydroxide (KOH) solution to maintain the medium pH at 7.5 (using a 1:1 molar ratio of butyric acid to KOH). One tributyrin hydrolysis unit (TBU) was considered as the quantity of micromoles of KOH consumed per minute (1 TBU = 1 μmol_{KOH}/min).

4.2.3.8 GC analysis

4.2.3.8.1 FAIEs quantification

Quantification of the FAIEs was performed by GC-FID analysis using a chromatograph (Model 7890A, Agilent Technologies, Santa Clara, CA, USA) equipped with a capillary column (Rtx-Wax, 30 m × 0.25 mm × 0.25 μm; Restek Co., Bellefonte, PA, USA). The injector was operated at 250 °C, with a split ratio of 31.25:1. The carrier gas was helium, supplied at a pressure of 13.593 psi and total flow rate of 67.5 mL/min. The oven had a temperature ramp of 150 °C (hold time and rum time of 2 min), 180 °C (rate of 10 °C/min, hold time of 3 min and rum time until 8 min) and 230 °C (rate of 10 °C/min, hold time of 12 min and rum time until 25 min). The FID was operated at 250 °C, with hydrogen, synthetic air, and nitrogen flow rates of 30, 400, and 25 mL/min, respectively. The sample injection volume was 1 μL. Isopropanol and hexene were used to clean the injection syringe.

The samples consisted of approximately 50 mg of dry sample (weighed out using a high precision balance) and 1 mL of a solution of 1 mg/mL methyl heptadecanoate in heptane. Equation 3 was used to calculate the reaction yield percentage (Y, wt.%):

$$Y\ [wt.\%] = 100 \cdot \frac{\sum A_i}{A_{standard}} \cdot \frac{C_{standard} \cdot V_{standard}}{m_{sample}} \quad (3)$$

where, A_i is the sum of the areas of the FAIE peaks in the chromatogram, $A_{standard}$ is the area of the methyl heptadecanoate peak, $C_{standard}$ is the mass concentration of methyl heptadecanoate solution in heptane (1 mg/mL), $V_{standard}$ is the volume of the methyl heptadecanoate heptane solution (1 mL), and m_{sample} is the mass of sample used in the reaction (~50 mg).

4.2.3.8.2 Quantification of acylglycerides and glycerin

The contents of monoglycerides, diglycerides, triglycerides, and glycerin were quantified by GC-FID, according to the ASTM D6584 standard (American Society for Testing and Materials, 2018), using a chromatograph (Model 7890A, Agilent Technologies, Santa Clara, CA, USA) equipped with a Select Biodiesel for Glycerides column (15 m × 0.32 mm × 0.1 µm + 2 m RG, Agilent Technologies, Santa Clara, CA, USA). The carrier gas was helium, at a pressure of 7.52 psi and flow rate of 3 mL/min. The oven had a temperature ramp of 50 °C (hold time and rum time of 1 min), 180 °C (rate of 15 °C/min, hold time of 0 min and rum time until 9.67 min), 230 °C (rate of 7 °C/min, hold time of 0 min and rum time until 16.81 min) and 380 °C (rate of 30 °C/min, hold time of 10 min and rum time until 31.81 min). The FID was operated at 300 °C, with hydrogen, synthetic air, and nitrogen flow rates of 30, 400, and 25 mL/min, respectively. Injection was made of 1 µL of dry sample, with isopropanol and hexene used to clean the injection syringe.

4.2.3.9 Chemical and physicochemical characterizations of biolubricant products

4.2.3.9.1 FAIEs synthesis for the characterization tests

It was necessary to perform 4 batches, using 150 mL of SODD for each batch, in order to obtain the amount of sample required for the characterization measurements. Each batch was performed in a jacketed reactor at 40 °C, without desiccant salt, using 1.0 mol $SODD_{Sap}$: 3.51 mol isoamyl alcohol, under mechanical stirring at 800 rpm with a straight blade impeller, until maximum Y was reached. Before the first batch, the hNF-PFL was placed in ~40 mL of reaction medium, and submitted to a blood roller mixer for 1 h, at room temperature, followed by centrifugation at 10707 rpm and 25 °C for 5 min to separate the hNF-PFL. The first batch had 100 TBU of hNF-PFL available for each 1 mL of SODD, while the subsequent batches used the hNF-PFL recovered at the end of each previous batch. After each batch, the liquid phase was drained from the reactor, centrifuged at 10707 rpm and 25 °C for 5 min (to separate the remaining suspended hNF-PFL), and transferred to a separation funnel. It was then washed two

times with water at boiling point (3:1 v/v water : SODD ratio) and the nonpolar phase was stored in a refrigerator.

After the 4 batches, the washed nonpolar phase was transferred to a rotary evaporator, at 75 °C and -710 mm Hg, for evaporation of the remaining moisture and isoamyl alcohol (volatile light phase). The heavy phase with FAIEs (nonvolatile phase) was divided into two equal parts, one of which was treated with 4% (w/v) sodium hydroxide (NaOH) solution (caustic polishing, CP), using a ratio of 1 mol of FFA to 1.15 mol of NaOH (Miranda et al., 2020), with roller agitation for 30 min at room temperature. The CP FAIEs sample was washed five times with water at room temperature (1 mL of water for each mL of sample), in a separation funnel, followed by drying the CP-treated and untreated FAIEs samples overnight in an oven at 60 °C.

4.2.3.9.2 Chemical and physicochemical characterization tests for the oils

Determinations of moisture (Karl Fisher method), acid value, and saponification value were performed according to the AOCS Ca 2e-84, Cd 3d-63, and Cd 3-25 standard methods, respectively (American Oil Chemists' Society, 2004). The viscosities at 40 and 100 °C, viscosity index (VI), density, pour point, and flash point were determined according to ASTM standards D88, D2270, D1298, D97, and D92, respectively (American Society for Testing and Materials, 2018). The latter tests were performed at Lubrin Tribological Analyses (São Paulo, SP, Brazil).

4.2.3.10 Scanning electron microscopy

Scanning electron microscopy (SEM) analyses were performed using a Philips XL-30 microscope equipped with a field emission gun and a Bruker energy dispersive X-ray spectroscopy (EDS) accessory, at the Structural Characterization Laboratory of the Materials Engineering Department, Federal University of São Carlos (São Carlos, SP, Brazil).

4.2.4 Results

4.2.4.1 Lipase screening

Among the six lipases analyzed, PFL showed a very high transesterification capacity and a good capacity for esterification employing isoamyl alcohol, when compared with the other lipases (Table 4.2-05). CALB presented a very high esterification capability, but almost no transesterification capability, under the test conditions. The differences in the reaction yields

(RY) observed for the lipases were probably related to structural differences, with effects on substrate affinity, interfacial activation mechanisms, and optimum operational conditions. Based on the lipase screening results (Table 4.2-05), PFL was selected as the catalyst in the subsequent experiments.

Table 4.2-05. Reaction yields (RY) for esterification of oleic acid and transesterification of soybean oil with isoamyl alcohol. Molar ratios of 1 mol : 1 mol of oleic acid/isoamyl alcohol and 1 mol : 3 mol soybean oil/isoamyl alcohol. The experiments were conducted in a shaker at 37.5 °C and 250 rpm, during 12 h, using 600 TBU per g of acyl donor (oleic acid or soybean oil) for each lipase.

	Oleic Acid	Soybean Oil
Lipase	Reaction Yield (%)	Reaction Yield (%)
ETL 2.0	4.40 ± 0.31	0.92 ± 0.31
CALB	38.02 ± 0.54	0.17 ± 0.04
TLL	4.66 ± 0.17	7.03 ± 0.87
CRL	5.04 ± 0.08	8.61 ± 0.95
RNL	4.54 ± 0.00	2.22 ± 0.08
PFL	7.43 ± 0.32	41.39 ± 1.01

4.2.4.2 Optimization of hNF hNF-PFL immobilization parameters

An experimental design for a quadratic model, with broad ranges of the variables C_{prot}, C_{CuSO_4}, and PBS pH, was used as a first approach to identify their appropriate levels and to better understand the relations among the variables. The variation of C_{prot}, C_{CuSO_4}, and PBS pH in the proposed ranges resulted in IY varying from 0.04 %TBU (Exp. 6) to 34.55 %TBU (Exp. 5), as shown in Table 4.2-06.

Table 4.2-06. Immobilization yields (IY) of hNF-PFL for the different experimental conditions of C_{prot}, C_{CuSO_4}, and PBS pH, as described in Table 4.2-01. Incubation at 25 °C for 3 days.

Exp.	C_{prot}	C_{CuSO_4}	PBS pH	IY (%TBU)
1	1	1	0	21.97
2	1	-1	0	3.46
3	1	0	1	17.02
4	1	0	-1	1.31
5	0	1	1	34.55
6	0	1	-1	0.04
7	0	-1	1	14.41
8	0	-1	-1	7.72
9	-1	1	0	0.32
10	-1	-1	0	5.02
11	-1	0	1	6.68
12	-1	0	-1	5.40
13	0	0	0	22.64
14	0	0	0	20.33
15	0	0	0	24.54
16	0	0	0	24.83

The coefficients of the second-degree equation obtained are shown in Table 4.2-07. Many of these coefficients had p-value slightly higher than 0.05. Analysis of variance (ANOVA) applied to the model (Table 4.2-08) showed that it had slight lack of fit, as indicated by a small difference between the calculated and tabulated F values. However, R^2 was relatively high, indicating satisfactory agreement between the model and the experimental data (IY values in Table 4.2-06). Comparison of the experimental data with the values predicted using the quadratic equation (coefficients in Table 4.2-07) showed that the experimental and predicted data were similar (Table 4.2-09).

Table 4.2-07. Coefficients calculated for the quadratic model based on the results data set of Table 4.2-06.

Coefficients		Standard Error	p-value
Independent (a_0)	23.09	2.14	3.80×10^{-5}
C_{prot}	3.29	1.52	7.29×10^{-2}
C_{CuSO_4}	3.28	1.52	7.35×10^{-2}
PBS pH	7.27	1.52	3.02×10^{-3}
C_{prot} x C_{CuSO_4}	5.80	2.14	3.53×10^{-2}
C_{prot} x PBS pH	3.61	2.14	1.44×10^{-1}
C_{CuSO_4} x PBS pH	6.96	2.14	1.76×10^{-2}
C_{prot}^2	-10.99	2.14	2.17×10^{-3}
$C_{CuSO_4}^2$	-4.41	2.14	8.57×10^{-2}
PBS pH^2	-4.50	2.14	8.09×10^{-2}

For a 95% of confidence level, the p-value for the coefficients must be < 0.05.

Table 4.2-08. ANOVA for the quadratic equation model with the coefficients of Table 4.2-07.

	SS	DF	MS	F calculated	F tabulated
Regression	1618.06	9	179.78	9.7693	4.0990
Residual	110.42	6	18.40		
Total	1728.48	15	115.23		
Residue					
Pure Error	12.99	3	4.33	7.5026	9.2766
Lack of Fit	97.43	3	32.48		
R^2	0.93612	R	0.96753		
R_{max}^2	0.99249	R_{max}	0.99624		

SS: Sum of Square; DF: Degrees of Freedom; MS: Mean Square

Table 4.2-09. Experimental data from Table 4.2-06 and the corresponding predicted results using the quadratic model with the coefficients of Table 4.2-07.

	IY (%TBU)	
Exp.	Experimental	Predicted
1	21.97	20.07
2	3.46	1.90
3	17.02	21.77
4	1.31	0.02
5	34.55	31.70
6	0.04	3.24
7	14.41	11.21
8	7.72	10.58
9	0.32	1.88
10	5.02	6.92
11	6.68	7.97
12	5.40	0.64
13	22.64	23.09
14	20.33	23.09
15	24.54	23.09
16	24.83	23.09

Considering the significant coefficients (p-value < 0.05), shown in Table 4.2-07, it was not possible to disregard any of the variables, since all had at least one significant coefficient. When a regression was performed with only the significant coefficients, the model showed substantial lack of fit and the R^2 value decreased to 0.71415. The predicted values generated also became worse than the predicted values obtained using all the coefficients of Table 4.2-07, when compared with the experimental data. Therefore, the response surfaces were constructed using a model with all the coefficients of Table 4.2-07.

Figure 4.2-01 shows a trend of higher IY with increasing C_{CuSO_4}, obtaining the best IY at C_{prot} and C_{CuSO_4} of 0.14 mg_{prot}/mL and 1.75 mM, respectively. Figure 4.2-02 evidences a trend of higher IY at more alkaline PBS pH, with the best IY at C_{prot} and PBS pH of 0.14 mg_{prot}/mL and 7.92, respectively. Figure 4.2-03 confirms the two trends towards higher IY provided by increasing C_{CuSO_4} and PBS pH, with the best IY observed at the extreme of the graph, at C_{CuSO_4} and PBS pH of 2.00 mM and 8.00, respectively. An experimental point made at C_{prot}, C_{CuSO_4}, and PBS pH of 0.14 mg_{prot}/mL, 2.00 mM, and 8.00, respectively, resulted in IY = 34.83 ± 1.53 %TBU, while the predicted value for the same conditions (using the coefficients of Table 4.2-07) was 34.52 %TBU.

Figure 4.2-01. Response surface for the quadratic model obtained using the coefficients of Table 4.2-07 for the variables C_{prot} and C_{CuSO_4}.

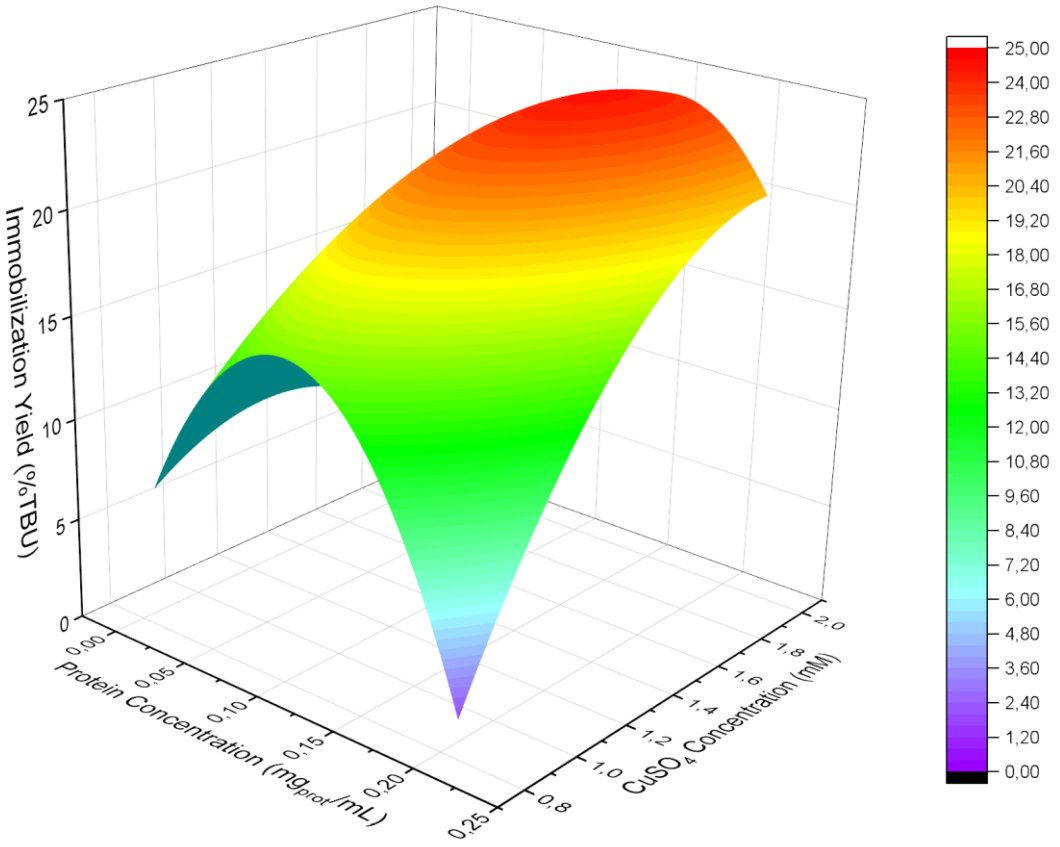

Figure 4.2-02. Response surface for the quadratic model obtained using the coefficients of Table 4.2-07 for the variables C_{prot} and PBS pH.

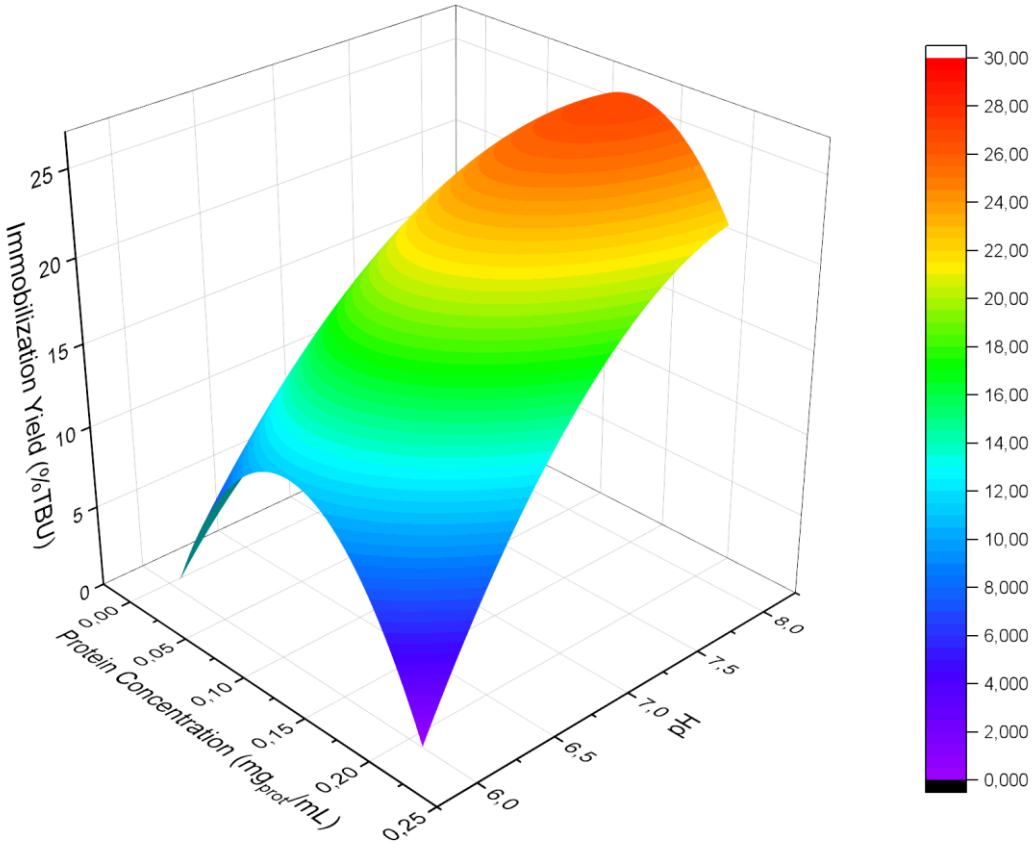

Figure 4.2-03. Response surface for the quadratic model obtained using the coefficients of Table 4.2-07 for the variables C_{CuSO_4} and PBS pH.

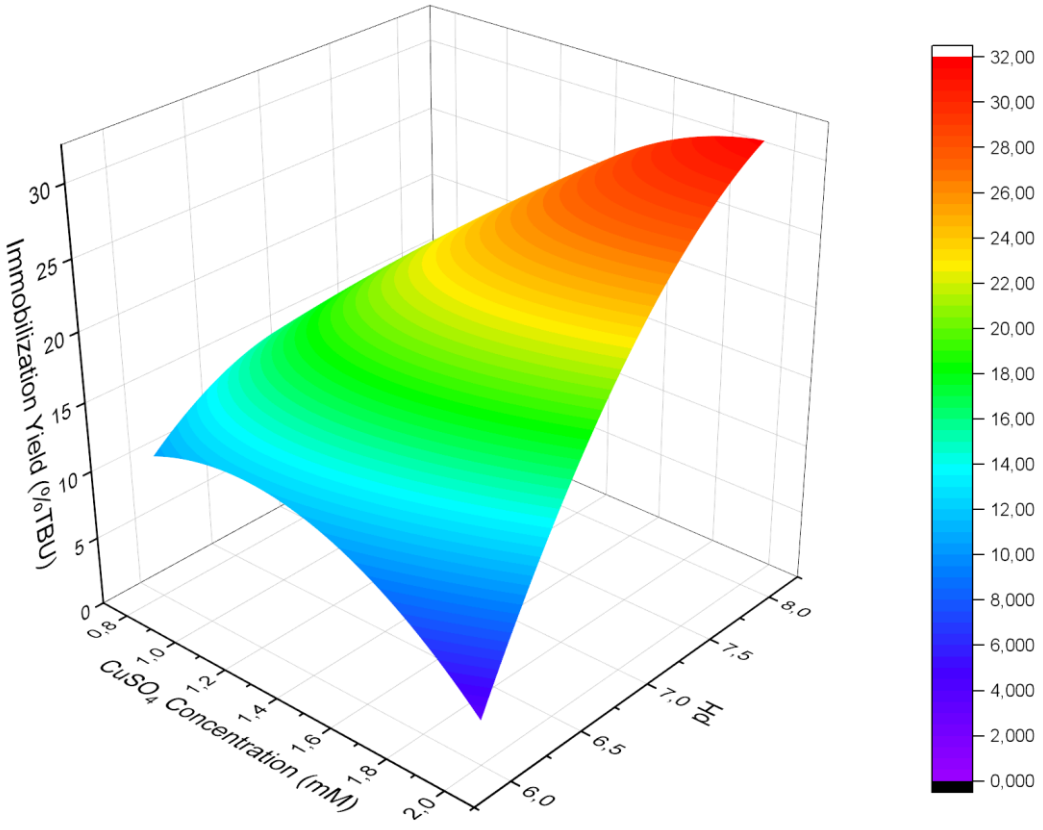

The results shown by the response surfaces (Figures 4.2-01, 4.2-02, and 4.2-03) indicated that further investigation was required of the effect of increasing C_{CuSO_4}. It was not possible to increase PBS pH, due to the pH limitation of the phosphate buffer required to compose the inorganic matrix of the hNFs. Therefore, C_{CuSO_4} was increased, using C_{prot} and PBS pH of 0.14 mg_{prot}/mL and 8.00, respectively. Figure 4.2-04 shows increases of IY and IA to 45.75 ± 0.46 %TBU and 51.26 ± 0.50 %TBU, respectively, at C_{CuSO_4} of 7.04 mM.

Figure 4.2-04. Influence of C_{CuSO_4} on IY and IA for C_{prot} of 0.14 mg_{prot}/mL and PBS pH of 8.0. Incubation at 25 °C for 3 days.

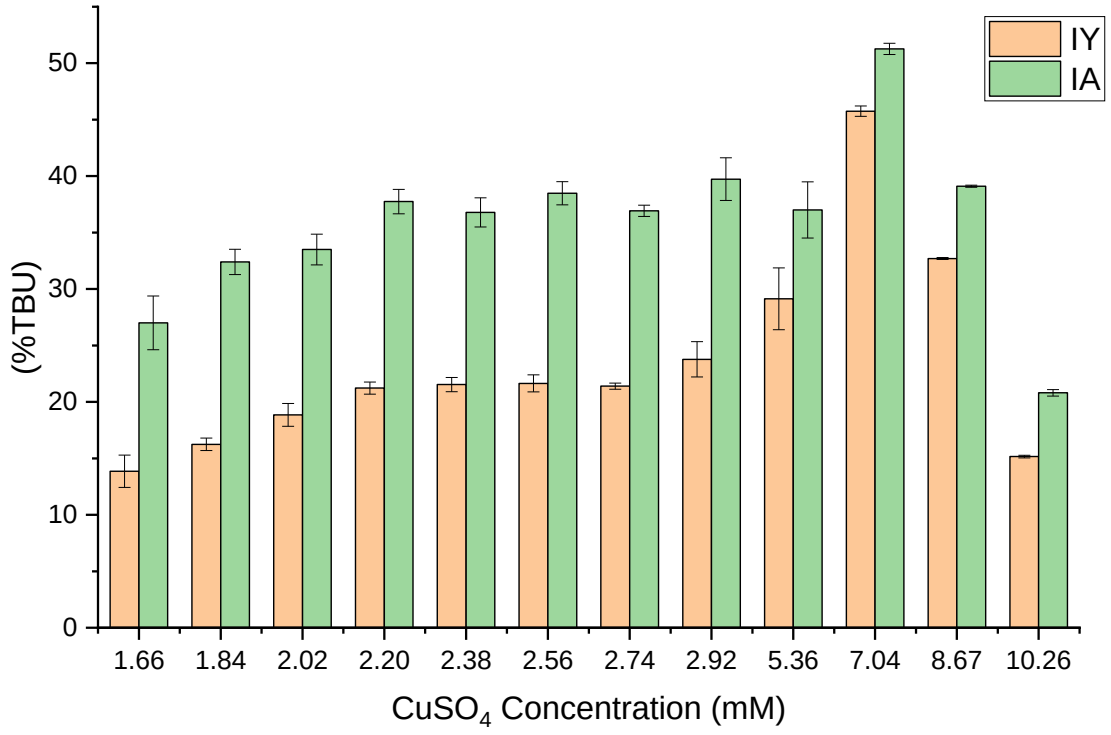

The literature concerning enzymes immobilized by hNFs frequently reports hyperactivation of enzymes. For example, immobilization of a PPL tII using hNFs achieved an immobilized activity of 876% (Li et al., 2016). Therefore, aiming at improving the hNF-PFL immobilized activity, changes were made in the incubation step, together with the application of surfactants. Soni et al. (2018) used the hNF method to immobilize BCL, with pretreatment using sodium dodecyl sulfate and incubation of the immobilization medium at 25 °C for 3 days, resulting in 399% immobilized activity (compared to the free lipase). When the immobilization medium was incubated using ultrasonication for 7.5 min, the immobilized activity reached 423%. Dwivedee et al. (2018) reported an immobilized activity increase of 89% (from 826.3 to 1562.7%) for a PFL hNF produced with cobalt metal, when the incubation was changed from static at 25 °C for 3 days to 10 min under ultrasonication. Cui et al. (2016) used 0.25 mM of cetyl trimethyl ammonium bromide (CTAB) as surfactant to activate BPL tII during the hNF immobilization, obtaining immobilized activities of 460% and 200%, compared to the free lipase and BPL tII hNF without surfactant, respectively. Li et al. (2020) reported immobilized activity of 172%, compared to the free lipase, using 0.15 mM of Tween 80 in the preparation of hNFs with AOL. In the absence of the surfactant, immobilized activity of 75% was obtained.

In the present work, the changes studied in the incubation step of the PFL-hNF synthesis were as follows: use of ultrasound before the 3 days of static incubation at 25 °C; use of ultrasound alone, without the 3 days of static incubation; use of stirring by flask rotation for 3 days at 25 °C; static incubation at 35 °C for 3 days; and no incubation at all. Investigation was also made of the influence of different concentrations of three nonionic surfactants: Triton X-100 (TX-100), Tween 20 (T-20), and Tween 80 (T-80). None of the incubation alterations or surfactants had any significative effect on the IY or IA of the hNF-PFL (Figures 4.2-05 and 4.2-06). The use of ultrasound (for 20 or 60 min) or static incubation at 35 °C for 3 days resulted in practically the same IY and IA as obtained using static incubation at 25 °C for 3 days. Given the considerable reduction of the incubation time from 3 days to 20 min, an incubation step of 20 min under ultrasonication was selected in the subsequent tests.

Figure 4.2-05. Comparison of different strategies for incubation of the hNF-PFL immobilization medium. Immobilization conditions: C_{prot} of 0.14 mg_{prot}/mL, C_{CuSO_4} of 7.04 mM, and PBS pH of 8.0. US: ultrasound; LR: low speed rotation; MR: medium speed rotation.

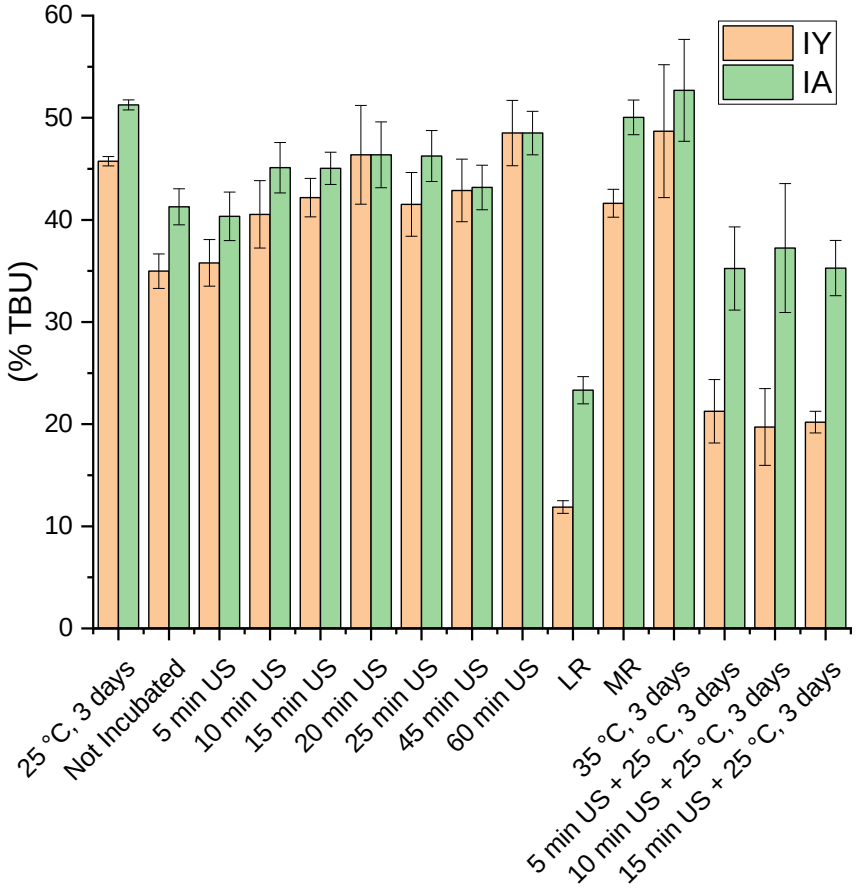

Figure 4.2-06. Comparison of the effects of different concentrations of three nonionic surfactants on the IY and IA of the hNF-PFL. Immobilization conditions: C_{prot} of 0.14 mg_{prot}/mL, C_{CuSO_4} of 7.04 mM, and PBS pH of 8.0. Incubation for 20 min under ultrasonication. TX-100: Triton X-100; T-20: Tween 20; T-80: Tween 80.

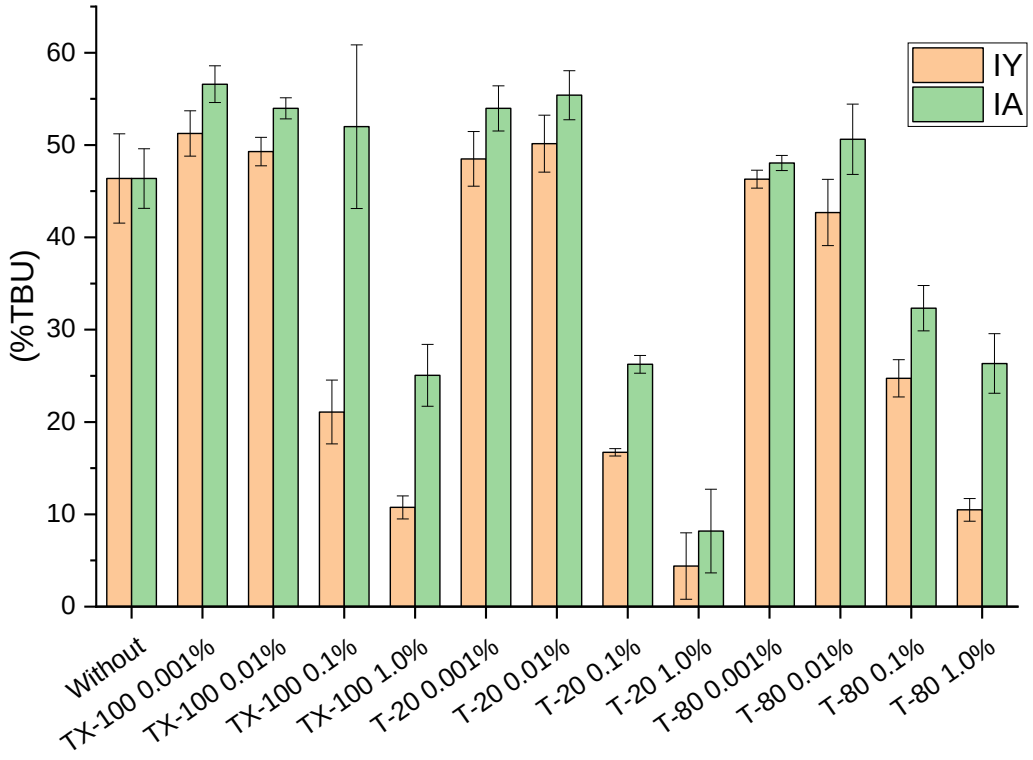

Finally, fine tuning of C_{prot} and C_{CuSO_4} was performed using experimental design (quadratic model). The assays employed PBS at pH 8.0, with incubation of the immobilization medium for 20 min under ultrasonication. Table 4.2-10 shows the IY results for the different experimental conditions, with the values varying from 40.63 %TBU (Exp. 6) to 54.96 %TBU (Exp. 7).

Table 4.2-10. IY results for the fine tuning of the hNF-PFL synthesis. The experiments were conducted using PBS at pH 8.0, with incubation for 20 min under ultrasonication.

Exp.	C_{prot} (mg_{prot}/mL)	C_{CuSO_4} (mM)	IY (%TBU)
1	1	1	51.70
2	1	-1	52.04
3	-1	1	45.42
4	-1	-1	43.53
5	0	-1.414	52.91
6	-1.414	0	40.63
7	0	1.414	54.96
8	1.414	0	52.59
9	0	0	51.26
10	0	0	50.44
11	0	0	49.30

The first attempt revealed that C_{CuSO_4} was not statistically significant, as shown in Table 4.2-11. This could have been due to the previous optimization of C_{CuSO_4} and the more restricted range adopted.

Table 4.2-11. Coefficients of the quadratic model for the variables C_{prot} and C_{CuSO_4}, based on the data set of Table 4.2-10.

Coefficients		Standard Error	p-value
Independent (a_0)	50.34	0.88	3.07×10^{-8}
C_{prot}	3.96	0.54	7.27×10^{-4}
C_{CuSO_4}	0.56	0.54	3.48×10^{-1}
$C_{prot} \times C_{CuSO_4}$	-0.56	0.76	4.96×10^{-1}
C_{prot}^2	-2.39	0.64	1.36×10^{-2}
$C_{CuSO_4}^2$	1.27	0.64	1.04×10^{-1}

For a 95% confidence level, the p-value for the coefficients must be < 0.05.

Disregarding the C_{CuSO_4} variable, a new regression showed that the C_{prot} coefficients were significant (Table 4.2-12). Application of ANOVA (Table 4.2-13) and comparison of the calculated and tabulated F values showed that the model provided a satisfactory fit to the experimental data, with relatively high R^2. The experimental data and the predicted values were very similar (Table 4.2-14).

Table 4.2-12. Coefficients of the quadratic model for the variable C_{prot}, based on the data set of Table 4.2-10.

Coefficients		Standard Error	p-value
Independent (a_0)	51.53	0.73	1.90×10^{-12}
C_{prot}	3.96	0.62	2.07×10^{-4}
C_{prot}^2	-2.76	0.70	4.38×10^{-3}

For a 95% of confidence level, the p-value for the coefficients must be < 0.05.

Table 4.2-13. ANOVA results for the quadratic equation model of C_{prot}, with the coefficients of Table 4.2-12.

	SS	DF	MS	F calculated	F tabulated
Regression	172.78	2	86.39	28.2456	4.4590
Residual	24.47	8	3.06		
Total	197.25	10	19.72		
Residue					
Pure Error	21.43	6	3.57	0.4255	5.1433
Lack of Fit	3.04	2	1.52		
R^2	0.87595	R	0.93592		
R_{max}^2	0.89136	R_{max}	0.94412		

SS: Sum of Square; DF: Degrees of Freedom; MS: Mean Square

Table 4.2-14. Comparison of the experimental data from Table 4.2-10 and the predicted values obtained using the model with the coefficients of Table 4.2-12.

	IY (%)	
Exp.	Experimental	Predicted
1	51.70	52.74
2	52.04	52.74
3	45.42	44.81
4	43.53	44.81
5	52.91	51.53
6	40.63	40.41
7	54.96	51.53
8	52.59	51.62
9	51.26	51.53
10	50.44	51.53
11	49.30	51.53

The response surface based on the coefficients of Table 4.2-12 (Figure 4.2-07) showed an optimum C_{prot} of 0.1688 mg_{prot}/mL, predicting hNF-PFL with IY of 52.96 %TBU. Therefore, hNF-PFL synthesis was performed using C_{prot}, C_{CuSO_4}, and PBS pH values of 0.1688 mg_{prot}/mL, 7.0 mM, and 8.00, respectively. The resulting material presented IY of 53.94 ± 1.29 %TBU and IA of 63.98 ± 1.87 %TBU.

Figure 4.2-07. Response of the C_{prot} model using the coefficients of Table 4.2-12.

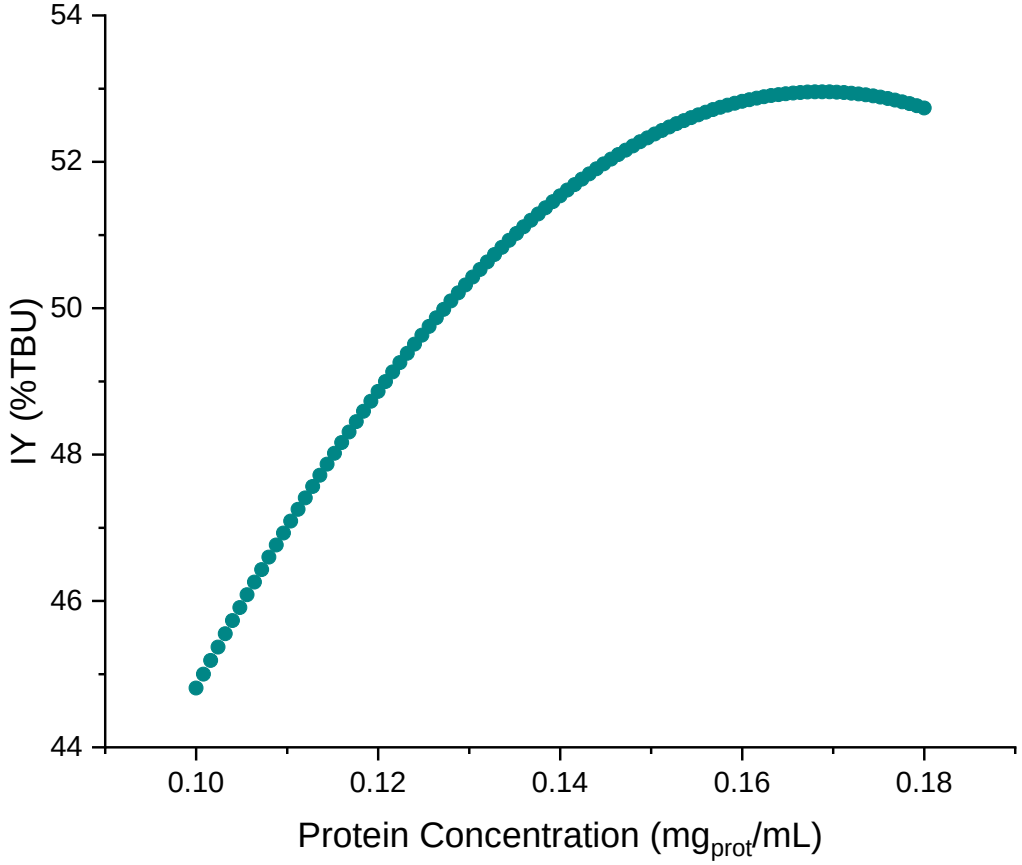

Analysis of the hNF-PFL obtained under the optimized conditions was performed using scanning electron microscopy (SEM), with elemental mapping by energy dispersive X-ray spectroscopy (EDS). Figure 4.2-08 (a-b) shows the formation of hNF-PFL structures, which were highly porous and with diameters varying from ~1 to ~9 µm. EDS elemental mapping (Figure 4.2-08 (c-g)) showed that the enzyme was homogeneously distributed in the hNF-PFL structures, as indicated by the nitrogen and carbon elements, which corresponded to 1.08 ± 0.97 and 16.99 ± 2.64 wt.%, respectively (Table 4.2-15).

Figure 4.2-08. (a) and (b) High resolution SEM images of hNF-PFL. EDS elemental mapping of copper (c), phosphorus (d), oxygen (e), nitrogen (f), and carbon (g), and SEM image (h).

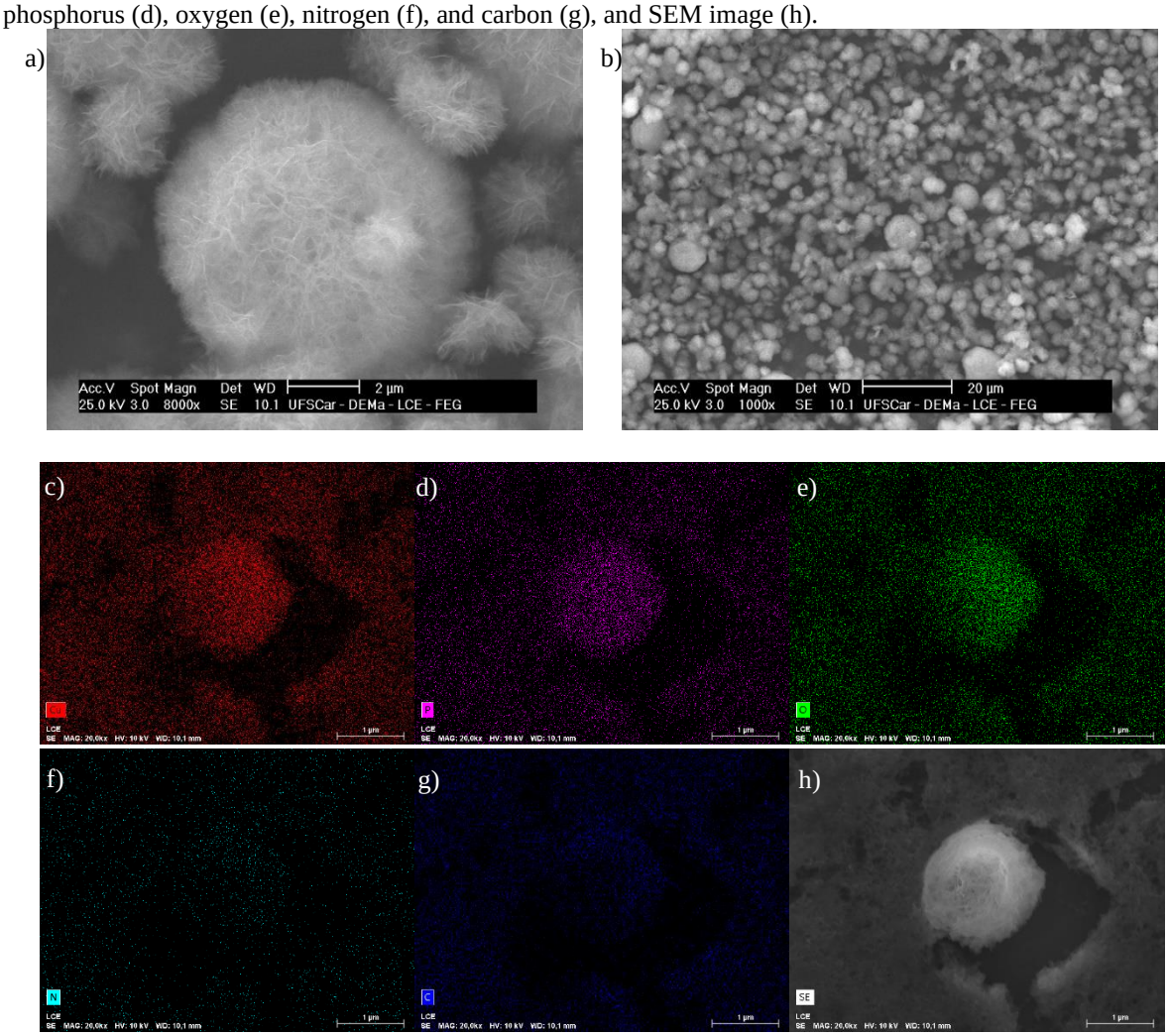

Table 4.2-15. EDS elemental analysis of hNF-PFL.

Element	Nitrogen	Carbon	Phosphorus	Oxygen	Copper
Mass (wt.%)	1.08 ± 0.97	16.99 ± 2.64	10.41 ± 0.81	25.00 ± 1.14	46.51 ± 1.12

4.2.4.3 Optimization of reaction conditions for obtaining FAIEs from SODD

In order to establish the optimal conditions for production of FAIEs from SODD, catalyzed by hNF-PFL, a screening of the variables was first performed according to an experimental design for a quadratic model, based on the range conditions used in the SODD FAIEs studies reported by Araujo-Silva et al. (2022). The reaction yield (RY) results for the different conditions of $R_{isoamyl}$, T, and $m_{desiccant\ salt}$ applied in the synthesis of FAIEs from SODD using hNF-PFL as catalyst are provided in Table 4.2-16. The lowest and highest observed RY values were 4.59 wt.% (Exp. 7) and 12.54 wt.% (Exp. 2), respectively.

Table 4.2-16. FAIEs reaction yields (RY) for the experimental design conditions of Table 4.2-03, with 100 TBU/mL of SODD, in a shaker at 250 rpm for 24 h.

Exp.	$R_{isoamyl}$ (mol $SODD_{Sap}$: mol isoamyl alcohol)	T (°C)	$m_{desiccant\ salt}$ (wt.%)	Reaction Yield, RY (wt.%)
1	-1	-1	-1	9.65
2	-1	-1	1	12.54
3	-1	1	-1	7.30
4	-1	1	1	11.49
5	1	-1	-1	6.59
6	1	-1	1	8.43
7	1	1	-1	4.59
8	1	1	1	5.55
9	0	0	0	9.57
10	0	0	0	9.79
11	0	0	0	9.02
12	0	0	0	8.91
13	0	0	0	10.11
14	-1.68	0	0	5.76
15	0	-1.68	0	9.28
16	0	0	-1.68	7.02
17	1.68	0	0	5.19
18	0	1.68	0	6.88
19	0	0	1.68	8.48

The quadratic model obtained presented many indicators of lack of fit, so cubic terms were inserted in the model, improving the lack of fit and increasing R^2 from 0.76356 to 0.91537. The variable T was not statistically significant for variation of the results (considering a confidence level of 95%), so a model with the two remaining variables ($R_{isoamyl}$ and $m_{desiccant\ salt}$) and cubic terms was evaluated. This model generated the coefficients shown in Table 4.2-17. The ANOVA results, shown in Table 4.2-18, indicated that the model had low lack of fit, with a small difference between the calculated and tabulated values of F. The R^2 value was moderate, but was close to the R_{max}^2 value. Comparison between the experimental data and the predicted values (calculated using the coefficients of Table 4.2-17) showed that they were similar (Table 4.2-19).

Table 4.2-17. Coefficients of the proposed model for $R_{isoamyl}$ and $m_{desiccant\ salt}$, with cubic terms, for the data set of Table 4.2-16.

Coefficients		Standard Error	p-value
Independent (a_0)	9.23	0.49	1.04×10^{-9}
$R_{isoamyl}$	-2.97	0.79	3.17×10^{-3}
$m_{desiccant\ salt}$	1.68	0.79	5.74×10^{-2}
$R_{isoamyl} \times m_{desiccant\ salt}$	-0.53	0.47	2.80×10^{-1}
$R_{isoamyl}^2$	-1.10	0.36	1.01×10^{-2}
$m_{desiccant\ salt}^2$	-0.30	0.36	4.16×10^{-1}
$R_{isoamyl}^3$	0.99	0.40	3.08×10^{-2}
$m_{desiccant\ salt}^3$	-0.44	0.40	2.95×10^{-1}

For a 95% confidence level, the p-value for the coefficients must be < 0.05.

Table 4.2-18. ANOVA of the model with the coefficients of Table 4.2-17.

	SS	DF	MS	F calculated	F tabulated
Regression	64.37	7	9.20	5.1934	3.0123
Residual	19.48	11	1.77		
Total	83.84	18	4.66		
Residue					
Pure Error	16.17	10	1.62	2.0456	4.9646
Lack of Fit	3.31	1	3.31		
R^2	0.76771	R	0.87619		
R_{max}^2	0.80716	R_{max}	0.89842		

SS: Sum of Square; DF: Degrees of Freedom; MS: Mean Square

Table 4.2-19. Experimental RY data and predicted values calculated using the coefficients of Table 4.2-17.

	RY (wt.%)	
Exp.	Experimental	Predicted
1	9.65	8.03
2	12.54	11.57
3	7.30	8.03
4	11.49	11.57
5	6.59	5.14
6	8.43	6.55
7	4.59	5.14
8	5.55	6.55
9	9.57	9.23
10	9.79	9.23
11	9.02	9.23
12	8.91	9.23
13	10.11	9.23
14	5.76	6.39
15	9.28	9.23
16	7.02	7.65
17	5.19	5.82
18	6.88	9.23
19	8.48	9.10

Not all the coefficients of Table 4.2-17 were significant, so a new regression was performed using only the significant coefficients. Tables 4.2-20 and 4.2-21 present the new coefficient values and the ANOVA results for the model obtained using only the significant coefficients. All the coefficients of Table 4.2-20 were significant (p-value < 0.05) and there were improvements in the lack of fit, indicated by the F values, although R^2 decreased slightly to 0.69985 (Table 4.2-21). The experimental data and the predicted values were still close (Table 4.2-22).

Table 4.2-20. Coefficients of the new model using only the significant coefficients of Table 4.2-17.

Coefficients		Standard Error	p-value
Independent (a_0)	8.98	0.40	2.22×10^{-12}
$R_{isoamyl}$	-2.97	0.80	2.24×10^{-3}
$m_{desiccant\ salt}$	0.90	0.36	2.61×10^{-2}
$R_{isoamyl}^2$	-1.07	0.36	9.64×10^{-3}
$R_{isoamyl}^3$	0.99	0.40	2.77×10^{-2}

For a 95% confidence level, the p-value for the coefficients must be < 0.05.

Table 4.2-21, ANOVA results for the model of Table 4.2-20.

	SS	DF	MS	F calculated	F tabulated
Regression	58.68	4	14.67	8.1608	3.1122
Residual	25.17	14	1.80		
Total	83.84	18	4.66		
Residue					
Pure Error	16.17	10	1.62	1.3911	3.4780
Lack of Fit	9.00	4	2.25		
R^2	0.69985	R	0.83657		
R_{max}^2	0.80716	R_{max}	0.89842		

SS: Sum of Square; DF: Degrees of Freedom; MS: Mean Square

Table 4.2-22. Experimental RY data and predicted values calculated using the coefficients of Table 4.2-20.

	RY (wt.%)	
Exp.	Experimental	Predicted
1	9.65	8.99
2	12.54	10.80
3	7.30	8.99
4	11.49	10.80
5	6.59	5.04
6	8.43	6.84
7	4.59	5.04
8	5.55	6.84
9	9.57	8.98
10	9.79	8.98
11	9.02	8.98
12	8.91	8.98
13	10.11	8.98
14	5.76	6.25
15	9.28	8.98
16	7.02	7.47
17	5.19	5.69
18	6.88	8.98
19	8.48	10.50

The response surface obtained using the coefficients of Table 4.2-20 (Figure 4.2-09) indicated the need to increase $m_{desiccant\ salt}$, in order to increase RY. A simple study of $m_{desiccant\ salt}$ was conducted to determine a more appropriate range for a new experimental design. The assays used $R_{isoamyl}$ of 1 mol of $SODD_{Sap}$ to 2.3 mol of isoamyl alcohol (suggested from the response surface of Figure 4.2-09) and T of 40 °C (since the temperature was regarded as not

significant, it was fixed at its level zero value). As shown in Figure 4.2-10, increase of $m_{desiccant\ salt}$ to 14 wt.% increased RY by 35% (from 14.5 to 19.6 wt.%).

Figure 4.2-09. Response surface of the cubic model of $R_{isoamyl}$ and $m_{desiccant\ salt}$ using the coefficients of Table 4.2-20.

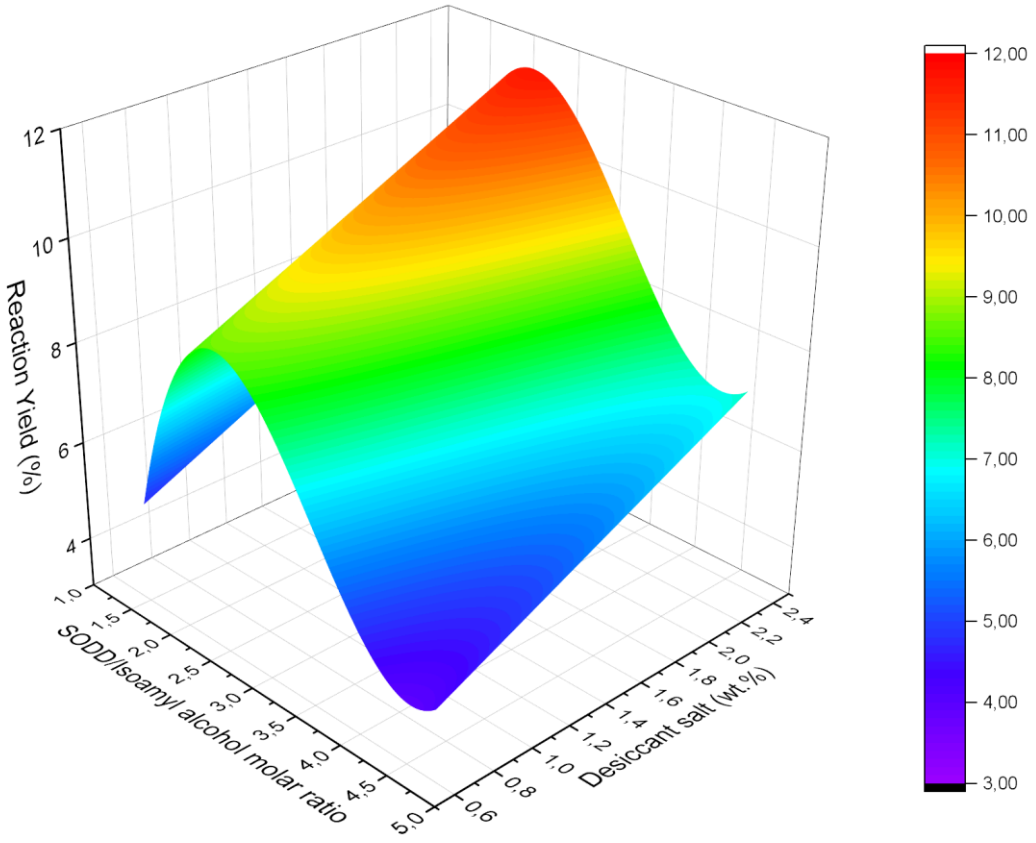

Figure 4.2-10. Influence of $m_{desiccant\ salt}$ on RY. Reaction conditions: 100 TBU/mL of SODD, $R_{isoamyl}$ of 1 mol of $SODD_{Sap}$ to 2.3 mol of isoamyl alcohol, and T of 40 °C, in a shaker at 250 rpm for 24 h.

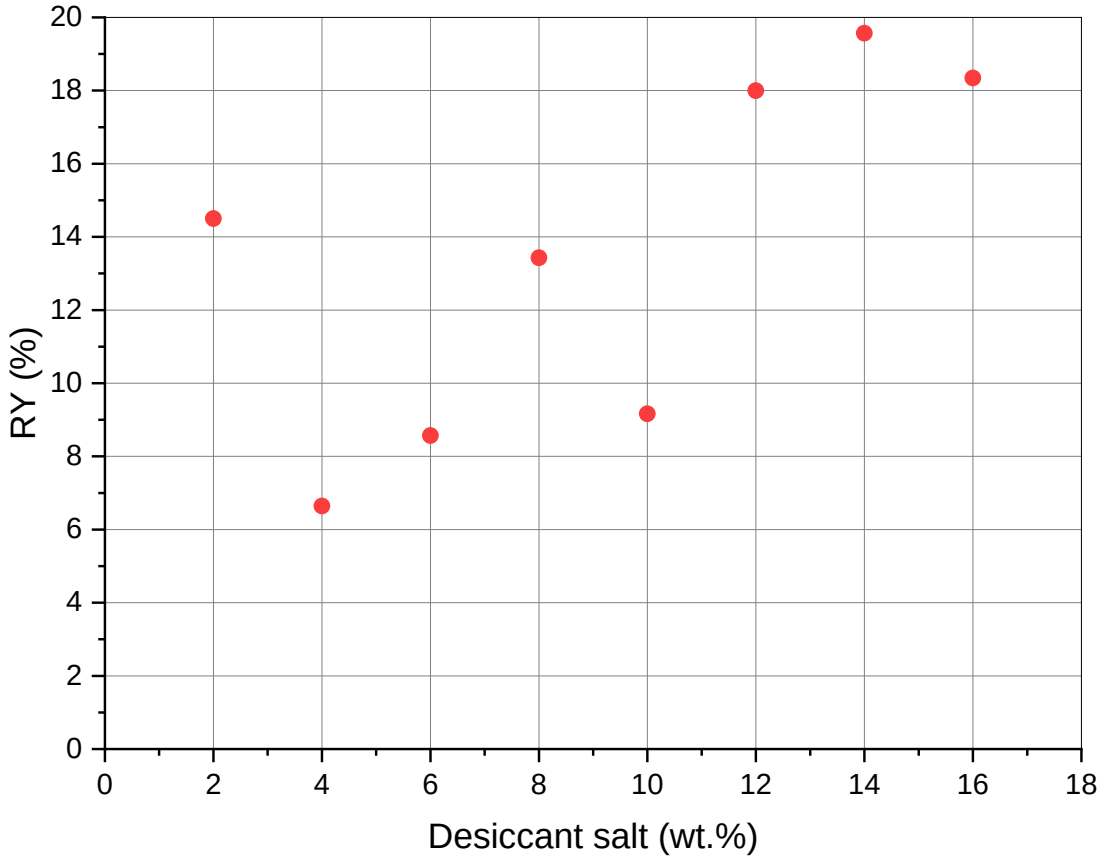

A refinement using experimental design for a quadratic model with the variables $R_{isoamyl}$ and $m_{desiccant\ salt}$ was conducted to identify the optimum conditions for higher RY. The results (Table 4.2-23) showed RY from 13.80 wt.% (Exp. 6) to 27.65 wt.% (Exp. 3 and Exp. 4). The results for a quadratic model were not satisfactory, so it was necessary to introduce cubic terms in the model. The coefficients of the cubic model are shown in Table 4.2-24, and the ANOVA results are provided in Table 4.2-25.

Table 4.2-23. FAIEs reaction yields (RY) for the experimental design conditions of Table 4.2-04, with 100 TBU/mL of SODD, in a shaker at 250 rpm and 40 °C for 24 h.

Exp.	$R_{isoamyl}$ (mol $SODD_{Sap}$: mol isoamyl alcohol)	$m_{desiccant\ salt}$ (wt.%)	RY (wt.%)
1	-1	-1	19.06
2	-1	1	16.57
3	1	-1	27.65
4	1	1	27.65
5	-1.414	0	19.61
6	1.414	0	13.80
7	0	-1.414	21.29
8	0	1.414	25.88
9	0	0	23.74
10	0	0	23.70
11	0	0	24.75

Table 4.2-24. Coefficients of the model for $R_{isoamyl}$ and $m_{desiccant\ salt}$ with cubic terms for the data set of Table 4.2-23.

Coefficients		Standard Error	p-value
Independent (a_0)	24.06	1.25	3.08×10^{-4}
$R_{isoamyl}$	11.89	2.43	1.63×10^{-2}
$m_{desiccant\ salt}$	-2.88	2.43	3.21×10^{-1}
$R_{isoamyl} \times m_{desiccant\ salt}$	0.62	1.08	6.06×10^{-1}
$R_{isoamyl}^2$	-3.03	0.91	4.50×10^{-2}
$m_{desiccant\ salt}^2$	0.41	0.91	6.86×10^{-1}
$R_{isoamyl}^3$	-6.97	1.53	2.00×10^{-2}
$m_{desiccant\ salt}^3$	2.25	1.53	2.39×10^{-1}

For a 95% confidence level, the p-value for the coefficients must be < 0.05.

Table 4.2-25. ANOVA results for the model with the coefficients of Table 4.2-24.

	SS	DF	MS	F calculated	F tabulated
Regression	189.66	7	27.09	5.7554	8.8867
Residual	14.12	3	4.71		
Total	203.79	10	20.38		
Residue					
Pure Error	0.71	2	0.36	37.7450	18.5128
Lack of Fit	13.41	1	13.41		
R^2	0.93070	R	0.96473		
R_{max}^2	0.99651	R_{max}	0.99825		

SS: Sum of Square; DF: Degrees of Freedom; MS: Mean Square

As shown in Table 4.2-24, the variable $m_{desiccant\ salt}$ was not statistically significant (considering a confidence level of 95%) for the variation of the results, in the range considered (from ~10 to ~20 wt.% of desiccant salt). The model presented substantial lack of fit, as indicated by the F values, but high R^2 was obtained, due to the similarity between the experimental data and the predicted values (Table 4.2-26).

Table 4.2--26. Experimental RY data and predicted values calculated using the coefficients of Table 4.2-24.

	RY (wt.%)	
Exp.	Experimental	Predicted
1	19.06	17.77
2	16.57	15.27
3	27.65	26.36
4	27.65	26.35
5	19.61	20.90
6	13.80	15.09
7	21.29	22.58
8	25.88	27.18
9	23.74	24.06
10	23.70	24.06
11	24.75	24.06

When regression was performed using only the significant coefficients shown in Table 4.2-24, all of them remained significant (Table 24.2-7) and the lack of fit improved considerably, as indicated by the F values (Table 4.2-28). The R^2 decreased from 0.93070 to 0.85900, but the experimental data and the predicted values were still very similar (Table 4.2-29).

Table 4.2-27. Coefficients of the model using only the $R_{isoamyl}$ variable and the data of Table 4.2-23.

Coefficients		Standard Error	p-value
Independent (a_0)	24.45	0.85	1.59E-08
$R_{isoamyl}$	11.89	2.27	1.19E-03
$R_{isoamyl}^2$	-3.15	0.81	6.13E-03
$R_{isoamyl}^3$	-6.97	1.43	1.82E-03

For a 95% confidence level, the p-value for the coefficients must be < 0.05.

Table 4.2-28. ANOVA results for the model using the coefficients of Table 4.2-27.

	SS	DF	MS	F calculated	F tabulated
Regression	175.05	3	58.35	14.2152	4.3468
Residual	28.73	7	4.10		
Total	203.79	10	20.38		
Residue					
Pure Error	11.73	4	2.93	1.9340	6.5914
Lack of Fit	17.01	3	5.67		
R^2	0.85900	R	0.92682		
R_{max}^2	0.94246	R_{max}	0.97080		

SS: Sum of Square; DF: Degrees of Freedom; MS: Mean Square

Table 4.2-29. Experimental RY data and predicted values calculated using the coefficients of Table 4.2-27.

	RY (wt.%)	
Exp.	Experimental	Predicted
1	19.06	16.38
2	16.57	16.38
3	27.65	26.21
4	27.65	26.21
5	19.61	21.05
6	13.80	15.24
7	21.29	24.45
8	25.88	24.45
9	23.74	24.45
10	23.70	24.45
11	24.75	24.45

The response graph for the model obtained using the coefficients of Table 4.2-27 (Figure 4.2-11) showed an optimum point at 3.5 mol of isoamyl alcohol (per 1 mol of $SODD_{Sap}$), with RY of 28.94 wt.%. The $m_{desiccant\ salt}$ value selected in the subsequent experiments was at the experimental design level zero (15 wt.%). Experimental confirmation under the optimum

conditions ($R_{isoamyl}$ of 1 mol of $SODD_{Sap}$ to 3.5 mol of isoamyl alcohol, $m_{desiccant\ salt}$ of 15 wt.%, and T of 40 °C) resulted in an observed RY of 23.80 ± 2.32 wt.%.

Figure 4.2-11. Response of the model using the coefficients of Table 4.2-27.

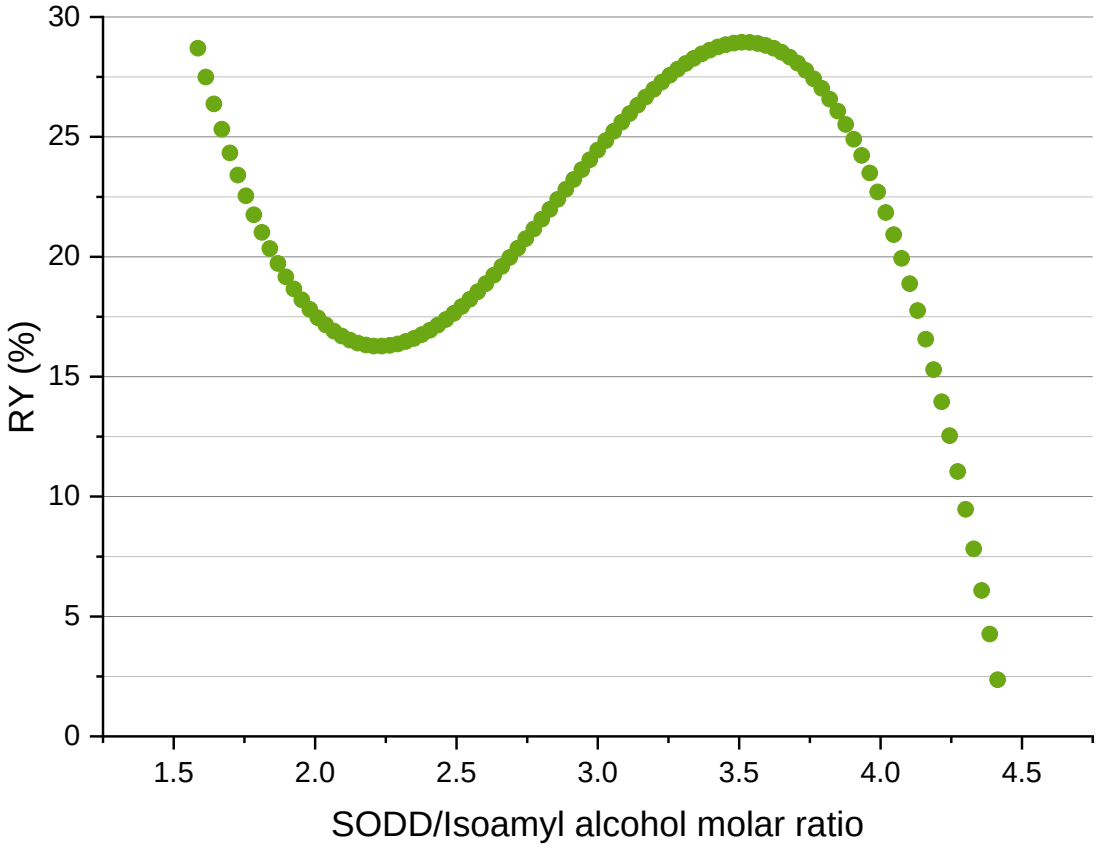

4.2.4.4 Time courses of the FAIEs reactions

The courses of the reactions for SODD FAIEs synthesis using hNF-PFL and free PFL as catalysts, shown in Figure 4.2-12, were evaluated using the conditions of $R_{isoamyl}$, T, and $m_{desiccant\ salt}$ identified in the previous section (1 mol of $SODD_{Sap}$ to 3.5 mol of isoamyl alcohol, T of 40 °C, and $m_{desiccant\ salt}$ of 15 wt.%). Different to the optimization step, these reactions were conducted in a jacketed reactor with mechanical stirring using a straight blade impeller at 1250 rpm. The reaction using hNF-PFL was initially very fast, up to 12 h (RY = 29.0 ± 0.7 wt.%), after which the velocity showed a small decrease between 12 and 32 h (RY = 40.1 ± 0.8 wt.%). After 32 h, the reaction proceeded very slowly, until reaching the maximum RY at 70 h (RY = 46.2 ± 10.7 wt.%). The reaction using free PFL was initially slightly slower than obtained with hNF-PFL, in the first 6 h, but was nevertheless also very fast, reaching RY = 49.4 ± 5.6 wt.% at 24 h, after which the reaction velocity decreased drastically, with maximum RY of 58.6 ±

2.1 wt.% reached at 100 h. Neither of the reactions (using hNF-PFL or free PFL) achieved the maximum RY of 68.1 ± 1.4 wt.% reported by Araujo-Silva et al. (2022).

Figure 4.2-12. Courses of the SODD FAIEs synthesis reactions using hNF-PFL (15 wt.% of $m_{desiccant\ salt}$), free PFL (15 wt.% of $m_{desiccant\ salt}$), and hNF-PFL without desiccant salt (WOSS – 0 wt.% of $m_{desiccant\ salt}$). Reaction conditions: 1 mol of $SODD_{Sap}$ to 3.5 mol of isoamyl alcohol, 40 °C, and 1250 rpm.

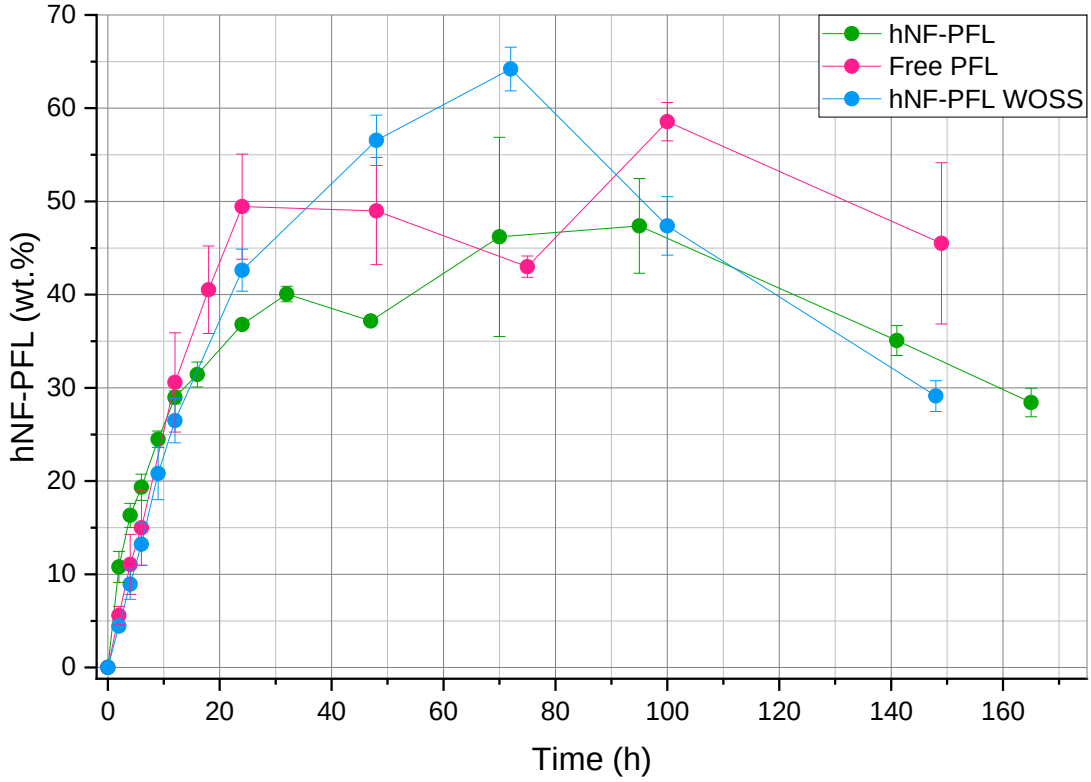

SEM images of the hNF-PFL after 165 h of reaction (Figure 4.2-13) revealed that the hNF structure had been compromised, with the catalyst changing from a solid form to a gelatinous material during the synthesis. Further tests with incubation of the hNF-PFL in the reaction medium components SODD, isoamyl alcohol, and 1 M Na_2SO_4 aqueous solution (Figure 4.2-14) indicated that the presence of Na_2SO_4 affected the hNF-PFL structure, resulting in fusion of the hNF spheres (Figure 4.2-14c). This was not observed in the presence of SODD or isoamyl alcohol (although the images were not very clear, due to interferences of organic compounds in the SEM analysis). Fusion of the spheres would require partial solubilization of the hNF-PFL, suggesting that when this occurred in the reaction medium (composed mainly of FAIEs, SODD, isoamyl alcohol, Na_2SO_4, and a small amount of water), the organic compounds could had interfered in the fusion process, so that the structures became gelatinous, rather than undergoing fusion.

Figure 4.2-13. SEM images of the hNF-PFL structures before (a and b) and after (c and d) the reaction.

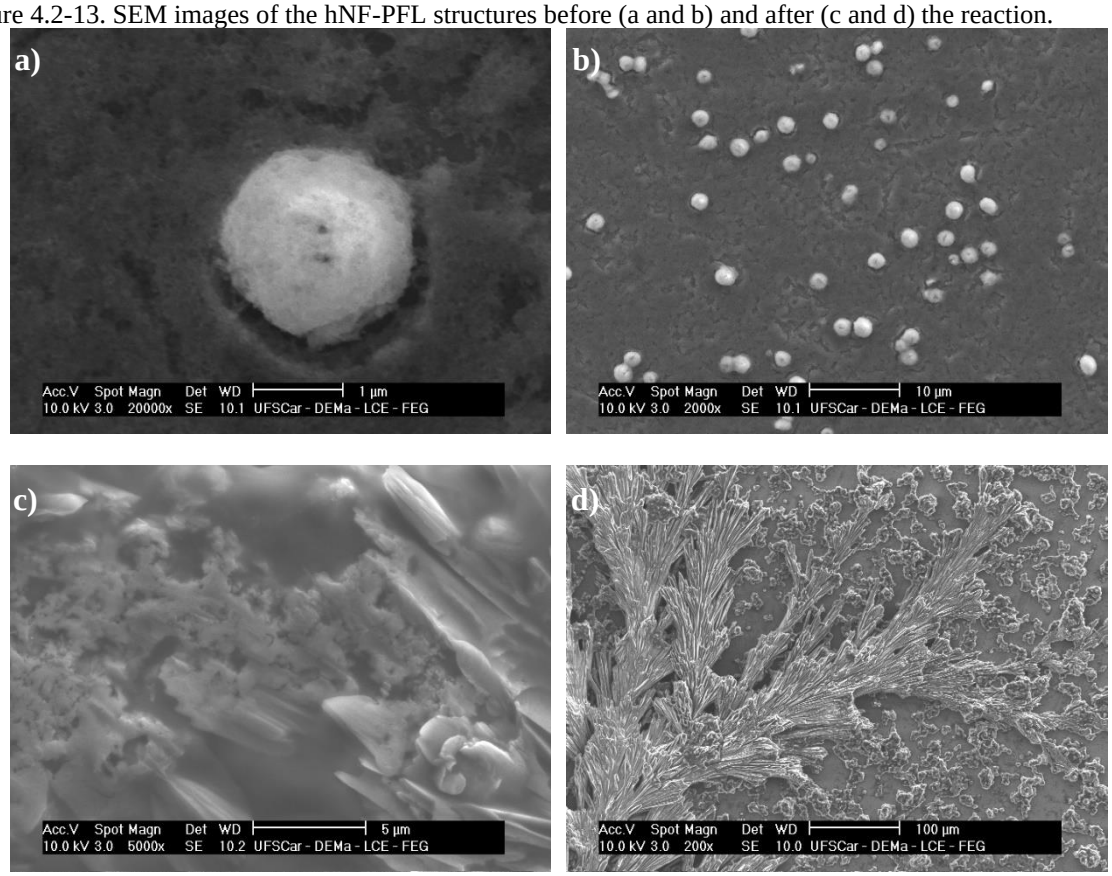

Figure 4.2-14. SEM images of the hNF-PFL after incubation in SODD (a), isoamyl alcohol (b), and 1 M Na_2SO_4 aqueous solution (c), compared to the control (d).

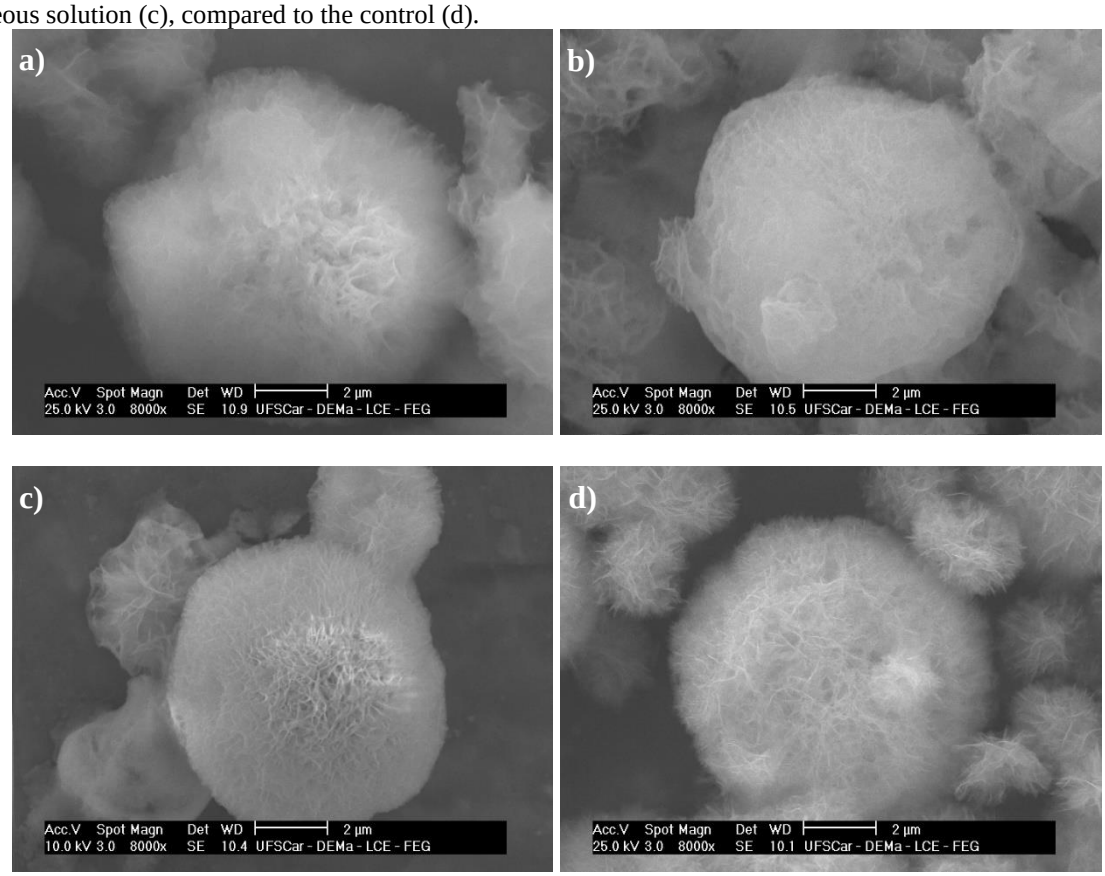

Given the evidence that Na_2SO_4 affected the hNF-PFL structure and that the velocity of the SODD FAIEs reaction at low $m_{desiccant\ salt}$ could be similar to the velocity obtained with 2 wt.% $m_{desiccant\ salt}$ (Figures 4.2-09 and 4.2-10), there were two possibilities: either change the desiccant material or operate without a desiccant. Therefore, a SODD FAIEs reaction, catalyzed by hNF-PFL, was performed without any desiccant (hNF-PFL WOSS curve in Figure 4.2-12). In the first 12 h, the behavior was similar to that observed using the free PFL, after which the reaction velocity gradually decreased until reaching the maximum RY of 64.2 ± 2.3 wt.% at 72 h.

In all the tests, decrease of the FAIEs content occurred after reaching the maximum RY (Figure 4.2-12). A possible explanation for this behavior was oxidation of the double bonds present in the fatty acid chains, due to the high contact of the reaction medium with oxygen (dos Santos et al., 2011), promoted by the agitation at 1250 rpm. It is also possible that hydrolysis of the FAIEs formed could have occurred, due to the equilibrium shift caused by a higher content of water (Yahya et al., 1998) produced from esterification reactions and from the oxidation reactions involving the fatty acid chain double bonds. This behavior could be more easily observed in the reaction without desiccant, compared to those with desiccant.

4.2.4.5 hNF-PFL reuse assay

At this stage, the use of a desiccant was discarded. Each batch employed 1 mol of $SODD_{Sap}$ to 3.5 mol of isoamyl alcohol, with 500 TBU/mL of SODD, under mechanical stirring at 40 °C for 24 h. At the end of each batch, the solid and liquid phases were separated by centrifugation, all the liquid was drained, and a new reaction medium was poured into the reactor with the solids.

Figure 4.2-15 presents the results for the synthesis of SODD FAIEs during 10 batches of 24 h. The first batch showed an unexpected RY value of 16.0 ± 1.1 wt.%, rather than an expected value similar to the RY of 42.6 wt.% previously achieved at 24 h in the reaction using the hNF-PFL without desiccant (Figure 4.2-12). At the end of the first batch, it was observed that the liquid phase in the centrifuge tube had separated into two layers, with a very small one at the bottom of the tube (aqueous phase about 1 mm in height) and a predominant upper layer (nonpolar organic phase about 20 mm in height). This phase separation indicated saturation of the reaction medium with water, which could explain the low RY observed for the first batch. The second batch showed RY of 53.8 wt.%, in better agreement with the RY of 42.3 wt.% at 24 h observed previously (Figure 4.2-12). The difference in RY between the 1st and 2nd batches of the reuse assay suggested that the hNF-PFL could still retain considerable amounts of moisture, even after centrifuging and draining of the water, which was sufficient to affect the FAIEs conversion. The RY remained fairly stable and above 50 wt.% during 7 batches (2nd to 8th), followed by a decrease to 39 wt.% in the 9th and 10th batches. From the results shown in Figure 4.2-15, it could be inferred that the hNF-PFL was very stable during synthesis of the SODD FAIEs and was not difficult to recover, since the RY remained practically unchanged during operation for 192 h. There was a 20% decrease of RY between the 8th and 9th batches, while the RY for the 10th batch was the same as for the 9th batch.

Figure 4.2-15. RY values for consecutive batches of reuse of hNF-PFL for SODD FAIEs synthesis.

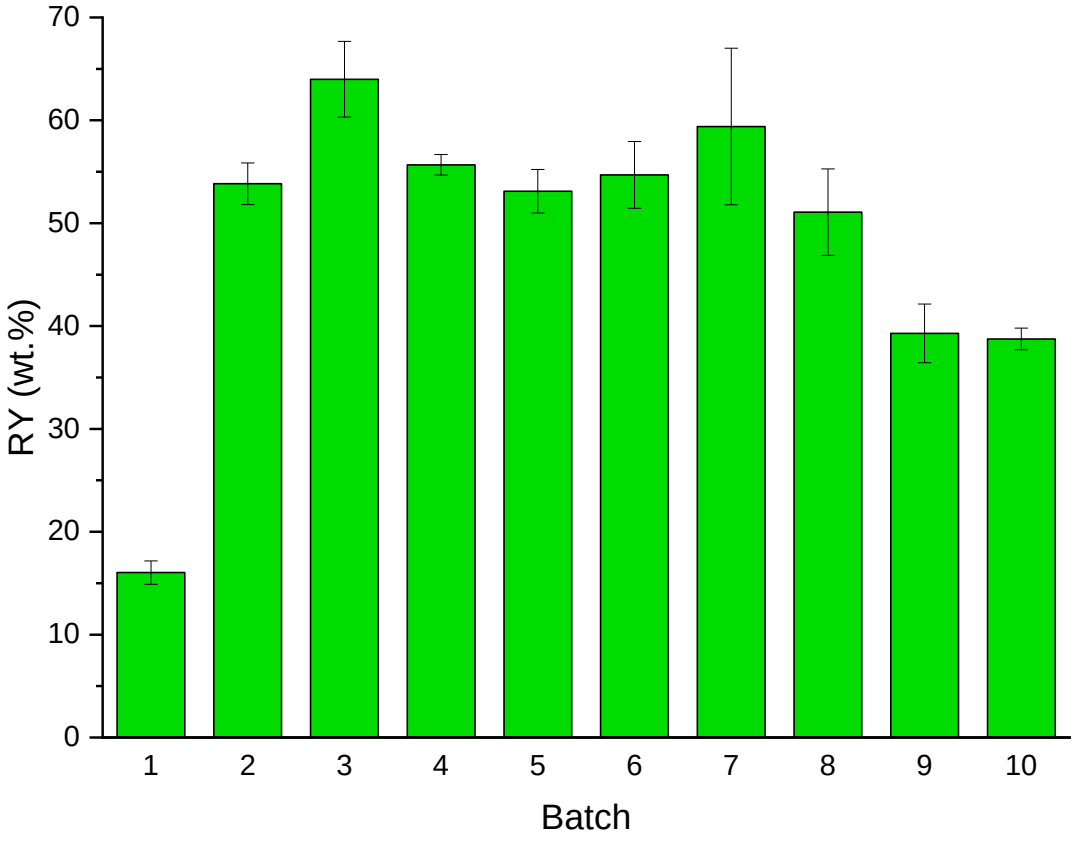

4.2.4.6 Chemical and physicochemical characterizations of the SODD FAIEs obtained using the hNF-PFL catalyst

Chemical and physicochemical characterizations of the SODD FAIEs obtained in the reaction catalyzed by hNF-PFL (Table 4.2-30) were performed after washing and evaporation of the residual isoamyl alcohol (Biolubricant sample), as well as after subsequent caustic polishing (CP Biolubricant sample), in an attempt to reduce the FFAs content. The CP treatment was not suitable, since the hydrolysis of mono- and diglycerides caused an increase of FFAs that could not be removed from the CP Biolubricant sample. The CP treatment had no significant impact on the FAIEs content. The main problem observed in the CP treatment was the difficulty in separating the aqueous and organic phases, which had formed a persistent emulsion. The two biolubricant samples showed similar physicochemical characteristics, despite differences in the FFAs and glycerides chemical compositions.

Table 4.2-30. Comparison of chemical and physicochemical characteristics of the SODD FAIEs biolubricants without (Biolubricant) and with caustic polishing (CP Biolubricant).

Parameters	Biolubricant	CP Biolubricant	SODD[a]	Unit	Standard
Reaction Yield	56.94	55.91	0.0	wt.%	-
Conversion of $SODD_{Sap}$ to FAIEs	75.70	75.37	0.0	wt.%	-
Viscosity at 40 °C	15.0	12.9	33.5	cSt	ASTM D445
Viscosity at 100 °C	3.9	3.7	7.3	cSt	ASTM D445
Viscosity Index	166.3	186.2	191.6	-	ASTM 2270
Relative Density	0.9046	0.8958	0.9211	-	ASTM D1298
Pour Point	-6.0	-9.0	-3.0	°C	ASTM D97
Flash Point	202[b]	202[b]	210[c]	°C	[b]ASTM D92 / [c]ASTM D93
Moisture (Karl Fischer)	0.083 ± 0.016	0.531 ± 0.048	0.185 ± 0.004	wt.%	AOCS Ca 2e-84
Saponification Value	151.76 ± 1.09	149.66 ± 5.24	186.75 ± 4.25	mg_{KOH}/g	AOCS Cd 3-25
Saponifiables[d]	75.22 ± 0.54	74.18 ± 2.60	92.56 ± 2.11	wt.%	AOCS Cd 3-25
Acid Value	9.15 ± 0.04	36.99 ± 0.26	36.85 ± 0.07	mg_{KOH}/g	AOCS Cd 3d-63
Free Fatty Acids[e]	4.54 ± 0.02	18.33 ± 0.13	18.52 ± 0.03	wt.%	AOCS Cd 3d-63
Monoglycerides	10.08	1.16	1.38	wt.%	ASTM D6584
Diglycerides	6.74	1.78	4.39	wt.%	ASTM D6584
Triglycerides	0.53	0.88	69.5	wt.%	ASTM D6584
Free Glycerol	0.066	0.008	0.003	wt.%	ASTM D6584

[a]Data from Araujo-Silva et al. (2022). [b]Open cup Flash Point test. [c]Closed cup Flash Point test. [d]Calculated based on the saponification value. [e]Calculated based in acid value.

Compared to the SODD, both biolubricants presented lower viscosities at 40 and 100 °C, as well as lower viscosity indexes. The hNF-PFL was able to significantly reduce the SODD FFA and triglyceride contents. The relative density and flash point values were similar for the two biolubricants and were slightly lower than for the SODD. The biolubricant RY values were similar to the RY of 55.3 wt.% reported for SODD FAIEs obtained by catalysis using free Eversa Transform 2.0 lipase (Araujo-Silva et al., 2022). The chemical and physicochemical characteristics were also similar.

The Biolubricant and CP Biolubricant samples presented values for viscosity at 40 and 100 °C, viscosity index, density, flash point, and saponification that were similar to those observed for commercial biolubricant base stocks (BASF, 2016), while the acid values were higher, compared to commercial base stocks.

4.2.5 Conclusions

Among the six lipases studied, PFL provided the best transesterification and the second best esterification, using isoamyl alcohol, so it was selected for hNF immobilization. The modifications performed in incubation of the hNF-PFL enabled reduction of the incubation time from 72 h to only 20 min, without compromising IY and with almost the same IA. The use of the surfactants Triton X-100, Tween 20 and Tween 80 did not lead to any significant improvement in IY or IA. The best hNF-PFL immobilization condition achieved IY of 53.94 ± 1.29 %TBU and IA of 63.98 ± 1.87 %TBU, using C_{prot}, C_{CuSO_4}, and PBS pH of 0.1688 mg_{prot}/mL, 7.0 mM, and 8.0, respectively, with incubation under ultrasonication for 20 min. The expected hyperactivation of PFL by immobilization using the hNF technique was not observed in this study. The use of SEM images and EDS mapping showed that the hNF-PFL consisted of highly porous spheres presenting hNF characteristics, ~1 to ~9 μm in diameter, with the enzyme being well distributed throughout the hNF structure. In the synthesis of SODD FAIEs catalyzed by hNF-PFL, higher RY (64. 2 ± 2.3 wt.%) was achieved without the use of a desiccant salt for moisture control, since it was found that the desiccant affected the structural integrity of the hNF-PFL. The results of the reuse assay, performed without an agent to control moisture, reinforced the importance of avoiding excess water in the reaction medium. The hNF-PFL showed high operational stability, maintaining practically the same RY during 192 h (8 cycles). The SODD FAIEs obtained in the reaction catalyzed by hNF-PFL were chemically and physicochemically characterized before and after caustic polishing treatment to remove FFAs. Although this treatment was ineffective, both products presented physicochemical characteristics similar to those of commercial biolubricant base stocks.

4.2.6 Funding

This work was funded by Fundação de Amparo à Pesquisa do Estado de São Paulo (FAPESP, grant 2016/10636-8), Conselho Nacional de Desenvolvimento Científico e Tecnológico (CNPq, grant 308212/2017-7), and in part by Coordenação de Aperfeiçoamento de Pessoal de Nível Superior – Brasil (CAPES, Finance Code 001).

4.2.7 Acknowledgments

The authors thank Novozymes Latin America (Araucária, PR, Brazil) for supplying the *Candida antarctica* lipase B (CALB) and COCAMAR (Maringá, PR, Brazil) for supplying the soybean oil deodorizer distillate (SODD).

4.2.8 References

Altinkaynak, C., Gulmez, C., Atakisi, O., & Özdemir, N. (2020). Evaluation of organic-inorganic hybrid nanoflower's enzymatic activity in the presence of different metal ions and organic solvents. *International Journal of Biological Macromolecules*, *164*, 162–171. https://doi.org/10.1016/j.ijbiomac.2020.07.118

American Oil Chemists' Society. (2004). *Official Methods and Recommended Pratices of the AOCS* (D. Firestone (ed.); 15th ed.). American Oil Chemists' Society.

American Society for Testing and Materials. (2018). *ASTM International*. https://www.astm.org/

Araujo-Silva, R., Vieira, A. C., de Campos Giordano, R., Fernandez-Lafuente, R., & Tardioli, P. W. (2022). Enzymatic Synthesis of Fatty Acid Isoamyl Monoesters from Soybean Oil Deodorizer Distillate: A Renewable and Ecofriendly Base Stock for Lubricant Industries. *Molecules*, *27*(9), 2692. https://doi.org/10.3390/molecules27092692

Bart, J. C. J., Gucciardi, E., & Cavallaro, S. (2013). Renewable lubricants. In J. C. J. Bart, E. Gucciardi, & S. Cavallaro (Eds.), *Biolubricants: Science and technology* (p. 944). Woodhead Publishing.

BASF. (2016). *Esters – Base Stocks Selection Guide for Lubricants and Metalworking Fluids* (p. 2). https://www.btc-europe.com/fileadmin/user_upload/Downloads/Pdf_s/Industries/Brochure_Selection-Guide-Base-Stocks-Esters.pdf

Bradford, M. M. (1976). A rapid and sensitive method for the quantitation of microgram quantities of protein utilizing the principle of protein-dye binding. *Analytical Biochemistry*, *72*(1–2), 248–254. https://doi.org/10.1016/0003-2697(76)90527-3

Cecilia, J. A., Ballesteros Plata, D., Alves Saboya, R. M., Tavares de Luna, F. M., Cavalcante, C. L., & Rodríguez-Castellón, E. (2020). An Overview of the Biolubricant Production Process: Challenges and Future Perspectives. *Processes*, *8*(3), 257. https://doi.org/10.3390/pr8030257

Cui, J., Zhao, Y., Liu, R., Zhong, C., & Jia, S. (2016). Surfactant-activated lipase hybrid nanoflowers with enhanced enzymatic performance. *Scientific Reports*, *6*(29), 1–13. https://doi.org/10.1038/srep27928

dos Santos, V. M. L., da Silva, J. A. B., Stragevitch, L., & Longo, R. L. (2011). Thermochemistry of biodiesel oxidation reactions: A DFT study. *Fuel*, *90*(2), 811–817. https://doi.org/10.1016/j.fuel.2010.09.017

Dwivedee, B. P., Soni, S., Laha, J. K., & Banerjee, U. C. (2018). Self Assembly through Sonication: An Expeditious and Green Approach for the Synthesis of Organic-Inorganic Hybrid Nanopetals and their Application as Biocatalyst. *ChemNanoMat*, *4*(7), 670–681. https://doi.org/10.1002/cnma.201800110

European Environmental Agency. (2020). *Transport: increasing oil consumption and greenhouse gas emissions hamper EU progress towards environment and climate objectives*. https://www.eea.europa.eu/publications/transport-increasing-oil-consumption-and

Ferreira, M. C., Meirelles, A. J. A., & Batista, E. A. C. (2013). Study of the fusel oil distillation process. *Industrial and Engineering Chemistry Research*, *52*(6), 2336–2351. https://doi.org/10.1021/ie300665z

Fotiadou, R., Patila, M., Hammami, M. A., Enotiadis, A., Moschovas, D., Tsirka, K., Spyrou, K., Giannelis, E. P., Avgeropoulos, A., Paipetis, A., Gournis, D., & Stamatis, H. (2019). Development of Effective Lipase-Hybrid Nanoflowers Enriched with Carbon and Magnetic Nanomaterials for Biocatalytic Transformations. *Nanomaterials*, *9*(6), 808. https://doi.org/10.3390/nano9060808

Ge, J., Lei, J., & Zare, R. N. (2012). Protein-inorganic hybrid nanoflowers. *Nature Nanotechnology*, *7*(7), 428–432. https://doi.org/10.1038/nnano.2012.80

Gunawan, S., Kasim, N., & Ju, Y. (2008). Separation and purification of squalene from soybean oil deodorizer distillate. *Separation and Purification Technology*, *60*(2), 128–135. https://doi.org/10.1016/j.seppur.2007.08.001

Hua, X., Xing, Y., & Zhang, X. (2016). Enhanced Promiscuity of Lipase-Inorganic Nanocrystal Composites in the Epoxidation of Fatty Acids in Organic Media. *ACS Applied Materials & Interfaces*, *8*(25), 16257–16261. https://doi.org/10.1021/acsami.6b05061

Jiang, W., Wang, X., Yang, J., Han, H., Li, Q., & Tang, J. (2018). Lipase-inorganic hybrid nanoflower constructed through biomimetic mineralization: A new support for biodiesel synthesis. *Journal of Colloid and Interface Science*, *514*, 102–107. https://doi.org/10.1016/j.jcis.2017.12.025

Ke, C., Fan, Y., Chen, Y., Xu, L., & Yan, Y. (2016). A new lipase–inorganic hybrid nanoflower with enhanced enzyme activity. *RSC Advances*, *6*(23), 19413–19416. https://doi.org/10.1039/C6RA01564F

Lee, H. R., Chung, M., Kim, M. Il, & Ha, S. H. (2017). Preparation of glutaraldehyde-treated lipase-inorganic hybrid nanoflowers and their catalytic performance as immobilized enzymes. *Enzyme and Microbial Technology*, *105*, 24–29. https://doi.org/10.1016/j.enzmictec.2017.06.006

Li, C., Zhao, J., Zhang, Z., Jiang, Y., Bilal, M., Jiang, Y., Jia, S., & Cui, J. (2020). Self-assembly of activated lipase hybrid nanoflowers with superior activity and enhanced stability. *Biochemical Engineering Journal*, *158*, 107582. https://doi.org/10.1016/j.bej.2020.107582

Li, K., Wang, J., He, Y., Abdulrazaq, M. A., & Yan, Y. (2018). Carbon nanotube-lipase hybrid nanoflowers with enhanced enzyme activity and enantioselectivity. *Journal of Biotechnology*, *281*, 87–98. https://doi.org/10.1016/j.jbiotec.2018.06.344

Li, Y., Fei, X., Liang, L., Tian, J., Xu, L., Wang, X., & Wang, Y. (2016). The influence of synthesis conditions on enzymatic activity of enzyme-inorganic hybrid nanoflowers. *Journal of Molecular Catalysis B: Enzymatic*, *133*, 92–97. https://doi.org/10.1016/j.molcatb.2016.08.001

Lin, J., Zhong, C., Lu, Q., & Lin, Z. (2020). Room-Temperature Synthesis of Trypsin-Inorganic Hybrid Nanocomposites for Fast and Efficient Protein Digestion. *ChemistrySelect*, *5*(40), 12500–12504. https://doi.org/10.1002/slct.202002859

Liu, Y., Shao, X., Kong, D., Li, G., & Li, Q. (2021). Immobilization of thermophilic lipase in inorganic hybrid nanoflower through biomimetic mineralization. *Colloids and Surfaces B: Biointerfaces*, *197*, 111450. https://doi.org/10.1016/j.colsurfb.2020.111450

Luther, R. (2014). Bio-Based and Biodegradable Base Oils. In T. Mang (Ed.), *Encyclopedia of Lubricants and Lubrication - Vol. 1* (p. 2413). Springer.

Miranda, L. P., Guimarães, J. R., Giordano, R. C., Fernandez-Lafuente, R., & Tardioli, P. W. (2020). Composites of Crosslinked Aggregates of Eversa® Transform and Magnetic Nanoparticles. Performance in the Ethanolysis of Soybean Oil. *Catalysts*, *10*(8), 817. https://doi.org/10.3390/catal10080817

Mohammadi-Mahani, H., Badoei-dalfard, A., & Karami, Z. (2021). Synthesis and characterization of cross-linked lipase-metal hybrid nanoflowers on graphene oxide with increasing the enzymatic stability and reusability. *Biochemical Engineering Journal*, *172*, 108038. https://doi.org/10.1016/j.bej.2021.108038

Nowak, P., Kucharska, K., & Kamiński, M. (2019). Ecological and Health Effects of Lubricant Oils Emitted into the Environment. *International Journal of Environmental Research and Public Health*, *16*(16), 3002. https://doi.org/10.3390/ijerph16163002

Ocsoy, I., Dogru, E., & Usta, S. (2015). A new generation of flowerlike horseradish peroxides as a nanobiocatalyst for superior enzymatic activity. *Enzyme and Microbial Technology*, *75–76*, 25–29. https://doi.org/10.1016/j.enzmictec.2015.04.010

Parkin, K. L. (2017). Enzymes. In S. Damodaran & K. L. Parkin (Eds.), *Fennema's Food Chemistry* (5th ed., p. 1125). CRC Press.

Ramos, M. D., Miranda, L. P., Giordano, R. L. C., Fernandez-Lafuente, R., Kopp, W., & Tardioli, P. W. (2018). 1,3-Regiospecific ethanolysis of soybean oil catalyzed by crosslinked porcine pancreas lipase aggregates. *Biotechnology Progress*. https://doi.org/10.1002/btpr.2636

Sharma, N., Parhizkar, M., Cong, W., Mateti, S., Kirkland, M. A., Puri, M., & Sutti, A. (2017). Metal ion type significantly affects the morphology but not the activity of lipase–metal–phosphate nanoflowers. *RSC Advances*, *7*(41), 25437–25443. https://doi.org/10.1039/C7RA00302A

Sherazi, H. S. T., Mahesar, S. A., & Sirajuddin. (2016). Vegetable Oil Deodorizer Distillate: A Rich Source of the Natural Bioactive Components. *Journal of Oleo Science*, *65*(12), 957–966. https://doi.org/10.5650/jos.ess16125

Somturk, B., Hancer, M., Ocsoy, I., & Özdemir, N. (2015). Synthesis of copper ion incorporated horseradish peroxidase-based hybrid nanoflowers for enhanced catalytic activity and stability. *Dalton Trans.*, *44*(31), 13845–13852. https://doi.org/10.1039/C5DT01250C

Somturk, B., Yilmaz, I., Altinkaynak, C., Karatepe, A., Özdemir, N., & Ocsoy, I. (2016). Synthesis of urease hybrid nanoflowers and their enhanced catalytic properties. *Enzyme and Microbial Technology*, *86*, 134–142. https://doi.org/10.1016/j.enzmictec.2015.09.005

Soni, S., Dwivedee, B. P., & Banerjee, U. C. (2018). An Ultrafast Sonochemical Strategy to Synthesize Lipase-Manganese Phosphate Hybrid Nanoflowers with Promoted Biocatalytic Performance in the Kinetic Resolution of β-Aryloxyalcohols. *ChemNanoMat*, *4*(9), 1007–1020. https://doi.org/10.1002/cnma.201800250

Talens-Perales, D., Fabra, M. J., Martínez-Argente, L., Marín-Navarro, J., & Polaina, J. (2020). Recyclable thermophilic hybrid protein-inorganic nanoflowers for the hydrolysis of milk lactose. *International Journal of Biological Macromolecules*, *151*, 602–608. https://doi.org/10.1016/j.ijbiomac.2020.02.115

Tsagaraki, E., Karachaliou, E., Delioglanis, I., & Kouzi, E. (2017). *Bio-based products and applications potential*. https://www.bioways.eu/download.php?f=150&l=en&key=441a4e6a27f83a8e828b802c37adc6e1

Wang, A., Chen, X., Yu, J., Li, N., Li, H., Yin, Y., Xie, T., & Wu, S. G. (2020). Green preparation of lipase@Ca3(PO4)2 hybrid nanoflowers using bone waste from food production for efficient synthesis of clindamycin palmitate. *Journal of Industrial and Engineering Chemistry*, *89*, 383–391. https://doi.org/10.1016/j.jiec.2020.06.007

Wu, Z., Li, X., Li, F., Yue, H., He, C., Xie, F., & Wang, Z. (2014). Enantioselective transesterification of (R,S)-2-pentanol catalyzed by a new flower-like nanobioreactor. *RSC Adv.*, *4*(64), 33998–34002. https://doi.org/10.1039/C4RA04431B

Xin, Y., Gao, Q., Gu, Y., Hao, M., Fan, G., & Zhang, L. (2020). Self-assembly of metal-cholesterol oxidase hybrid nanostructures and application in bioconversion of steroids derivatives. *Frontiers of Chemical Science and Engineering*. https://doi.org/10.1007/s11705-020-1989-7

Yahya, A. R. ., Anderson, W. A., & Moo-Young, M. (1998). Ester synthesis in lipase-catalyzed reactions. *Enzyme and Microbial Technology*, *23*(7–8), 438–450. https://doi.org/10.1016/S0141-0229(98)00065-9

Yin, Y., Xiao, Y., Lin, G., Xiao, Q., Lin, Z., & Cai, Z. (2015). An enzyme–inorganic hybrid nanoflower based immobilized enzyme reactor with enhanced enzymatic activity. *J. Mater. Chem. B*, *3*(11), 2295–2300. https://doi.org/10.1039/C4TB01697A

Yu, J., Wang, C., Wang, A., Li, N., Chen, X., Pei, X., Zhang, P., & Wu, S. G. (2018). Dual-cycle immobilization to reuse both enzyme and support by reblossoming enzyme–inorganic hybrid nanoflowers. *RSC Advances*, *8*(29), 16088–16094. https://doi.org/10.1039/C8RA02051E

Zainal, N. A., Zulkifli, N. W. M., Gulzar, M., & Masjuki, H. H. (2018). A review on the chemistry, production, and technological potential of bio-based lubricants. *Renewable and Sustainable Energy Reviews*, *82*, 80–102. https://doi.org/10.1016/j.rser.2017.09.004

Zhang, B., Li, P., Zhang, H., Wang, H., Li, X., Tian, L., Ali, N., Ali, Z., & Zhang, Q. (2016). Preparation of lipase/Zn3(PO4)2 hybrid nanoflower and its catalytic performance as an immobilized enzyme. *Chemical Engineering Journal*, *291*, 287–297. https://doi.org/10.1016/j.cej.2016.01.104

Zhang, L., Ma, Y., Wang, C., Wang, Z., Chen, X., Li, M., Zhao, R., & Wang, L. (2018). Application of dual-enzyme nanoflower in the epoxidation of alkenes. *Process Biochemistry*, *74*, 103–107. https://doi.org/10.1016/j.procbio.2018.08.029

Zhang, Y., Sun, W., Elfeky, N. M., Wang, Y., Zhao, D., Zhou, H., Wang, J., & Bao, Y. (2020). Self-assembly of lipase hybrid nanoflowers with bifunctional Ca2+ for improved activity and stability. *Enzyme and Microbial Technology*, *132*, 109408. https://doi.org/10.1016/j.enzmictec.2019.109408

Zhang, Z., Zhang, Y., He, L., Yang, Y., Liu, S., Wang, M., Fang, S., & Fu, G. (2015). A feasible synthesis of Mn3(PO4)2@BSA nanoflowers and its application as the support nanomaterial for Pt catalyst. *Journal of Power Sources*, *284*, 170–177. https://doi.org/10.1016/j.jpowsour.2015.03.011

Zhong, L., Jiao, X., Hu, H., Shen, X., Zhao, J., Feng, Y., Li, C., Du, Y., Cui, J., & Jia, S. (2021). Activated magnetic lipase-inorganic hybrid nanoflowers: A highly active and recyclable nanobiocatalyst for biodiesel production. *Renewable Energy*, *171*, 825–832. https://doi.org/10.1016/j.renene.2021.02.155

5 CONCLUSIONS

The results obtained in this work showed the feasibility of using SODD as a source of fatty acids (free or in the form of glycerides) for the enzyme-catalyzed production of isoamyl esters. The lipases Eversa Transform 2.0 (in the free form) and from *Pseudomonas fluorescens* (free and immobilized by the hNF method) provided high conversions of the fatty acid source material to fatty acid isoamyl esters (FAIEs). The products obtained, with different concentrations of FAIEs, presented physicochemical properties similar to those of commercial biolubricant base materials. These proprieties also enable their use as biolubricant additives or as hydraulic fluids.

The immobilization of PFL by the hNF technique did not present the expected hyperactivation characteristic of this method, which has been observed for other lipases, although relatively high hNF-PFL immobilization yield and immobilized activity were achieved. The structures of the hNF-PFL were typical of the hNF technique, with sizes ranging from ~1 to ~9 μm and the enzyme being well dispersed in the hybrid matrix. Alteration of the incubation method, from static conditions at 25 °C for 3 days (72 h) to ultrasonication for 20 min, significantly reduced the preparation time of the hNF-PFL, without loss of immobilization yield or immobilized activity. The use of sodium sulfate as a drying salt to control the moisture of the reaction medium during the synthesis of FAIEs from SODD had a negative effect on the hNF-PFL structure. With the organic compounds present in the reaction medium for synthesis of FAIEs from SODD, it was observed that the medium with the drying salt promoted the gelatinization of the hNF-PFL. When the FAIEs synthesis reaction was made without the drying salt, no gelatinization was observed. In the absence of organic compounds, using aqueous sodium sulfate solution, it was observed the fusion of the hNF-PFL particles. The assays of reuse of the hNF-PFL in the synthesis of FAIEs from SODD, were performed without the use of sodium sulfate or any other drying agent, and the hNF-PFL presented high stability, with almost the same reaction yield during 8 cycles, totaling 192 h of operation.

APPENDIX A: PRELIMINARY TESTS OF ENZYME IMMOBILIZATION USING THE HYBRID NANOFLOWERS TECHNIQUE

Attempts were made to immobilize enzymes employing the hNF procedures described by Ge et al. (2012) and Li et al. (2016), but without success. Therefore, in an attempt to solve this problem, several modifications of the procedures were introduced. The possible interference of impurities in the hNFs preparation procedure was investigated using enzymatic solutions that underwent centrifugation, dialysis, and precipitation with acetone. Solutions of PBS and $CuSO_4$ were filtered through 0.22 μm filters, before being used in the immobilization, and biomolecular grade water was used for preparation of these solutions in all the immobilizations. Immobilizations using the hNF technique were performed with two β-amylases as model enzymes, one from crude barley extract (CBE), and the other with high purity from sweet potato (PSP). Proteins were measured according to the procedures described by Bradford (1976) and Lowry et al. (1951). 5 mL Eppendorf tubes and flat-bottomed amber glass flasks were used to incubate the immobilization medium. PBS stock solution (10x), incubation temperatures of 25 and 4 °C, incubation times of 7, 15, and 30 days, and successive precipitations with the same immobilization medium were also evaluated. However, none of these approaches provided satisfactory results.

Due the lack of success and delay of the several hNF reproduction efforts, it was decided to go to the next stage of the work, the evaluation of the feasibility of producing esters for application as biolubricant using SODD and isoamyl alcohol (Section 4.1). At the same time, further efforts were made to reproduce the technique described by Ge et al. (2012), this time using the enzymatic solution in PBS buffer or enzymatic solution in PBS and $CuSO_4$ pretreated or/and incubated in ultrasound, which finally showed promising results.

The next section provides a description of the methodologies used in the attempts at immobilization according to the methods of Ge et al. (2012) and Li et al. (2016), including the reaction times, the conditions of the reaction media submitted to ultrasonication, and the results obtained.

A.1. Materials and methodologies for immobilizations using the hNF method

A.1.1. Materials

Lipases from *Candida rugosa* (CRL), porcine pancreas (PPL), and *Rhizopus niveus* (RNL), β-amylases from crude barley extract (CBE) and with high purity from sweet potato (PSP), and biomolecular grade water were acquired from Sigma-Aldrich (St. Louis, MO, USA). *Candida antarctica* lipase B (CALB) was kindly donated by Novozymes (Araucária, Brazil). All the other reagents used in synthesis of the hNFs were analytical grade.

A.1.2. Methodology of Ge et al. (2012) for hNF synthesis

Lipases CALB, CRL, and RNL, and β-amylases CBE and PSP, were immobilized according to the conditions described by Ge et al. (2012). In each assay, one of the enzymes was added in sufficient quantity to obtain a protein concentration of 0.02 mg_{prot}/mL in 3 mL of 1x PBS buffer (with concentrations of ~12 mM PO_4^{3-} and ~140 mM Cl^-) at pH 7.4. The medium was vortexed agitated until solubilization of the enzyme, followed by addition of 20 µL of 120 mM $CuSO_4$ solution and further agitation. The medium was incubated for 3 days at 25 °C in a thermostatic bath, after which it was centrifuged and the supernatant was separated for measurement of the hydrolytic activity. The precipitate was washed with 3 mL of distilled water, centrifuged, and resuspended in 3 mL of distilled water for measurement of the hydrolytic activity of the hNFs. A blank assay was performed without addition of $CuSO_4$, enabling calculation of the immobilization yield (IY) (Equation A.1-1).

$$IY(\%) = 100 \times \frac{A_{hNF}}{A_{blank}} \qquad \text{(Equation A.1-1)}$$

where, A_{hNF} is the hydrolytic activity (per mL) of the resuspended hNF and A_{blank} is the hydrolytic activity (per mL) of the blank (final or initial). The residual activity in the supernatant after immobilization of the enzymes (SA) (Equation 4.1-2) was calculated analogously to IY:

$$SA(\%) = 100 \times \frac{A_{supernat}}{A_{blank}} \qquad \text{(Equation A.1-2)}$$

where, $A_{supernat}$ is the hydrolytic activity (per mL) in the supernatant.

A.1.3. Methodology of Li et al. (2016) for hNF synthesis

PPL was added in a sufficient amount to obtain a protein concentration of 0.25 mg_{prot}/mL in 3 mL of 1x PBS buffer (containing ~12 mM PO_4^{3-} and ~140 mM Cl^-) at pH 6.0. The medium was vortexed agitated until solubilization of the enzyme, followed by addition of 20 µL of 120 mM $CuCl_2$ solution and further agitation. The medium was then incubated at 25 °C for 3 days in a thermostatic bath, centrifuged, and the supernatant was separated for

measurement of hydrolytic activity. The precipitate was washed with 3 mL of distilled water, centrifuged, and resuspended in 3 mL of distilled water for measurement of the hydrolytic activity of the hNFs. A blank assay was performed without addition of $CuCl_2$, enabling calculation of IY and SA (Equations A.1-1 and A.1-2).

A.1.4. Treatment using ultrasonication

Different solutions of PBS with enzyme, before and after addition of $CuSO_4$, were submitted to pretreatment or/and incubation in an ultrasonic bath (MaxiClean 1450, Unique, Indaiatuba, SP, Brazil) for different time intervals. Three conditions were evaluated:

A) PBS + CALB (before addition of $CuSO_4$);

B) PBS + CALB + $CuSO_4$ (after addition of $CuSO_4$);

C) PBS + CALB and PBS + CALB + $CuSO_4$ (before and after addition of $CuSO_4$).

Blank assays were performed without addition of the copper salt, enabling calculation of IY and SA (Equations A.1-1 and A.1-2). The immobilized activity (IA) values of these hNFs were calculated according to Equation A.1-3:

$$IA(\%) = 100 \times \frac{A_{hNF}}{A_{final\ blank} - A_{supernat}} \qquad \text{(Equation A.1-3)}$$

A.1.5. Measurements of enzymatic activities

A.1.5.1. Lipase activity

Determination of lipase hydrolytic activity was performed using the initial rates, quantified by measuring the volume of potassium hydroxide (KOH) required to neutralize butanoic acid, generated by the hydrolysis of tributyrin in buffered aqueous medium. The assays were performed at constant pH and temperature, under mechanical agitation, using an automated pH-STAT instrument (Pharm 907 Titrando, Metrohm, Herisau, Switzerland) operated with Metrohm tiamo™ software (Guimarães et al., 2021). A jacketed reactor, at 37.0 °C, was filled with 22.5 mL of 26.7 mM sodium phosphate buffer solution (pH 7.5) and 1.5 mL of tributyrin, followed by addition of between 0.1 to 0.5 mL (depending on the activity of the lipase evaluated) of enzyme solution (blank or supernatant) or lipase-hNF suspension, under constant mechanical agitation at 900 rpm using a straight stirrer. The pH was maintained constant by adding aliquots of 20 mM KOH solution to the system. The reaction was monitored during 5 min, obtaining a table with values recorded every 2 s for the volume of KOH solution added. Using the stoichiometric ratio of 1 mol of KOH to 1 mol of butanoic acid, it was possible

to determine the units of activity (TBU) for the hydrolysis of tributyrin by lipase, as mols of KOH consumed per minute (1 TBU = 1 mol KOH/min).

A.1.5.2. β-Amylase activity

The activities of the β-amylases were determined according to a published method (Sigma-Aldrich, 2014), based on the work of Bernfeld (1955), using a jacketed reactor maintained at a controlled temperature of 20 °C, under mechanical agitation with a straight stirrer. The reactor was filled with 5 mL of 16 mM sodium acetate buffer solution (pH 4.8) containing 1% (w/v) of soluble starch (previously solubilized at boiling temperature for 10 min), followed by addition of 0.5 mL of a solution containing free or immobilized β-amylase. The reaction was monitored for 12 min, with periodic removal of aliquots for determination of total reducing sugars by the dinitrosalicylic acid (DNS) method. A standard curve was constructed using maltose. The units of starch hydrolysis by β-amylase (βU) were defined as mg of maltose generated per minute ($mg_{maltose}$/min).

A.2. Results and Discussion

The different attempts to replicate the hNF techniques were unsuccessful. Several strategies were studied in order to try to understand the problem, as described in Section A.1. The results of these attempts were unsatisfactory (Table A.2-1), since high IY and low SA were expected, based on the high IA or IY reported by Ge et al. (2012) and Li et al. (2016). In cases where IY was not zero, the values were very low, while the SA values were very high, indicating low IA.

Table A.2-1. Results obtained in attempts to produce hNFs with different enzymes, using various adjustments of the synthesis methods.

Description of alteration of the hNF methods	**Enzyme used**	**IY (%)[a]**	**IY (%)[b]**	**SA (%)[a]**	**SA (%)[b]**	
Dialysis of the enzymes	CALB	0	0	-	78.14	
	PPL	0	0	-	0	
Clarification by centrifugation	CALB	0	0	-	84.49	
	PPL	0	0	48.86	4.36	[c]
Using an Eppendorf tube (Epp) or glass flask (GF) in a cold chamber	CALB (Epp)	0	0	93.49	84.03	
	CALB (GF)	0	0	92.66	83.27	
Use of a cold chamber and different inorganic salts	PPL ($CuCl_2$)	0	0	54.65	53.06	[c]
	PPL ($CuSO_4$)	0	0	54.4	52.81	[c]
Comparison of the purity of hNFs containing β-amylases from purified sweet potato (PSP) and crude barley extract (CBE)	β-amylase PSP	0	0	81.5	57.69	
	β-amylase CBE	0	0	0	0	
Protein concentrations of 0.01, 0.02, and 0.03 mg_{prot}/mL	CALB 0.01	9.23	8.74	100.14	94.84	[d]
	CALB 0.02	8.72	8.26	106.28	100.66	[d]
	CALB 0.03	4.16	3.94	103.77	98.27	[d]
Filtration of inorganic salt solutions using a 0.22 μm filter	CALB	4.68	-	87.98	-	
2nd successive immobilization	CALB	5.01	4.68	79.16	74.01	
Purification by precipitation with acetone and growth of the crystals after 3, 7, 15, and 30 days	CALB 3	1.63	1.55	98.28	93.69	
	CALB 7	3.12	2.65	94.67	80.38	
	CALB 15	4.41	3.73	96.61	87.57	
	CALB 30	4.01	3.41	97.2	88.15	
Temperature of 25 °C in a thermostatic bath	CRL	0	0	-	-	
	RNL	0	0	-	-	
Temperature of 4 °C in a thermostatic bath	CRL	0	0	-	-	
	RNL	0	0	-	-	

[a] In relation to the final blank; [b] In relation to the initial blank; [c] With formation of blue crystals; [d] Values with possible experimental error.

In several cases, with or without any IY, there was the formation of characteristic hNF structures. For example, Figure A.2-1 shows scanning electron microscopy (SEM) and energy dispersive spectroscopy (EDS) images of a CALB-hNF sample with IY = 1.63%. It can be seen in the SEM images (Figure A.2-1a) that the structures formed had characteristic hNF shapes and sizes, with high uniformity. The EDS images (Figure A.2-1b) showed low amounts of

carbon (C) and almost no nitrogen (N), which is a characteristic element present in proteins, indicating their absence.

Figure A.2-1. SEM and EDS images of CALB-hNF prepared using CALB purified by precipitation with acetone and 3 days of crystal growth.

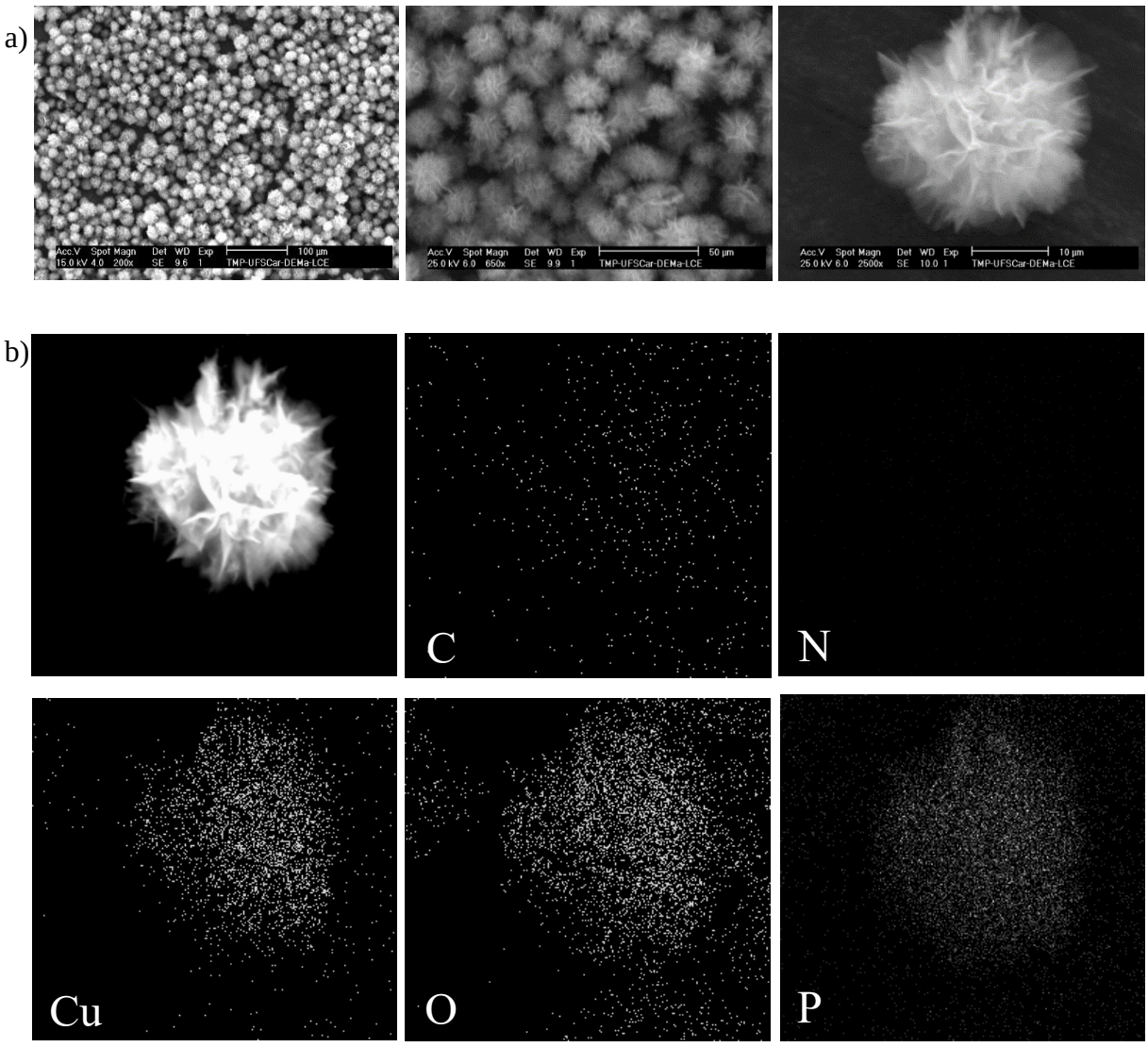

C: carbon; N: nitrogen; Cu: copper; O: oxygen; P: phosphate.

The use of ultrasonication resulted in much higher IY (Table A.2-2), in some cases achieving values of over 40%. However, SA remained high, indicating low IY. Some IA values reached over 100%, typical of the hNF technique.

Table A.2-2. Results for immobilization of *Candida antarctica* lipase B (CALB) using the hNF technique with ultrasonication.

Conditions	Time (min)	IY (%)	SA (%)	IA (%)
A	20	41.02	78.92	194.54
	40	20.42	76.37	86.43
	60	8.86	89.83	87.13
B	20	40.77	82.23	229.41
	40	10.48	90.49	110.23
	60	24.27	93.76	388.60
C	10 and 10	12.20	107.73	-
	20 and 20	12.20	73.88	46.71

(A) PBS + CALB (before addition of $CuSO_4$); (B) PBS + CALB + $CuSO_4$ (after addition of $CuSO_4$); (C) PBS + CALB and PBS + CALB + $CuSO_4$ (before and after addition of $CuSO_4$).

Based on the data shown in Table A.2-2, new syntheses of hNFs employing ultrasonication were studied.

A.3. References

Bernfeld, P. (1955). Amylases, α and β. In S. P. Colowick & N. O. Kaplan (Eds.), *Methods in Enzymology* (pp. 149–158). Academic Press. https://doi.org/10.1016/0076-6879(55)01021-5

Bradford, M. M. (1976). A rapid and sensitive method for the quantitation of microgram quantities of protein utilizing the principle of protein-dye binding. *Analytical Biochemistry*, *72*(1–2), 248–254. https://doi.org/10.1016/0003-2697(76)90527-3

Ge, J., Lei, J., & Zare, R. N. (2012). Protein-inorganic hybrid nanoflowers. *Nature Nanotechnology*, *7*(7), 428–432. https://doi.org/10.1038/nnano.2012.80

Guimarães, J. R., Miranda, L. P., Fernandez-Lafuente, R., & Tardioli, P. W. (2021). Immobilization of Eversa® Transform via CLEA Technology Converts It in a Suitable Biocatalyst for Biolubricant Production Using Waste Cooking Oil. *Molecules*, *26*(1), 193. https://doi.org/10.3390/molecules26010193

Li, Y., Fei, X., Liang, L., Tian, J., Xu, L., Wang, X., & Wang, Y. (2016). The influence of synthesis conditions on enzymatic activity of enzyme-inorganic hybrid nanoflowers. *Journal of Molecular Catalysis B: Enzymatic*, *133*, 92–97. https://doi.org/10.1016/j.molcatb.2016.08.001

Lowry, O., Rosebrough, N., Farr, A. L., & Randall, R. (1951). PROTEIN MEASUREMENT WITH THE FOLIN PHENOL REAGENT. *Journal of Biological Chemistry*, *193*(1), 265–275. https://doi.org/10.1016/S0021-9258(19)52451-6

Sigma-Aldrich. (n.d.). *Enzymatic Assay of β-AMYLASE (EC 3.2.1.2)*. Retrieved February 20, 2014, from http://www.sigmaaldrich.com/technical-documents/protocols/biology/enzymatic-assay-of-bamylase

APPENDIX B: PERMISSIONS OF IMAGES REPRODUCTIONS

B.1. Permission to reproduce Figure 2.4-1

Marketplace™

Order Number: 1267584
Order Date: 12 Sep 2022

Payment Information

Rafael Araujo Silva
[redacted]
Payment method: Invoice

Billing Address:
Dr. Rafael Araujo Silva
General
São Paulo, São Paulo
Brazil
[redacted]
com

Customer Location:
Dr. Rafael Araujo Silva
General
São Paulo, São Paulo
Brazil

Order Details

1. Green chemistry : an international journal and green chemistry resource : GC

Billing Status: Open

Article: The use of lipases as biocatalysts for the epoxidation of fatty acids and phenolic compounds

Order License ID	1267584-1	Type of use	Republish in a thesis/dissertation
Order detail status	Completed		
ISSN	1463-9262	Publisher	ROYAL SOC OF CHEM
		Portion	Chart/graph/table /figure

0.00 USD
Republication Permission

LICENSED CONTENT

Publication Title	Green chemistry : an international journal and green chemistry resource : GC	Rightsholder	Royal Society of Chemistry
		Publication Type	Journal
		Start Page	1740
Article Title	The use of lipases as biocatalysts for the epoxidation of fatty acids and phenolic compounds	End Page	1754
		Issue	4
		Volume	16
Author/Editor	Royal Society of Chemistry (Great Britain)		
Date	01/01/1999		
Language	English		
Country	United Kingdom of Great Britain and Northern Ireland		

REQUEST DETAILS

B.2. Permission to reproduce Figure 2.4-2

ELSEVIER LICENSE
TERMS AND CONDITIONS

Sep 12, 2022

This Agreement between Dr. Rafael Araujo Silva ("You") and Elsevier ("Elsevier") consists of your license details and the terms and conditions provided by Elsevier and Copyright Clearance Center.

License Number	5386580561398
License date	Sep 12, 2022
Licensed Content Publisher	Elsevier
Licensed Content Publication	Biotechnology Advances
Licensed Content Title	Structural traits and catalytic versatility of the lipases from the Candida rugosa-like family: A review
Licensed Content Author	Jorge Barriuso,María Eugenia Vaquero,Alicia Prieto,María Jesús Martínez
Licensed Content Date	September–October 2016
Licensed Content Volume	34
Licensed Content Issue	5
Licensed Content Pages	12
Start Page	874

B.3. Permission to reproduce Figures 2.5-1 and 2.5-2

SPRINGER NATURE LICENSE
TERMS AND CONDITIONS

Sep 12, 2022

This Agreement between Dr. Rafael Araujo Silva ("You") and Springer Nature ("Springer Nature") consists of your license details and the terms and conditions provided by Springer Nature and Copyright Clearance Center.

License Number	5386581168492
License date	Sep 12, 2022
Licensed Content Publisher	Springer Nature
Licensed Content Publication	Nature Nanotechnology
Licensed Content Title	Protein–inorganic hybrid nanoflowers
Licensed Content Author	Jun Ge et al
Licensed Content Date	Jun 3, 2012
Type of Use	Thesis/Dissertation
Requestor type	non-commercial (non-profit)
Format	electronic
Portion	figures/tables/illustrations
Number of figures/tables /illustrations	2

B.4. Permission to reproduce Figure 2.5-3

ELSEVIER LICENSE
TERMS AND CONDITIONS

Sep 12, 2022

This Agreement between Dr. Rafael Araujo Silva ("You") and Elsevier ("Elsevier") consists of your license details and the terms and conditions provided by Elsevier and Copyright Clearance Center.

License Number	5386581387107
License date	Sep 12, 2022
Licensed Content Publisher	Elsevier
Licensed Content Publication	Journal of Biotechnology
Licensed Content Title	Carbon nanotube-lipase hybrid nanoflowers with enhanced enzyme activity and enantioselectivity
Licensed Content Author	Kai Li,Jianhua Wang,Yaojia He,Miaad Adnan Abdulrazaq,Yunjun Yan
Licensed Content Date	Sep 10, 2018
Licensed Content Volume	281
Licensed Content Issue	n/a
Licensed Content Pages	12
Start Page	87

B.5. Permission to reproduce Figure 2.5-4

ELSEVIER LICENSE
TERMS AND CONDITIONS

Sep 12, 2022

This Agreement between Dr. Rafael Araujo Silva ("You") and Elsevier ("Elsevier") consists of your license details and the terms and conditions provided by Elsevier and Copyright Clearance Center.

License Number	5386601078998
License date	Sep 12, 2022
Licensed Content Publisher	Elsevier
Licensed Content Publication	Renewable Energy
Licensed Content Title	Activated magnetic lipase-inorganic hybrid nanoflowers: A highly active and recyclable nanobiocatalyst for biodiesel production
Licensed Content Author	Le Zhong,Xiaobo Jiao,Hongtong Hu,Xuejian Shen,Juan Zhao,Yuxiao Feng,Conghai Li,Yingjie Du,Jiandong Cui,Shiru Jia
Licensed Content Date	Jun 1, 2021
Licensed Content Volume	171
Licensed Content Issue	n/a
Licensed Content Pages	8
Start Page	825

B.6. Permission to reproduce Figure 2.5-5

ELSEVIER LICENSE
TERMS AND CONDITIONS

Sep 12, 2022

This Agreement between Dr. Rafael Araujo Silva ("You") and Elsevier ("Elsevier") consists of your license details and the terms and conditions provided by Elsevier and Copyright Clearance Center.

License Number	5386601272619
License date	Sep 12, 2022
Licensed Content Publisher	Elsevier
Licensed Content Publication	Materials Letters
Licensed Content Title	In situ growth of hybrid nanoflowers on activated carbon fibers as electrodes for mediatorless enzymatic biofuel cells
Licensed Content Author	Thuan Ngoc Vo,Tai Duc Tran,Hoang Kha Nguyen,Do Yun Kong,Moon Il Kim,Il Tae Kim
Licensed Content Date	Dec 15, 2020
Licensed Content Volume	281
Licensed Content Issue	n/a
Licensed Content Pages	1
Start Page	128662

B.7. Permission to reproduce Figure 2.5-6

ELSEVIER LICENSE
TERMS AND CONDITIONS

Sep 12, 2022

This Agreement between Dr. Rafael Araujo Silva ("You") and Elsevier ("Elsevier") consists of your license details and the terms and conditions provided by Elsevier and Copyright Clearance Center.

License Number	5386601445918
License date	Sep 12, 2022
Licensed Content Publisher	Elsevier
Licensed Content Publication	Journal of Hazardous Materials
Licensed Content Title	Supported growth of inorganic-organic nanoflowers on 3D hierarchically porous nanofibrous membrane for enhanced enzymatic water treatment
Licensed Content Author	Mengying Luo,Mufang Li,Shan Jiang,Hao Shao,Joselito Razal,Dong Wang,Jian Fang
Licensed Content Date	Jan 5, 2020
Licensed Content Volume	381
Licensed Content Issue	n/a
Licensed Content Pages	1